POTENTIAL ANTIDOTES TO PHOSPHINE POISONING

by

Kimberly Kinter Garrett

BS, Allegheny College, 2015

MPH, University of Pittsburgh, 2017

Submitted to the Graduate Faculty of the

Graduate School of Public Health in partial fulfillment

of the requirements for the degree of

Doctor of Philosophy

University of Pittsburgh

2021

UNIVERSITY OF PITTSBURGH

GRADUATE SCHOOL OF PUBLIC HEALTH

This dissertation was presented

by

Kimberly Kinter Garrett

It was defended on

August 10, 2021

and approved by

Dissertation Advisor:

James Peterson, PhD, Associate Professor, Department of Environmental and Occupational Health, Graduate School of Public Health, University of Pittsburgh

Committee Members:

Linda L. Pearce, PhD, Assistant Professor, Department of Environmental and Occupational Health, Graduate School of Public Health, University of Pittsburgh

George D. Leikauf, PhD, Professor, Department of Environmental and Occupational Health, Graduate School of Public Health, University of Pittsburgh

Jill Millstone, PhD, Associate Professor, Department of Chemistry, Dietrich School of Arts and Sciences, University of Pittsburgh

POTENTIAL ANTIDOTES TO PHOSPHINE POISONING

Kimberly K. Garrett, PhD

University of Pittsburgh, 2021

Globally, phosphine gas released from metal phosphides is responsible for more poisonings (both intentional and accidental) than any other chemical agent. Metal phosphides (e.g. Ca_3P_2, AlP) produce phosphine through hydrolysis and can react with moisture in ambient air. Phosphine is used as a fumigant pesticide and is a workplace hazard in agriculture, shipping, pest control, and the semiconductor industry where it is used as a doping agent. However, the majority of phosphine exposures are suicidal in nature. No antidote to phosphine is currently available. Most purposeful phosphine poisonings occur through the ingestion of metal phosphides, which results in continuous exposure to phosphine gas. Therefore, an antidote with both prophylactic and therapeutic activity may be beneficial. Phosphine is associated with the inhibition of mitochondrial respiration at complex IV, cytochrome *c* oxidase, but the full implication of this inhibition as it relates to phosphine toxicity is not completely understood.

Because the mechanism is incomplete, a decorporation strategy, useful against two other mitochondrial poisons (cyanide and azide), was adopted. Based on inorganic principles, Au(I) and Ag(I) complexes were selected as potential decorporating antidotes against phosphine toxicity. In addition, some Co(II/III) complexes, shown to be effective against other complex IV inhibitors, were also tested. A novel method for screening potential antidotes to phosphine toxicity using *Galleria mellonella* larvae is described in this work. Antidotes that proved effective against phosphine toxicity in the larvae were subsequently examined in mice by a behavioral method. Methemoglobinemia, negatively associated with survival, and hemolysis have been reported in

cases of phosphine poisoning. Murine blood exposed to phosphine was studied over the course of 1-2 hours, both *in vivo* and *in vitro*, for the presence of methemoglobin and potential hemolysis.

TABLE OF CONTENTS

LIST OF TABLES

LIST OF FIGURES

LIST OF EQUATIONS

ABBREVIATIONS AND NOMENCLATURE

AA	Ascorbic acid
ACS	American Chemical Society
AEGL	Acute Exposure Guideline
Ag	Silver
$Ag(MTZ)_2NO_3$	Silver(I) bis(metronidazole) nitrate
$AgNO_3$	Silver(I) nitrate
$Al(OH)_3$	Aluminum Hydroxide
AlP	Aluminum phosphide
ATP	Adenosine Triphosphate
Au	Gold
AuTG	Aurothioglucose
AuTM	Sodium aurothiomalate
AuTS	Auro-sodium bisthiosulfate
Br	Bromine
BR	Breathing rate
C	Carbon
c	Concentration
$Ca(OH)_2$	Calcium hydroxide
Ca_3P_2	Calcium phosphide
CFW	Carworth Farms White
CN^-	Cyanide
Co	Cobalt
$Co(II)N_4[11.3.1]$	Cobalt(II)2,12-dimethyl-3,7,11,17-tetraazabicyclo-[11.3.1]-heptadeca-1(17)-2,11,13,15-pentaenyl dibromide
$Co(II)N_4[14]$	(5,7,7,12,14,14-Hexymethyl-1,4,8,11-tetraazacyclotetradeca-4,11-diene cobalt (II) dibromide dehydrate)
$CoBr_2$	Cobalt(II) bromide

D_{abs}	Absorbed dose
D_{exp}	Exposure/inhaled dose
DHAA	Dehydroascorbic acid
DMSO	Dimethylsulfoxide
EDTA	Ethylenediaminetetraacetic acid
EPR	Electron Paramagnetic Resonance spectroscopy
ESI-MS	Electrospray Ionization Mass Spectrometry
ε	Molar absorptivity
Fe	Iron
FT-IR	Fourier Transform Infrared spectroscopy
H	Hydrogen
H_2O	Water
H_2O_2	Hydrogen peroxide
H_2PO	Phosphinite
H_2SO_4	Sulfuric acid
H_3PO	Phosphinous acid
H_3PO_2	Phosphinic acid
H_3PO_3	Phosphorous acid
H_3PO_4	Phosphoric acid
H_4P_2	Phosphanylphosphane
HEPES	4-(2-hydroxyethyl)-1-piperazineethanesulfonic acid
IDLH	Immediately Dangerous to Life or Health
IP	Intraperitoneal
IUPAC	International Union of Pure and Applied Chemistry
KCl	Potassium chloride
K_{eq}	Equilibrium constant
K_{ow}	1-octanol/water partition coefficient
K_{sp}	Solubility product constant
M	Metal

m	Mass
MetHb	Methemoglobin
MTZ	1-(2-hydroxyethyl)-2-methyl-5-nitro-1H-imidazole
N	Nitrogen
N_3^-	Azide
$Na_2S_2O_3$	Sodium thiosulfate
NADPH	Nicotinamide adenine dinucleotide phosphate
NIOSH	National Institute of Occupational Safety and Health
NOAEL	No Observed Adverse Effect Level
O_2	Oxygen
OH^-	Hydroxide
OSHA	Occupational Safety and Health Administration
OxyHb	Oxyhemoglobin
P_2O_5	Phosphorous pentoxide
PBS	Phosphate Buffered Saline
PEL	Permissible Exposure Limit
PH_3	Phosphine
RBC	Red Blood Cell
t	Time
WHO	World Health Organization
λ	Wavelength (nm)

ACKNOWLEDGEMENTS

This work would not have been possible without the support of so many. I'd like to thank my primary advisors Dr. Jim Peterson and Dr. Linda Pearce for your invaluable mentorship, teaching, and patience. Thank you for sharing your lab and expertise with me. Thank you to the other members of my committee, Dr. George Leikauf and Dr. Jill Millstone. Thank you both for feedback and encouragement. To my lab-mates, both former and current, thank you for your hands-on help and your friendship. Thank you Samantha Carpenter-Totoni for sharing your mouse-wrangling skills and Cody Madison for being my co-parent to thousands of caterpillars.

Thank you to the department of environmental and occupational health and to Bryanna Schneider and Adam Orbell who I appreciate so much. Thank you to Dr. Michael Hendrich of Carnegie Mellon University who allows us to use his EPR system and software. This work was supported by the National Institutes of Health CounterACT Program, National Institutes of Health Office of the Director (NIH OD), and the National Institute of Environmental Health Sciences (NIEHS): Award R21 ES029310 (to L.L.P. and J.P).

I'd like to give special thanks to the University of Pittsburgh Graduate Student Organizing Committee. Learning and organizing with you has been one of the greatest parts of the past five years. Everyone deserves to be safe and empowered at work and the graduate student organizing committee works every day to reach that goal not only for grad workers but for the whole campus community.

I would not have reached this milestone without the support and community of my friends. I'd like to acknowledge a few for being the very best: Pat Healy, Tory Irwin, Allison Shafer, Dr.

Emily Ackerman, Dr. Melissa Yang, Sarah E. Scherk, David Maynard, Sarah La Rue, Gabe Miller, Madeline Barber, Will Brown, and Jess Schombert.

I'm so thankful to my partner and best friend, Matt Demers. You've been supportive through so much, especially over the past year and I'm thankful for you every day. To my parents, Roger and Susie Garrett, I love you so much. Thank you for continuous love and for teaching me to love nature, science, and medicine. Finally, I'd like to recognize my distinguished coo-leagues, Cooper and Lady Pigeon for being the best animal companions I could ever ask for.

1.0 INTRODUCTION

Phosphine (PH_3) is used as an agricultural fumigant and dopant in the semi-conductor industry. The gas is released from metal phosphide tablets upon reaction with water, even with moisture in ambient air [1, 2]. While phosphine is considered a primarily mitochondrial poison, case reports and recent developments in phosphine treatment suggest it may act through more diverse toxicity mechanisms including erythrocyte hemolysis and hemoglobin damage [3-7]. This possible role for the blood/vasculature might account for the sometimes suggested involvement of multiple organ systems [8, 9]. There is currently no antidote to phosphine available and poisoned patients are treated with supportive measures with inconsistent success [10-13]. The goal of this research is to identify and screen novel antidotes to phosphine poisoning and along the way, add to the body of knowledge about phosphine toxicity, specifically its impacts on the blood.

Previously identified cobalt-based compounds effectively ameliorated the toxicity of other mitochondrial poisons cyanide (CN^-) and azide (N_3^-) through decorporation, the strong binding of the poison ligand to an antidote metal forming a stable adduct, reducing the circulating level of the toxicant [14-16], and ultimately, promoting its excretion. In this work, transition-metal based compounds that may ameliorate phosphine toxicity through a similar decorporation mechanism have been investigated. Based on inorganic chemistry principles, some gold(I) and silver(I) compounds were initially selected as candidate antidotes [17, 18]. In addition, some cobalt compounds shown by our own group to be effective against CN^- and N_3^- have been examined for their putative antidotal effects against phosphine as well. Finally, the impact of phosphine on whole blood, which has been implicated in cases of human exposure to phosphine has been studied [5, 6, 19-25].

1.1 HUMAN EXPOSURES & PUBLIC HEALTH SIGNIFICANCE

Phosphine released from metal phosphide tablets is used as an agricultural fumigant around the world. It is useful as a nonspecific pesticide for food and materials storage; when used correctly, phosphine is produced and decomposes slowly over time in a sealed container, ultimately leaving no toxic products behind. Under normoxic conditions (O_2 = 21%) in moist air, phosphine eventually oxidizes to phosphoric acid [26]. The sale of metal phosphides is restricted in the United States but they are easily available to consumers in many countries [27-29]. The OSHA permissible exposure limit (PEL) for phosphine gas (PH_3) is 0.3 ppm over an 8-hour work day and the NIOSH immediately dangerous to life or health level (IDLH) is 50 ppm [2]. Immediately obvious symptoms of acute phosphine exposure include drowsiness, vomiting, ataxia, and cyanosis, followed by clinically determined effects including hypotension, tachycardia, pulmonary edema, and cardiac failure [2, 25, 30].

In 1980, Wilson and colleagues reported that 1% of known occupational exposures to phosphine occur on ships [31]. During storage and transport on ships, grain products are often fumigated with metal phosphides. Ideally, this fumigation occurs under properly ventilated conditions, but workers on ships are particularly vulnerable to exposure because of their confined environment. The authors report an incident in 1978 in which 29 out of 31 crew members were sickened and one child died after phosphine exposure due to a leaky fumigation hold [31]. Phosphine exposure is still a risk to freight workers; a 2020 study of Belgian and French maritime workers showed that the rate of occupational exposure to phosphine has been steadily increasing since 2000 [32].

In North America, most human exposures to phosphine are accidental and occupational. In 2014, 80% of California's reports of phosphine exposure occurred in the agricultural industry [30].

These exposures are often attributed to mishandling of and/or accidental release from metal phosphide pellets. For example, in 2013, a pistachio silo containing aluminum phosphide was damaged during a storm. The phosphide became wet, phosphine gas was released, and 10 workers were hospitalized for signs of phosphine exposure. Six out of ten showed signs of respiratory distress [33]. Phosphine gas is also a byproduct of clandestine methamphetamine production. Phosphine exposure and poisoning is reported among methamphetamine producers and first responders in the US [34-36]. Other exposures to phosphine in North America are related to residential fumigation [37-40]. While sale of metal phosphides is limited in the US, they are still accessible for both professional and amateur household pest control. In a tragic but characteristic case in Texas in 2017, a man spread metal phosphide pellets under his family's mobile home to address a pest problem. In response to the garlic-like odor of the pellets, he attempted to wash them away with water. This produced more phosphine gas and unfortunately, four children died and one woman was sickened after inhaling phosphine inside the home. The man had reportedly received the metal phosphide pellets in an unlabeled container from a friend [38].

Globally, most cases of phosphine poisoning occur in India and the Middle East [41-43]. Phosphine exposure accounted for 8% of all-cause mortality and at least 65% of all poisonings in India during the early 2000s [42]. While some of these exposures are accidental in nature and similar to those reported in North America, many are purposeful. Over the past 40 years, the global suicide rate has risen by 60% [43]. Of nearly 800,000 annual suicides, 79% occur in low-and middle-income countries. While the global suicide rate is 10.5 out of 100,000, India's is 16.5 and reaches 24 in some states [44, 45]. Intentional poisoning is the third most common route of suicide in Iran and phosphine was implicated in 81% of self-poisonings from 2011 to 2015 [46]. These suicides are part of an epidemic of farmer suicides in response to socioeconomic

disenfranchisement in the Middle East and India [42, 45]. Many of these suicides occur through the ingestion of agricultural chemicals including organophosphorus pesticides and metal phosphides, which are easily accessible in the countries with the highest rates of their use for suicide [42-44, 46, 47]. Suicide by phosphine is significantly correlated to low socioeconomic conditions including illiteracy and financial instability [42]. In a typical suicide case, the victim ingests metal phosphide tablets, which, depending on freshness, contain 1-3 grams of metal phosphide [1, 21, 42]. 1-2 tablets can produce a fatal dose of phosphine when ingested [21, 27, 48]. The pellets react with saliva and hydrochloric acid in the stomach and produce phosphine gas, which can be inhaled or absorbed through the gastrointestinal tract [21, 27]. Death from phosphide ingestion typically occurs 12-24 hours after exposure [2]. If the victim is taken to the hospital, they receive supportive care, as no antidote is currently available [10, 27]. Supportive measures are administered based on symptoms and typically consist of supplemental oxygen, and permanganate, bicarbonate, vegetable oil, and/or activated charcoal lavage [13, 49]. Supportive care yields inconsistent success; reports of mortality from the ingestion of metal phosphides ranges from 45-90% [48, 50].

Phosphine and metal phosphides are listed as Chemicals of Interest (COI) by the US Department of Homeland Security under the Chemical Facility Anti-Terrorism Standards regulation. This designation is due to the toxicity, reactivity, and accessibility of metal phosphides and (subsequently) phosphine [51]. Thus, there is much interest (worldwide) in developing a fast-acting antidote that would be useful in both individual and mass acute poisonings.

1.2 PHOSPHINE CHEMISTRY & TOXICITY

Phosphine, or "phosphane" (IUPAC) is a trigonal pyramidal molecule consisting of one phosphorous atom bonded to three hydrogen atoms (Figure 1). It is a gas under standard conditions and has a relative vapor density of 1.17 [48, 52]. Phosphine is produced by the reaction of metal phosphides with water or acids as shown in Equation 1. Metal phosphides are sold as solid tablets, typically AlP, Ca_3P_2, Mg_3P_2, or Zn_3P_2. Phosphine is frequently associated with a fishy or garlic-like odor but the gas itself is odorless [53]. The pungent smell is due to the reaction of impurities and formation of other phosphate species including H_4P_2 [54, 55].

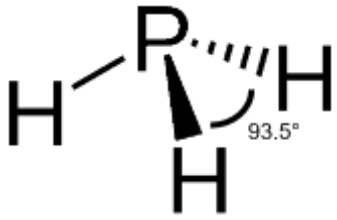

Figure 1. Chemical structure of phosphine.

$$Ca_3P_{2(s)} + 6\ H_2O_{(l)} \rightarrow 2\ PH_{3(g)} + 3\ Ca(OH)_{2(s)} \quad (1)$$

$$AlP_{(s)} + 3\ H_2O_{(l)} \rightarrow PH_{3(g)} + Al(OH)_{3(s)} \quad (2)$$

Equation 1. Phosphine production via hydrolysis of metal phosphides.

Reactions of two common metal phosphide salts used to produce phosphine gas through hydrolysis. (1) Calcium phosphide, (2) Aluminum phosphide.

Phosphine is oxidized to phosphoric acid through a series of intermediates (Equation 2). The first intermediate, phosphinous acid (H_3PO), is thermodynamically unstable and has in fact never been observed in the study of phosphine *in vivo* [26]. H_3PO has been isolated for spectral

analysis through the reaction of phosphine and ozone at very low temperature (12-18 K) in solid argon but is otherwise considered transient [56]. However, this intermediate is notable because in a 2011 review of phosphine toxicity, Nath and colleagues posit that phosphinous acid may in fact be the toxicant responsible for phosphine poisoning [57]. None of the other resulting oxo-phosphorous compounds have shown any toxicity commensurate with phosphine.

$$\underset{\text{Phosphine}}{PH_3} \xrightarrow{[O]_{(aq)}} \underset{\text{Phosphinous Acid}}{H_3PO} \xrightarrow{[O]} \underset{\text{Phosphinic Acid}}{H_3PO_2} \xrightarrow{[O]_{(aq)}} \underset{\text{Phosphorous Acid}}{H_3PO_3} \xrightarrow{[O]_{(aq)}} \underset{\text{Phosphoric Acid}}{H_3PO_4}$$

Equation 2. Oxidation of phosphine to phosphoric acid.

Specific dose and toxicity information (i.e. LD_{50}, LC_{50}) for phosphine and metal phosphides is not well-documented. Human data is collected retrospectively and mostly published through individual case reports. Exposure to metal phosphide tablets through ingestion is often reported as a mass of tablets consumed. However, phosphine production by metal phosphide tablets varies by tablet type [58], freshness [1, 50], particle size [1], and the ratio of active phosphide to other inert ingredients in the tablets [27, 42]. Generally for humans, survival is unlikely after the ingestion of 1.5-2 g of metal phosphides [59] but 150-500 mg ingested AlP is also reported as a lethal dose for adults [10, 24, 27]. Based on this information, the lethal dose for AlP ingestion for a 70 kg adult ranges from 2-28 mg/kg. In 2004, Dua and Gill [3] found the LD_{50} for AlP ingestion in rats to be 10 mg/kg and the LD_{100} to be between 15-25 mg/kg. Based on Dua and Gill's data [3], Anand and Colleagues [60] found that 20 mg/kg was an effective LD_{100} for AlP ingestion in rats. A 1997 publication by the International Programme on Chemical Safety reports that the LD_{50} for the ingestion of zinc phosphide in rats ranges from 2.9-40.5 mg/kg [61].

Inhalational phosphine exposure also depends upon characteristics of the source (e.g. metal phosphides vs purified gas), environmental conditions including ventilation, and duration of exposure [53, 58, 62, 63]. In reports of occupational exposure, exact phosphine concentrations are rarely reported but can be estimated from post-incident air sampling and records of metal phosphide use (i.e. mass reacted). A report of occupational phosphine exposure onboard a bulk grain carrier in 2008 [64], in which one worker died and others were sickened, estimates a peak phosphine concentration of 700 ppm in both a leaky fumigation chamber and the surrounding cabins. This estimate is based on the amount of aluminum phosphide used for fumigation: 1.5 g/m^3 which the authors report to be a common amount used in grain fumigation. The true exposure concentration is not known and may not actually have been 700 ppm; the air was not sampled quantitatively until two days after workers became ill and hours after cabin ventilation. From this sampling, the authors report a concentration of 0.24 ppm PH_3 outside of the fumigation chamber and "a trace" in the cabins [64]. A 1988 occupational health study of Indian agricultural fumigators found concentrations between 0.17 and 2.11 ppm PH_3 in their working environments [65]. The NIOSH IDLH for phosphine is 50 ppm and the NIOSH acute exposure guidelines (AEGL) suggest that concentrations as low as 4 ppm can result in serious effects and impair the ability to escape after just 10 minutes [53]. Exposure to 7.2 ppm for 10 minutes is considered life-threatening [53]. In a 2007 report, Assem & Takamiya [58] tabulated human exposure data and occupational standards and found that exposure to over 100 ppm PH_3 was associated with severe outcomes 30-60 min after exposure and exposure to over 400 ppm PH_3 was associated with death within 30-60 min. They also reported that the LC_{50} for rats is 1057 ppm for 35-50 min exposures, 498 ppm for 65-75 min, and 11 ppm for 4 hours [58]. Waritz and Brown found the rat LC_{50} for a 4 hr PH_3 exposure to be 8 ppm [66]. In 2017, Wong and colleagues [67] published a detailed study of

phosphine toxicity in rats. They found that phosphine exhibits a steep dose-response curve between 15000 and 30000 ppm·min with an LCt_{50} (concentration·time value associated with 50% mortality within 24 hours) of 23270 ppm·min [67]. As in humans, toxicity data for phosphine in rodents is varied and inconsistent (Table 1). Phosphine toxicity varies in different species of insects; the dose-response relationship is not linear and varies by the duration of exposure [62, 68]. In a 1969 study, Bond and colleagues [68] exposed insects to phosphine gas and monitored the phosphine concentration in the chamber over time by gas chromatography. Roaches (*Periplaneta americacna*) exhibited visible toxicity (decreased voluntary movement, muscle spasms) after 10 minutes of exposure to 500 ppm, which advanced to death (or non-recovery) between 3 and 5 hours of exposure [68]. In the same study, 24-hr LC_{100} values were determined to be at most 1380 ppm for mealworms (*Tenebrio molitor* larvae) and at most 1340 ppm for flour beetles (*Tribolium confusum*) under normal aerobic conditions [68]. In insects (at least), acute phosphine toxicity is dependent on available oxygen [59, 62, 63, 69] and is ineffective under anaerobic conditions [68]. Phosphine resistance has also been reported in insects, including Lepidoptera species [70, 71]. In a study of three Coleoptera species, Pimentel and colleagues [71] found that resistant organisms had LC_{95} values above doses recommended for insecticidal use. Phosphine resistance in insects is correlated with lowered respiration and active exclusion [71], though the exclusion mechanism is not clear and is not mediated by spiracle modification [68, 71]. To adjust for these factors, phosphine/phosphide insecticides are often used at a discriminating dose, or a dose expected to kill all susceptible insects. In their study of phosphine resistance in Coleoptera and Lepidoptera, Gautam and colleagues [70] reported a 20 hour exposure to 98.7 ppm PH_3 to be a discriminating dose.

In summary, phosphine toxicity is difficult to compare between species because of the diversity of exposure parameters but available data shows that humans are sensitive to gaseous phosphine at lower levels than rodents [58, 61] and insects [68] but are similarly sensitive to phosphine poisoning from metal phosphide ingestion [3, 10, 24, 27, 60].

Table 1. Available toxicity data for phosphine and metal phosphides.

Form	Organism	Route	Duration	Dose (mg/kg)	Concentration (ppm, v/v)	Concentration (ppm·min)	Effect	Ref.
AlP	Human*	Ingestion		2-28			LD	[24, 27, 59]
Zn_3P_2	Rat	Ingestion		2.9-40.5			LD_{50}	[61]
AlP	Rat	Ingestion		10			LD_{50}	[3]
AlP	Rat	Ingestion		15-20			LD_{100}	[3, 60]
$PH_{3(g)}$	Human	Inhalation			50		IDLH**	[72]
$PH_{3(g)}$	Human	Inhalation	10 min		7.2	72	AEGL3***	[53]
$PH_{3(g)}$	Rat	Inhalation	10-40 min			23270	LCt_{50}	[67]
$PH_{3(g)}$	Rat	Inhalation	4 hr		8-11	2640	LC_{50}	[58, 66]
$PH_{3(g)}$	Rabbit	Inhalation	25-30 min		500	12500	LD_{100}	[61]
$PH_{3(g)}$	Rabbit	Inhalation	4 hr		200	48000	LD_{100}	[61]
$PH_{3(g)}$	Coleoptera, Lepidoptera	Inhalation	20 hr		98.7	118800	Discriminating dose	[70]
$PH_{3(g)}$	Roach	Inhalation	3-5 hr		500	90000	LD_{100}	[68]
$PH_{3(g)}$	Mealworm	Inhalation	24 hr		1380	1987200	LD_{100}	[68]
$PH_{3(g)}$	Flour beetle	Inhalation	24 hr		1340	1929600	LD_{100}	[68]

*Collected from published reviews of phosphine poisoning, retrospective estimates based on patient or family reports.
** Immediately Dangerous to Life or Health limits are determined by NIOSH and OSHA to be an airborne concentration likely to immediately cause death, permanent adverse health impacts, or impair the ability to escape [72].
***Acute Exposure Guideline Level 3, reported by the National Oceanic and Atmospheric Administration, is the airborne concentration above which serious health effects or death are possible [73].

Phosphine is an inhibitor of mitochondrial respiration; it prevents oxygen consumption and ATP synthesis through the inhibition of the mitochondrial electron transport system (Figure 2) at complex IV, cytochrome *c* oxidase [3, 59, 74-78]. Normally, cytochrome *c* oxidase reduces oxygen to water through the oxidation of the electron carrier cytochrome *c*, which transfers electrons between complex III and complex IV via a heme-iron(II/III) binding site (Equation 3). Cytochrome *c* oxidase is responsible for oxygen consumption or "turnover" during respiration and

contributes to the proton gradient essential to ATP synthesis. When complex IV is inhibited, oxygen consumption and ATP synthesis slow and cytochrome *c* remains reduced.

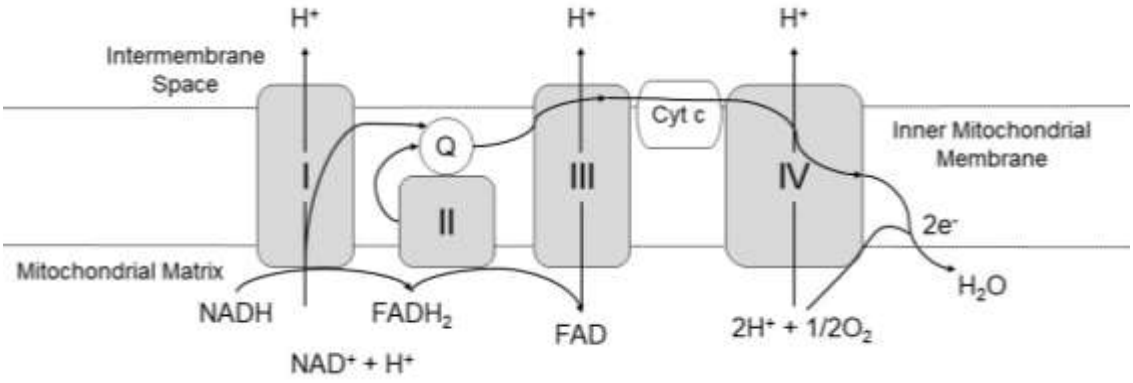

Figure 2. The mitochondrial electron transport system.

$$4\ Fe^{2+}\ \text{cytochrome}\ c + O_2 \rightarrow 4\ Fe^{3+}\ \text{cytochrome}\ c + H_2O$$

Equation 3. Reduction of oxygen to water by mitochondrial complex IV via the oxidation of cytochrome *c*.

1.2.1 Uncertainty in the mechanism of toxicity

Phosphine poisoning is associated with mitochondrial dysfunction characteristic of cytochrome *c* inhibition. Much of the early data on phosphine's mitochondrial activity comes from insect models, likely due to its popularity as an insecticide. A 1976 study by Chefurka et al. [74] reports that phosphine inhibits mitochondrial respiration in two species of insects and in mice. The authors noted that mitochondrial uncouplers do not improve respiration after phosphine exposure, which suggests a direct impact on the electron transport system. They also reported that cytochrome *c* oxidase is likely the specific target for phosphine toxicity [74]. This is one of many phosphine studies that report consistent mitochondrial inhibition across species and even phyla

[41, 60, 63, 67, 79]. Anand and colleagues reported structural damage to mitochondria including a 70% loss of functional cytochrome *c* in the liver tissue of mice exposed to phosphine [60] and Bumbrah and colleagues reported a 70% reduction in respiration and hypoxia-related organ damage in human patients exposed to phosphine via metal phosphides [41]. This mechanism may be similar to those of other complex IV inhibitors like cyanide and azide [15, 16, 79]. Also, like cyanide and azide, many of the effects of phosphine poisoning in humans reflect the inhibition of the electron transport system. These include cyanosis, reduction in cardiac output, respiratory distress, and pulmonary edema [2, 30, 42]. Death in cases of phosphine poisoning is usually attributed to heart failure resulting in cardiac arrest [41, 57, 58, 80].

While a wealth of data suggests that phosphine inhibits cytochrome *c* oxidase and it is widely regarded as a mitochondrial poison [3, 59, 74-77, 79], its entire mechanism of toxicity is not fully understood. It is known that phosphine toxicity is dependent upon environmental oxygen concentration in a positive but nonlinear correlation [7, 60, 63, 68]. Researchers have reported decreased respiration in humans and animals exposed to phosphine [41, 63]. Other groups have reported a lack of change in respiration in insect models exposed to phosphine but this has been correlated with population resistance [63, 81].

It has also been suggested that phosphine's toxicity is primarily due to oxidative damage through the generation of radical oxygen species [23, 59, 69, 82] and lipid peroxidation and/or protein interaction [7, 9, 57], perhaps leading to the breakdown of vascular tissue [49]. However, radical oxygen species and their indicators do not necessarily cause toxicity [83-85]. Lipid peroxidation and metabolic acidosis have indeed been reported in cases of phosphine poisoning and oxidative damage is frequently claimed to be associated with dysfunction of the electron transport system [20, 50, 67, 86, 87]. While the supportive treatment of metabolic acidosis using

sodium bicarbonate and potassium permanganate, typically used to oxidize phosphine to phosphate, is often recommended for phosphine poisoned patients [5, 11, 24, 27], little evidence exists to suggest that this significantly increases survival [13, 27]. Phosphine itself is a strong reductant, so oxidative damage, if important, is likely due to an indirect or secondary mechanism [20, 21, 88].

1.2.1.1 Potential impacts on blood

The oxidation of the iron atom in hemoglobin from Fe^{2+} to Fe^{3+} (methemoglobinemia) and red blood cell (RBC) lysis (hemolysis) have been reported in cases of phosphine poisoning in humans [5, 19, 20, 24, 25]. Methemoglobinemia has been negatively associated with survival in phosphine-poisoned patients; a 2011 case study by Mostafazadeh and colleagues reports a significant relationship between elevated methemoglobin level upon hospital admission and death from phosphine poisoning [20]. Methemoglobin levels of up to 46% have been reported in cases of phosphine poisoning [5, 24]. Methemoglobinemia due to other causes, however, is only associated with mortality at levels over 70% [89]. The concentration of ferrous hemoglobin (Fe^{2+}) in the blood is well maintained and blood typically contains less than 2% methemoglobin. Methylene blue, which accelerates NADPH methemoglobin reductase, is a common treatment for methemoglobinemia [88, 89]. A 2000 study in rats showed that methylene blue lavage improved outcomes after phosphine exposure [23]. However, it has not been widely studied against phosphine poisoning in humans and as of this writing has only been successfully used in human patients once [24, 25, 89]. Blood transfusion with fresh-packed red blood cells has recently been shown to improve outcomes from phosphine poisoning in rats [87]. In humans, however, data on whole-blood transfusion against phosphine poisoning is sparse [5, 6].

It is unclear if the observed methemoglobinemia and hemolysis are directly related to phosphine toxicity or if they are secondary symptoms [69, 88]. Additionally, it is not known if (or how) they are related to each other. Hemolysis and methemoglobinemia often appear together [88, 89]; RBCs containing methemoglobin are prone to rupture, which releases free ferric (Fe^{3+}) heme, which can induce hemolysis in other RBCs [90, 91]. On the other hand, free ferrous heme from ruptured RBCs is quickly oxidized to Fe^{3+} [90, 92]. These impacts do not appear uniformly in cases of phosphine poisoning and they are not always observed together or at all [19, 21, 22, 27, 69]. A 2016 case study of 50 patients presenting with acute phosphine poisoning found that only 8 had both methemoglobinemia and hemolysis, 3 had methemoglobinemia alone, and 3 had hemolysis alone [22]. Further, methemoglobinemia is associated with some oxidizing medications such as potassium permanganate, given to promote oxidation of phosphine to phosphite/phosphate in the gastrointestinal tract, and methemoglobinemia has indeed been observed in phosphine-poisoned patients after treatment with permanganate salts [19, 24, 93]. We are interested in characterizing the relationship between phosphine and blood because if phosphine indeed directly induces hemolysis or methemoglobinemia, it may impact the efficacy of our antidotes and change the required delivery method (i.e. exposure concentration may have to be reduced before reaching the blood stream).

Very little data is available on phosphine pharmacokinetics and biomarkers of exposure have yet to be determined. In fact, as of this writing, no formal studies have been conducted of phosphine absorption and distribution *in vivo*. Biomarkers of increased cardiac stress and respiratory failure have been reported in studies of phosphine poisoning [67, 69, 94] but cannot be correlated to exposure or effective dose in absence of a known toxicokinetic scheme. To delineate this scheme is outside the scope of this project. In the absence of a better understanding of the

complete toxic mechanism, we adopted the practical approach of selecting candidate antidotes with the intention of reducing circulating levels of phosphine *in vivo*.

1.3 POTENTIAL ANTIDOTES TO PHOSPHINE POISONING

Generalized supportive care is not necessarily enough to ensure positive outcomes for victims of phosphine poisoning [27, 41]. Fast-acting antidotes that can be administered after or during phosphine exposure are essential. A prophylactic antidote may be of some use in an occupational setting, but an antidote to be administered after the start of exposure would be useful in the majority of phosphine poisonings [95, 96]. The line, however, between prophylactic and therapeutic antidote is ambiguous in many cases of phosphine poisoning for the following reasons. As previously mentioned, ingested phosphide tablets produce phosphine gas in an ongoing reaction. In these cases, phosphine exposure can last for hours [23, 97]. This means that if given in time after ingestion, a nominally "prophylactic" antidote may prevent cumulative exposure and subsequent toxicity. In the absence of definitive knowledge of mechanism, possible approaches to phosphine antidote development are limited, which presents a crucial barrier to progress. Regardless of the ultimate toxicity mechanism, a decorporating/scavenging antidote may be beneficial for preventing phosphine poisoning. A decorporating agent reduces the circulating level of a toxicant and binds the toxicant ligand with high affinity, forming a stable and non-toxic adduct to be excreted [15, 16]. Ideally, scavenging occurs in the bloodstream and prevents the toxicant from reaching the target site(s) [15]. Decorporation is characterized by high binding affinity (K_{eq}) between a toxicant ligand and antidote [14-16]. Using a decorporating approach, we have identified transition-metal based compounds that successfully ameliorate cyanide and azide

toxicity in both an insect and mouse model [14, 15, 98]. We have utilized spectroscopic and respirometric methods to confirm that these candidate antidotes reduce the inhibition of cytochrome *c* oxidase and bind the toxicant ligands at reasonable rates and with relatively high affinity [15, 98].

Phosphine is easily polarized and is characterized as a "soft" ligand according to Pearson's hard-soft acid-base theory [99]. According to this principle, phosphine will bind to a "soft" metal with high affinity [17, 18, 99]. Gold(I) and silver(I) are among the softest metals [18, 99, 100] so may be useful as decorporating agents against phosphine toxicity. Additionally, many Au(I) and Ag(I) salts are known to be safe to humans; they are used in a variety of medical applications including the treatment of rheumatoid arthritis and bacterial infections [100-107]. Based on this knowledge, a variety of Au(I) and Ag(I) compounds were screened against phosphine toxicity in an insect and mouse model. Additionally, some cobalt(II/III) compounds that have been shown to be effective against cyanide and azide [14, 15, 98], were also screened as controls. These were not expected these to be very effective at decorporation based on Pearson's hard-soft acid-base series [18, 99].

1.3.1 Gold(I) Complexes

Gold(I) is the softest metal in Pearson's hard-soft-acid base series [99]. Au(I) is biologically active and has a variety of medical uses; it has been used in the treatment of rheumatoid arthritis for over 90 years [108]. The cation itself is unstable and can be oxidized to more toxic forms. However, when paired with "soft", polarizable ligands, Au(I) is fairly stable and has relatively low toxicity. Most Au(I) used in medicine is coordinated to ligands including thiol groups and phosphines, which help to prevent oxidation from Au(I) to highly toxic Au(III) [101,

108, 109]. We selected three Au(I) complexes with established safety in humans to screen as candidate antidotes to phosphine: Au(I) thiosulfate, Au(I) thioglucose, and Au(I) thiomalate (Figure 3).

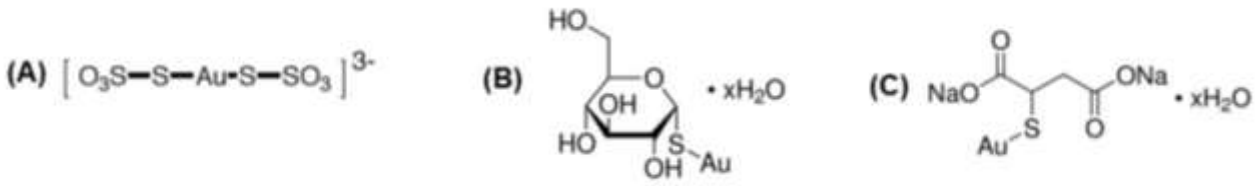

Figure 3. Candidate phosphine antidotes: Au(I) compounds.

Structures of Au(I) complexes tested against phosphine. (A) Au(I) thiosulfate, anion; (B) Au(I) thioglucose, (C), Au(I) thiomalate, disodium salt.

All of these candidate antidotes have been or are currently used as treatments for rheumatoid arthritis [108, 110-113] and the sodium salt of Au(I) thiosulfate was used historically as a treatment for tuberculosis [114, 115]. The anti-inflammatory mechanism of these Au(I) compounds is not fully understood but seems to be the result of diverse mechanisms. Au(I) compounds used against rheumatoid arthritis have been shown to inhibit the production of prostaglandins, interfere with the compliment cascade, and inhibit other pro-inflammatory enzymes [116]. The adverse effects of long-term treatment with Au(I) compounds include dermatitis, oral ulcers, and proteinuria. Other, more severe side effects including interstitial lung disease and liver toxicity have been reported but are quite rare. Again, these effects are associated with chronic exposure to Au(I) compounds [100, 116] and resolve when exposure is discontinued. Because of Au(I)'s affinity for soft ligands, low acute toxicity, and established use in humans, we proposed Au(I) thiosulfate, Au(I) thioglucose, and Au(I) thiomalate as potential decorporating antidotes to phosphine poisoning.

Gold is notoriously expensive. Currently, the aforementioned Au(I) compounds cost between $130 and $598 per gram [117-119]. While we expected Au(I) to be effective against phosphine poisoning, we searched for alternatives that may be less expensive to produce and obtain.

1.3.2 Silver(I) Complexes

We identified five readily available Ag(I) compounds that may also be effective antidotes against phosphine. Ag(I) is also among the softest ligands in Pearson's hard-soft-acid-base series and has strong affinity to other soft ligands [18, 99, 105]. Ag(I) compounds also boast established use in humans; many are antimicrobial and anti-inflammatory agents [105, 106]. In fact, in a 2014 paper, Barillo and Marx speculate that "there are few, if any compounds in contemporary medical practice with as lengthy a history as silver" [106]. We identified five Ag(I) compounds to screen against phosphine in an insect model: Ag(I) lactate, Ag(I) nitrate, Ag(I) bis(metronidazole)nitrate, Ag(I) thiosulfate, and Ag(I) sulfadiazine (Figure 4).

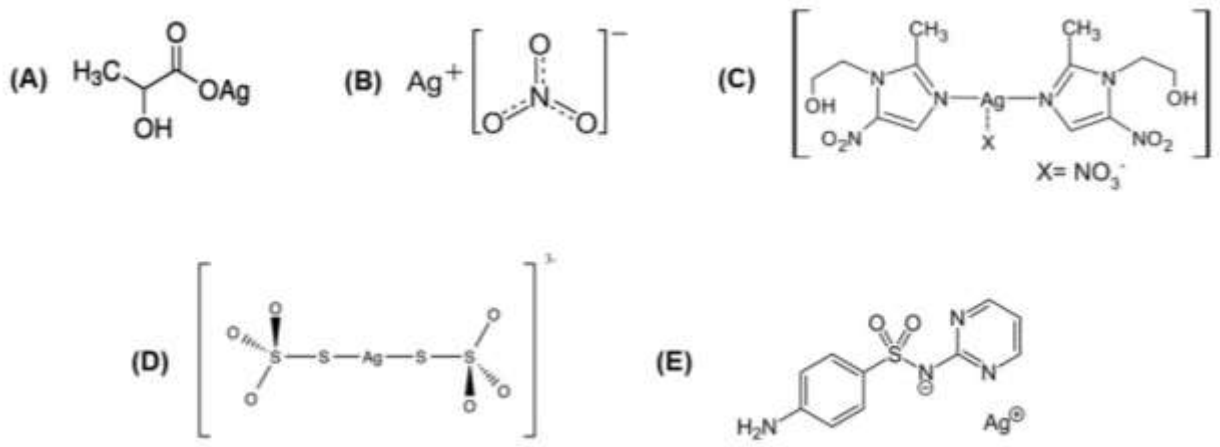

Figure 4. Candidate phosphine antidotes: Ag(I) compounds.

Structures of Ag(I) complexes tested against phosphine. (A) Ag(I) lactate, (B) Ag(I) nitrate, (C) Ag(I) metronidazole nitrate [120], (D) Ag(I) thiosfulate, (E) Ag(I) sulfadiazine.

Ag(I) lactate, Ag(I) nitrate, Ag(I) bis(metronidazole), and Ag(I) sulfadiazine are useful antimicrobials and Ag(I) sulfadiazine has been on the World Health Organization's List of Essential Medicines since 1987 [105, 121]. Ag(I) thiosulfate is used to inhibit ethylene production in plants and is found in the environment as a waste product of photographic film manufacturing [122]. It has not been assessed for medical use in humans but its toxicity in other organisms is low compared to other Ag(I) compounds, especially Ag(I) nitrate [123, 124]. The Ag^+ ion is responsible for these compounds' antimicrobial activity; it damages cell membranes and enzymes through protein interactions and is effective at very low concentrations. Sensitivity to the Ag^+ ion is related to genetic factors and rates of intracellular uptake; bacteria and fungi are more sensitive to the ion than mammalian cells [125, 126]. These compounds are associated with a variety of adverse effects, mostly cosmetic; Ag(I) nitrate stains the skin upon contact and chronic ingestion of Ag(I) compounds leads to systemic skin discoloration [126-128].

Overall, Ag(I) compounds have very low solubility in aqueous solutions. They are even less soluble in saline solutions, including the physiological fluids of many organisms [105, 129]. Silver is known to precipitate and accumulate in tissues and in the later 20th century, the use of oral Ag(I) drugs was reduced and substituted for other antibiotics [105, 123, 127]. Currently, most Ag(I) pharmaceuticals are applied dermally and used to treat skin conditions including severe burns [106]. Ag(I)'s low solubility may prove challenging for drug delivery and effectiveness, but is unlikely to endanger health upon acute exposure [106]. We selected candidate antidotes that can be dissolved in physiologically-appropriate buffers (with and/or without additional solubilizing agents as described in MATERIALS). Based on Ag(I)'s softness, solubility, and toxicity, we anticipated that the Ag(I) compounds would prove somewhat useful against phosphine poisoning but be less effective than Au(I). However, if effective at ameliorating phosphine toxicity, they may prove beneficial over Au(I) compounds based on their lower price point.

1.3.3 Cobalt(II) Complexes

Our group has identified and screened cobalt-containing candidate antidotes to other complex IV inhibitors [14-16, 130]. These cobalt-based macrocycles have proven effective against cyanide and azide toxicity in a variety of models, *in vitro* and *in vivo*. These antidotes work through decorporation, binding cyanide or azide ligands to the central cobalt with high affinity [15, 16]. These candidate complexes are based on the structure of hydroxocobalamin (Cb) (Figure 5A), an approved antidote to cyanide poisoning that binds one cyanide ligand to a central Co(III). Cb is indeed effective against cyanide, but is expensive and not shelf-stable in a useful form. It is not well-suited for use in a mass-casualty situation [14, 15]. Thus, we proposed smaller, less expensive antidotes to cyanide and azide based on the Cb structure. CoN_4[11.3.1] (Figure 5B) has been shown

to ameliorate cyanide and azide toxicity in animal models [14-16]. We have established toxicity data for these compounds in two animal models, *G. mellonella* larvae and mice [14-16, 131]. While none of these compounds were expected to lessen phosphine toxicity, (Co(II/III) is not considered a very soft metal and is unlikely to bind phosphine with strong affinity [18, 99]), it was thought that they might serve as good controls in the animal models.

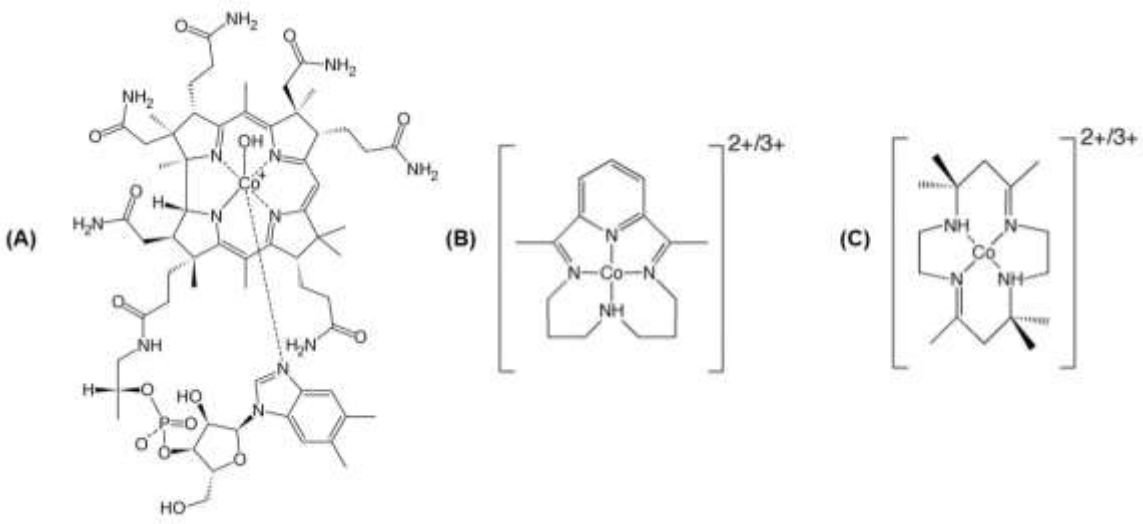

Figure 5. Candidate Phosphine Antidotes: Co(II/III) compounds.

Structures of Co(II/III) complexes tested against phosphine. (A) Hydroxocobalamin, (B) CoN_4[11.3.1] (Cobalt(II)2,12-dimethyl-3,7,11,17-tetraazabicyclo-[11.3.1]-heptadeca-1(17)-2,11,13,15-pentaenyl dibromide) (C) CoN_4[14] (5,7,7,12,14,14-Hexymethyl-1,4,8,11-tetraazacyclotetradeca-4,11-dienyl cobalt (II) dibromide dehydrate).

1.4 EXPERIMENTAL MODELS

We screened and tested the potential antidotes in two animal models, larvae of the greater wax moth, *Galleria mellonella*, and mice. *G. mellonella* larvae are used in fungal and bacterial study owing partly to their melanin-linked immune system with allows for visible infection

monitoring [132-136]. Our group has successfully utilized this insect model to identify and screen potential antidotes to other mitochondrial poisons that were subsequently found to be effective in mice [131]. These models are comparable for mitochondrial study because cytochrome *c* oxidase, the likely target of phosphine, is nearly identical between the two models [131]. Both models exhibit visible signs of toxicity (immobilization) when exposed to the other complex IV inhibitors azide and cyanide [131]. While mice have a closed circulatory system and an oxygen carrier (hemoglobin), *G. mellonella* larvae have an open circulatory system that lacks an active oxygen carrier. Instead, oxygen diffuses through the body cavity. The main body cavity is called the hemocoel and is washed in a lipid and mitochondria-rich substance that makes up an organ called the fat body. This model allows us to study phosphine toxicity without potential interference from hemoglobin (see section 1.2.1.1). In addition to whole-organism study, we utilized mitochondrial particles isolated from the fat body to study the action of phosphine on respiration *in vitro*. *G. mellonella* are an advantageous model because they are inexpensive (~$20 for 250 caterpillars) and have no special housing or food requirements. By using this model for preliminary antidote screening, we were able to collect hundreds of data points without sacrificing hundreds of mice. From reported toxicity data (see Table 1), insects appear to be more resistant to phosphine than mammals. This may require modulation of exposure conditions between models.

We identified promising candidate antidotes based on their efficacy in the insect model then tested them in mice. This model translates more closely to human physiology and allows us to study phosphine and potential antidotes in a circulatory environment more closely aligned with that of humans and in the presence of hemoglobin. To determine if phosphine's impacts on blood were relevant to antidote development, we compared antidote effectiveness between insects and mice. We also performed whole-blood experiments to determine if phosphine directly induces

hemolysis or methemoglobinemia and studied the blood of phosphine-exposed mice for indicators of these impacts.

1.5 SCOPE OF DISSERTATION AND STATEMENT OF HYPOTHESES

Phosphine gas (PH_3), typically released by the hydrolysis of metal phosphide salts, is responsible for more human poisonings (accidental and deliberate) worldwide than any other pesticide. In the US, phosphides (particularly of aluminum and zinc) are legally available from many commercial outlets for use as insecticide/rodenticide fumigants. The pellets release phosphine gas upon reaction with aqueous media and could conceivably be deployed as weapons. An antidote to phosphine/phosphide poisoning remains to be identified. Under non-laboratory conditions, lethal exposures to phosphine have invariably occurred over a duration of minutes to several hours, either through inhalation/ingestion of dispersed particulate phosphides or inhalation of phosphine gas in confined spaces. Phosphine (PH_3) is comparably soluble in lipids and aqueous media, so in addition to phosphide particulates in the airways and esophagus, accumulation of PH_3 in tissues can be expected to result in an ongoing phosphine exposure even though the victim may have been separated from the source. It follows that a decorporating approach should be of considerable value as a countermeasure to phosphine poisoning. We propose such an approach using metal-ion complexes chosen to have greater affinity for phosphine than any biological ligands present.

This work is a proof-of-concept study in early-stage drug development and aims to identify lead compounds that show efficacy against phosphine in animals. Funding was through the NIH CounterACT program, which primarily supports research into countermeasures to terrorism

resulting in mass-casualty events. Acute mass-exposures to phosphine would likely occur through inhalation and modeling exposure through ingestion falls outside the scope of the work. Some insights into phosphine's toxicity mechanism have been serendipitously discovered but not further developed as again, these lines of inquiry were outside of the scope of the funded project.

Aim 1. To determine if some univalent gold and related complexes are antidotal toward phosphine in mice. Some commercially available gold(I) complexes and similar silver(I) compounds will be screened for antidotal activity in an insect model and those exhibiting significant antidotal activity toward phosphine will be further tested in mice. **Hypothesis:** All phosphanes, including phosphine, are "soft" ligands according to Pearson's classification. They have higher affinity for soft cations like gold(I) and silver(I) than other "harder" ligands like the nitrogen-, oxygen-, sulfur-donors found in biological systems. Consequently, the proposed gold(I)/silver(I) antidotes should efficiently scavenge phosphine in animals, protecting the mitochondria. **Approach:** Unanesthetized mice will be exposed to phosphine generated by hydrolysis of aluminum or calcium phosphide (AlP, Ca_3P_2). The putative antidotes will be given either before or after toxicant exposure. Sub-lethal (pole climbing) assessments of the effectiveness of putative antidotes will be undertaken.

Aim 2. To show that phosphine causes methemoglobinemia and/or hemolysis in mice. Hemolysis and methemoglobinemia have repeatedly been reported in conjunction with phosphine/phosphide exposure but the extent and possible significance of this has not been recognized by many authors. Recently, blood transfusions have been shown to be helpful in remediating phosphine poisoning. **Hypothesis:** Exposure to phosphine results in methemoglobinemia and/or hemolysis and phosphine antidotes may protect against these conditions. **Approach:** Drawn blood samples from phosphine-challenged mice (with and without

potential antidotes) will be analyzed spectroscopically to assess methemoglobinemia, hemolysis, and verify protection of hemoglobin from phosphine-dependent damage.

2.0 MATERIALS AND METHODS

2.1 MATERIALS

All chemicals, unless otherwise stated, were ACS grade, purchased from Sigma-Aldrich or Fisher and used without further purification. Aluminum phosphide (AlP) was purchased from American Elements and argon gas (99.998%) was purchased from Matheson.

Phosphine gas was generated with the reaction of either calcium phosphide (Ca_3P_2) with sulfuric acid (H_2SO_4) or AlP with excess PBS (pH 7.4). For animal exposure models, 20 mL of 1.2 M H_2SO_4 was mixed with ~0.5 g Ca_3P_2 or 20 mL PBS was mixed with ~0.5 g AlP in a closed chamber (4.8 L volume). Time-dependent phosphine production was observed by infrared spectroscopy at 2325 cm^{-1} using a Thermo-Nicholet 6700 FT-IR spectrophotometer (Figure 6). Phosphine concentration was quantified from absorbance using Beer's law (Equation 4).

$$A = \varepsilon \cdot l \cdot c$$

Equation 4 Beer's Law.

Absorbance (A) is proportional to concentration (c) through a constant path length (l) and molar absorptivity (ε).

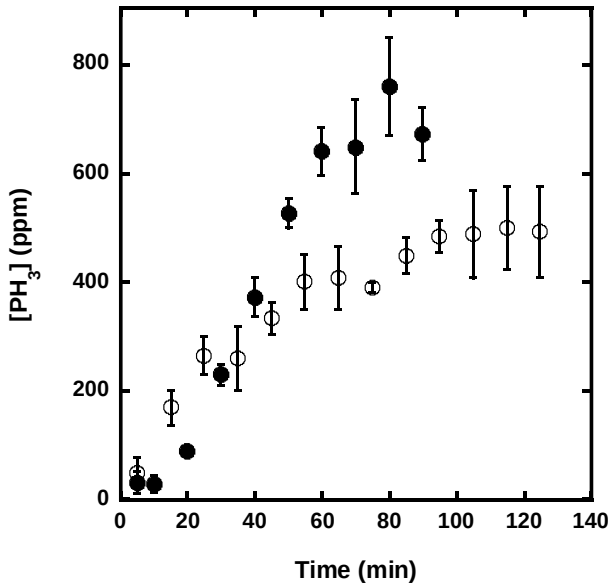

Figure 6. PH_3 production by AlP and Ca_3P_2 in animal exposure model.

PH_3 gas was generated in a sealed, 4.8 L chamber under aerobic conditions using 0.5 g AlP mixed with 20 mL PBS (closed circles) or Ca_3P_2 with 20 mL 1.2 M H_2SO_4 (open circles). PH_3 was monitored using IR spectroscopy and concentration was determined using Beer's law and absorbance values at 2325 cm^{-1}. Circles represent mean absorbance and bars standard error for 3-6 data sets.

Calibration was by a standard additions method using pure phosphine gas generated with H_2SO_4 and AlP. Exposure to phosphine gas is reported as integrated concentration (ppm) · time (min). Aqueous phosphine was generated using AlP and PBS under anaerobic conditions in a septum-sealed vial with minimal headspace as described by Hsu and colleagues [137]. The concentration of aqueous phosphine solutions was limited to 11.6 mM.

Au(I) compounds and sodium thiosulfate solutions were prepared in filtered PBS (pH 7.4).

The carrier molecule calix[4]arene sulfonate, tetrasodium, or tetrasodium;25,26,27,28-tetrahydroxypentacyclo[19.3.1.1^{3,7}.1^{9,13}.1^{15,19}]octacosa-1(24),3,5,7(28),9,11,13(27),15(26),16,18,21(25),22-dodecaene-5,11,17,23-tetrasulfonate(832.7

g/mol) (Figure 7) was synthesized by Karen Rodgers, University of Alabama. Solutions of calix[4]arene sulfonate, tetrasodium were prepared in 50 mM HEPES buffer, pH 7.4.

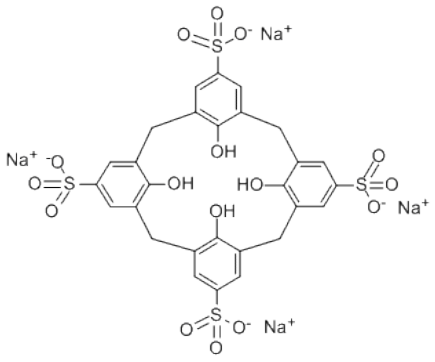

Figure 7. Structure of tetrasodium calix[4]arene sulfonate.

2.1.1 Synthesis and preparation of Ag(I) compounds

$Ag(MTZ)_2NO_3$ was prepared using the method described by Kalinowska et al [107]. 0.34 g metronidazole was dissolved in 20 mL ethanol at 60 °C. 10 mL of 1 mM $AgNO_3$ (dissolved in 5% ethanol) was added to the metronidazole solution and stirred at 60 °C for 30 minutes. The mixture was then evaporated under vacuum at 60 °C to half of the initial volume. The solution was then left to crystalize at room temperature for 24 hours. Crystals were then washed with anhydrous diethyl ether.

Silver(I) thiosulfate was prepared by combining 0.1 M solutions of $AgNO_3$ and $Na_2S_2O_3$ in a ratio of 1:4 and diluted to the desired concentration in 50 mM HEPES buffer (pH 7.4) as described by "Preparation of silver thiosulfate (STS) solution" [122].

Ag(I) lactate, Ag(I) nitrate, and Ag(I) thiosulfate were prepared in 50 mM filtered HEPES buffer (pH 7.4). Ag(I) bis(metronidazole) nitrate and Ag(I) sulfadiazine were prepared in 50 mM HEPES with or without 10% dimethylsulfoxide (DMSO, final concentration 5 mM) to improve

solubility. Where indicated, Ag(I) nitrate was combined with calix[4]arene sulfonate tetrasodium in a ratio of 2:1 in 50 mM filtered HEPES buffer (pH 7.4).

2.1.2 Synthesis of CoN_4[14]

CoN_4[14], (5,7,7,12,14,14-Hexymethyl-1,4,8,11-tetraazacyclotetradeca-4,11-diene cobalt (II) dibromide dehydrate) was prepared anaerobically under argon using trans-[14]-diene prepared as described by Hay et al. [138], adapted from Curtis [139]. Under argon, previously synthesized trans-[14]-diene (0.96 g) and 0.5 g cobalt acetate tetrahydrate were dissolved in 20 mL deoxygenated methanol. The solution was heated to 40 °C and stirred and refluxed for 2 hours. The solution was then evaporated overnight, leaving the orange CoN_4[14] powder. Elemental analysis for $Co(C_{16}H_{32}N_4)]Br_2 \cdot 2H_2O$ (Atlantic Microlab) calculated: 35.9% C, 6.78% H, 10.5% N, 29.9% Br. Found: 36.73% C, 6.99% H, 9.41% N, 26.71% Br. ESI-MS (positive ion mode) calculated for $CoC_{16}H_{32}N_4$ [M^{2+}] 339.4 [1/2 M^{2+}] 169.7; found [M^{2+}] 338.3 [1/2 M^{2+}] 169.6.

2.1.3 Synthesis of CoN_4[11.3.1]

Cobalt(II)2,12-dimethyl-3,7,11,17-tetraazabicyclo-[11.3.1]-heptadeca-1(17)-2,11,13,15-pentaenyl dibromide was synthesized as first described by Long and Busch [140], modified by Lacy and colleagues [141] and reported by Lopez-Manzano et al. [15]. Briefly, 1.35 g $CoBr_2$ and 1 g 2,6-diacetylpyridine were dissolved in a deoxygenated solution of 20 mL ethanol and 0.5 mL deionized water. 0.857 mL (6.13 mmol) 3-3'diaminodipropylamine was slowly added under argon. A color change from green to red was observed. Still under argon, 1 µL glacial acetic acid was added and the solution was heated to 50 °C for 12 hours with continuous stirring. The dark purple

solid was then washed with diethyl ether and dried over P_2O_5 for 24 hours then stored under anaerobic conditions. Elemental analysis was performed by Atlantic Microlab, Inc. for $C_{15}H_{22}N_4Br_2Co$. Calculated: 37.76% C, 4.65% H, 11.74% N, 33.5% Br. Reported: 37.4% C, 5.05% H, 11.42% N, 32.64% Br.

Co(III)N_4[11.3.1] was prepared from Co(II)N_4[11.3.1] by leaving a solution of Co(II)N_4[11.3.1] to oxidize in a fume hood under aerobic conditions for a minimum of 48 hours. Oxidation state and concentration were validated with EPR and electronic absorbance spectroscopy [16].

2.2 INSTRUMENTATION

2.2.1 High-resolution respirometry

Oxygen concentration was monitored using an Oroboros Instruments Oxygraph-2k high-resolution respirometer (Oroboros Instruments, Innsbruck, Austria) [142]. The instrument utilizes a Clark-type electrode to detect oxygen concentration through the reduction of oxygen via a gold catalyst. With constant stirring, molecular oxygen permeates a Teflon membrane in the reaction chamber and reaches the cathode, where it is reduced (Equation 5A). A silver/silver chloride anode provides electrons for this reaction (Equation 5B). The electrode consumes less than 3 pM/s·mL during operation. Temperature in the reaction chambers is maintained by a built-in Peltier thermostat [142].

$$O_2 + 2\ H_2O + 4\ e^- \xrightarrow{Au} 4\ OH^- \quad (A)$$

$$4\ Ag \rightarrow 4\ Ag^+ + 4\ e^- \quad (B)$$

Equation 5. Cathode and anode reactions for the Oroboros Oxygraph Clark-type electrode.

(A) Cathode reacction, reduction of oxygen through a gold catalyst. (B) Anode reaction using silver/silver chloride [142].

2.2.2 Other instrumentation

Anaerobic samples were prepared under argon in an Omni-Lab glovebox (Vacuum Atmosphere, <0.5 ppm O_2). Electronic absorption spectra were obtained with Shimadzu UV-1650PC and UV-2501PC spectrophotometers. Infrared spectroscopy was performed with a Nicolet 6700 FT-IR spectrometer. pH was monitored in solution using a Corning Pinnacle 555 pH/ion meter.

2.3 METHODS

2.3.1 *G. mellonella* model

Larvae of the greater wax moth, (*G. mellonella*) were purchased from Vanderhorst (St. Mary's, OH) and Fish On Bait & Tackle (Pittsburgh, PA), and acclimated at 25 °C for at least 48 hours. Groups of 10 caterpillars were exposed to phosphine generated as described above in a sealed container (4.8 L volume) for a duration of 20 minutes. A group of larvae were exposed to a vessel containing sulfuric acid placed in the inhalation chamber as an added control. Air was circulated every 5 minutes with a 30 mL syringe. After exposure, caterpillars were removed from

the container and monitored for paralysis and recovery. As described by Frawley et al., [131], recovery is characterized by repeated righting behavior. Candidate antidotes or buffer controls were administered five minutes before or immediately after the end of exposure via intrahemocoel injection through the left most distal proleg. Maximum injection volume was 10 μL. Buffers and candidate antidotes were screened for toxicity in *G. mellonella* to determine the appropriate dose. The buffer solutions (500 mM PBS, 50 mM HEPES, 50 mM HEPES with 5 mM DMSO) were not associated with any adverse outcomes at the experimental doses. Candidate antidote doses were selected based on solubility constraints and the no-observed-adverse-effect level (NOAEL). Larvae were monitored for knockdown or death for at least 120 minutes after exposure and/or antidote administration and then checked for survival 24 hours after exposure. Larvae were also monitored for immune activity signaled by a melanin-mediated color change [134].

G. mellonella mitochondrial particles were prepared by cooling about 20 larvae to 4 °C for 12 minutes. Cooled larvae were minced in 1 mL EDTA/KCl solution (154 mM KCl, 1 mM EDTA; pH adjusted to 6.8) [143]. Minced tissue was gently homogenized using a glass homogenizer in 5 mL EDTA/KCl solution, filtered through cheesecloth, and centrifuged at 1500 *g* at 4 °C for 8 minutes to pellet mitochondrial particles. The pellet was washed with 200 μL EDTA/KCl solution, suspended in 200 mL of the same solution, and placed on ice until use in respirometric experiments.

2.3.2 Mouse model

The University of Pittsburgh Institutional Animal Care and Use Committee (Protocol number 17091400) approved all animal protocols used in this study. The Division of Laboratory and Animal Research of the University of Pittsburgh provided all veterinary care during

experiments. Swiss-Webster (CFW) mice weighing 27-40 g and 6-7 weeks old were purchased from Taconic, Hudson, NY, housed four per cage, and allowed access to food and water *ad libitum*. Animals were allowed to adapt to their new environment for at least 1 week prior to carrying out experiments. All animals were randomly assigned to experimental groups of predetermined size. Mice were exposed to phosphine gas two at a time in a procedure that was otherwise identical to that used for the *G. mellonella* larvae (see above) for 15-20 minutes. For these paired exposures, one mouse received treatment with a candidate antidote while the other served as a phosphine-exposed control. Mice were paired by sex and weight and exposure time was adjusted for mean mass of the two exposed mice. Mean mass for the exposed pair was divided by 40 g, the reference mass for dosage calculations for a 20 min exposure. The resulting proportion was multiplied by 20 min to determine exposure time.

In the absence of biomarkers for phosphine poisoning (see section 1.2.1) we are limited in our ability to calculate the inhaled and effective dose of phosphine for our exposure experiments and must rely on the phosphine concentration within the exposure chamber (

Figure 6) for dosage estimations. Effective phosphine doses are notoriously difficult to estimate, even in post-mortem sampling in cases of ingested metal phosphides because phosphine

is degraded quickly to its oxidation products *in vivo*. We are unable to measure the blood level of phosphine of mice under our experimental conditions; the amount of circulating phosphine after a 20 minute exposure would likely be low and not easily correlated to an effective dose in the absence of a known *in vivo* oxidation rate. We estimated the inhaled phosphine concentration for mice using a generalized exposure dose (D_{Exp}) calculation as described in Equation 6.

$$D_{Exp} = c \cdot BR \cdot t$$

Equation 6. Inhaled dose calculation.

Equation used to estimate inhaled phosphine by mice. Exposure dose (D_{Exp}, mg/kg) is a function of concentration (c, mg/L), breathing rate (BR, L/min), and duration (t, min).

The absorbed dose was calculated by multiplying the inhaled dose by phosphine's 1-octanol-water partition coefficient (K_{ow} = 0.54 [144]) as shown in Equation 7. Average circulating phosphine concentration was estimated using the estimated absorbed dose and adjusted for blood volume.

$$D_{Abs} = D_{Exp} \cdot K_{ow}$$

Equation 7. Absorbed dose calculation.

Equation used to estimate absorbed phosphine dose in mouse model. Absorbed dose ($D_{Abs,}$ mg/kg) is equal to the exposure dose (D_{Exp}, mg/kg) modified by the diffusion coefficient (K_{ow}).

Candidate antidotes were injected intraperitoneally (IP) into mice either 5 minutes before or immediately after phosphine exposure. Injected solutions of Au(I) and Co(II) – based candidate antidotes were prepared in filtered PBS (pH 7.4) and Ag(I) – based antidotes were prepared in filtered 50 mM HEPES (pH 7.4) as previously described.

After phosphine exposure and antidote administration for therapeutic treatment groups, mice were assessed for toxicity using a modified pole test. This test evaluates the ability of the mouse to climb a lightly roughened, 24 inch pole (0.95 cm diameter) before and after exposure to a toxicant as well as recovery post-exposure after receiving treatment [131]. Briefly, the pole was placed in the horizontal position (45° angle) and the mouse was placed on to the end. The pole was

then gradually raised to the vertical position (90° angle). The mouse was scored based on its ability (or inability) to climb the pole from 0 (unable to grasp pole)-3 (climbs to the top readily without issue). The pole test began immediately after phosphine exposure and was repeated every 10 minutes up to 2 hours after exposure.

In these studies, the absence of normal open-field exploratory behavior when pole testing had otherwise indicated recovery to be underway was often an early indication of loss of vision. Mice were further assessed for vision impairment using an eye blink reflex test [145]. The lack of a blinking response upon approaching the eye with a gloved finger or cotton swab was taken to indicate visual impairment. Cataracts were identified by observing onset of lens opacity [146].

2.3.3 High-resolution respirometry

Oxygen concentration and flux was monitored with an Oxygraph O2k polarographic instrument (see section 2.2.1). For experiments using isolated mitochondrial particles of *G. mellonella,* the mitochondrial buffer MiRO5 (2.1 mL) was added to both chambers of the respirometer and left to equilibrate for 20 min at 25 °C before ~100 μL of mitochondrial particles (prepared as described in section 2.3.1) was added [147]. Mitochondrial respiration was observed with the addition of cytochrome *c* (final concentration 10 μM), succinate (final concentration 10 mM), and rotenone (to prevent back reaction through complex I, final concentration 0.5 μM). Phosphine was added in 25-100 μL increments to respiring mitochondrial particles from an aqueous phosphine solution prepared as described above.

For Oxygraph experiments with cobalt compounds and phosphine, 50 mM sodium or potassium phosphate buffer (pH 7.4) was added to each Oxygraph chamber and left to equilibrate for 20 minutes at room temperature under aerobic conditions [15]. Sodium ascorbate (0.25-1.5

mM), CoN_4[11.3.1] (25-150 μM), and/or aqueous PH_3 (30-300 μM) were added to the chamber in varying concentrations.

2.3.4 Product assay

Hydrogen peroxide was detected in solution using the H_2O_2/peroxidase marker Amplex® UltraRed (Invitrogen). Experimental samples contained Co(II)N_4[11.3.1] in PBS (pH 7.4) (final concentration 0.06-5 μM) and increasing amounts of aqueous phosphine (final concentration 5-6 mM, prepared as previously described in MATERIALS) up to a 100 fold excess over the cobalt complex. Three negative control groups were prepared; one containing PBS alone, another with 250 μM Co(II)N_4[11.3.1] in PBS , and one containing aqueous phosphine. Positive control samples contained 5 μM H_2O_2. Samples were plated in 96-well plates and incubated with Amplex® UltraRed and horseradish peroxidase according to manufacturer's instructions. Fluorescence was detected using a Cytation 5 Cell Imaging Multi-Mode Reader (BioTek) and quantified using BioTek Gen 5 data analysis software. Results were calibrated by a standard curve method using 0-5 μM H_2O_2.

2.3.5 Protein isolation and enzyme assay

Cytochrome *c* oxidase was prepared from intact bovine heart mitochondria using a modified Harzell-Beinert procedure (without the preparation of the Keilin-Hartree particles) as described by Pearce et al [148]. The enzyme was determined to be spectroscopically pure if the 444 to 424 nm ratio for the reduced enzyme was 2.2 or higher [149]. Enzyme concentrations were determined as a total heme *a* using the differential (absorption) extinction coefficient of $\Delta\varepsilon_{604}$ =

12 mM $^{-1}\cdot$ cm^{-1} for the reduced minus oxidized spectra of the mammalian and bacterial enzymes, respectively [150]. Concentrations throughout are given on a per enzyme concentration basis (i.e., [heme *a*]/2).

Steady-state kinetics were performed with the isolated enzyme as described by Nicholls et al [151]. The concentration changes of the electron donor, bovine ferrocyctochrome *c*, were monitored through its absorbance at 550 nm (minus 540 nm, an isosbestic point in the spectrum of cytochrome *c*) in the presence of excess sodium ascorbate (14.5 mM) in normoxic solution, 0.1 M potassium phosphate (pH 7.44), 0.02% laural maltoside (Anatrace). The fractional oxidase activity, [E], was determined by the following equation in which $[c^{2+}]_0$ = fraction at time 0, $[c^{3+}]_t$ = fraction at time *t*, $[c^{3+}]_0$ = fraction at time 0 and $[c^{2+}]_t$ = fraction at time *t.*

$$[E] = [c^{2+}]_0\cdot[c^{3+}]_t/[c^{3+}]_0\cdot[c^{2+}]_t$$

Equation 8. Fractional cytochrome *c* oxidase activity.

2.3.6 Electron paramagnetic resonance (EPR) spectroscopy

X-band (9 GHz) EPR spectra were recorded on a Bruker ESP 300 spectrometer equipped with an ESR 910 flow cryostat (Oxford Instruments) for ultralow-temperature measurements and analyzed with SpinCount software, provided by Professor Michael Hendrich, Carnegie Mellon University. Samples (~200 μL) were placed in quartz EPR tubes, frozen immediately, and stored in liquid nitrogen before analysis.

2.3.7 Phosphine binding affinity

In order to determine a binding constant (K = CoN_4[11.3.1]-PH_3/[PH_3][CoN_4[11.3.1]), phosphine was titrated into CoN_4[11.3.1] under anaerobic conditions, in septum-sealed quartz cuvettes with minimal headspace (1.5 mL volume). All transfers were performed using gastight syringes. Aqueous phosphine was prepared from AlP and PBS as described in section 2.1. Minimal volumes of aqueous phosphine were titrated into Co(II)N_4[11.3.1] (in 50 mM sodium phosphate buffer, pH 7.4) followed by rigorous mixing. The binding affinity was calculated from the absorbance data (recorded from 300-800 nm) using a nonlinear least squares fit of the values at λ = 425 nm to Equation 9 [152].

$$y = \varepsilon_1 + \left(\frac{(\varepsilon_2 \cdot k \cdot x)}{\left(1 + 0.5 \cdot \left(\sqrt{\left(1 - (k \cdot C) + (k \cdot x)\right) \cdot \left(1 - (k \cdot C) + (k \cdot x)\right) + (4 \cdot k \cdot C)} - \left(1 - (k \cdot C) + (k \cdot x)\right)\right)\right)} \right)$$
$$\cdot \left(\frac{\sqrt{\left(1 - (k \cdot C) + (k \cdot x)\right) \cdot \left(1 - (k \cdot C) + (k \cdot x)\right) + (4 \cdot k \cdot C)) - (1 - (k \cdot C) + (k \cdot x)))}}{2 \cdot k} \right.$$

Equation 9. Nonlinear least squares fit for determination of phosphine-Co(II)N_4[11.3.1] K_{eq}.

As described by Hargrove et al [152]. y = absorbance at 425 nm, x = concentration of ligand, ε_1 = extinction coefficient of CoN_4[11.3.1] at 425 nm, ε_2 = extnction coefficient of product/adduct at 425 nm, *C* = concentration of CoN_4[11.3.1], *k* = $K_{CoN4[11.3.1]\text{-}PH3}$.

2.3.8 Blood analysis

Whole-blood was obtained from mice via heart puncture immediately after sacrifice and mixed with 850 μM EDTA in PBS (pH 7.4). For EPR analysis, 200 μL samples were collected

from phosphine-exposed mice (controls), placed in EPR tubes, frozen and stored in liquid nitrogen until examination could occur. Red blood cells (RBCs) were isolated from fresh whole blood by pelleting at 10000 rpm for 3 min at 20 °C and subsequent re-suspension. Pelleted RBCs were re-suspended in 1 mL of either PBS (pH 7.4) (negative controls) or deionized water, which is not isotonic and induces hemolysis (positive controls). Pelleted experimental samples of RBCs were re-suspended in solutions (1 mL, in PBS) of 0.3–5.8 mM aqueous phosphine for 15 min prior to analysis. Other experimental samples were re-suspended in 5.8 mM phosphine for 20, 30, 45, or 60 min. The samples were then re-spun at 10000 rpm for 3 min at 20 °C and the resulting supernatant was diluted 1:100 in PBS and analyzed for free hemoglobin using electronic absorption spectroscopy. Oxyhemoglobin (oxyHb) concentration was quantified from absorbance at 415 nm using Beer's law (Equation 4) and normalized based on positive control values [153].

2.4 STATISTICAL ANALYSIS

Data was analyzed and presented using Kaleidagraph or GraphPad Prism software. A *p*-value ≤ 0.05 was considered significant. Survival, knockdown, and incidence data was compared using a two-tailed Fisher's exact test and animal recovery data and pole test scores were analyzed using a Kruskal-Wallis ranked sum test with chi-square approximation assuming a nonparametric distribution and/or a Wilcoxon ranked sign test for paired data assuming a nonparametric distribution.

3.0 ANTIDOTAL ACTION OF SOME GOLD (I) COMPLEXES TOWARD PHOSPHINE TOXICITY

Kimberly K. Garrett, Kristin L. Frawley, Samantha Carpenter Totoni, Yookyung Bae, Jim Peterson*, and Linda Pearce*

Department of Environmental and Occupational Health, Graduate School of Public Health, The University of Pittsburgh, Pittsburgh, Pennsylvania, 15219, United States

*Corresponding Authors: jimmyp@pitt.edu; lip10@pitt.edu

Supported by NIH Office of the Director (NIH OD) and the National Institute of Environmental Health Sciences (NIEHS): award R21 ES092310 (to L.L.P. and J.P)

Adapted from

With permission, Garrett, K. K., Frawley, K. L., Carpenter Totoni, S., Bae, Y., Peterson, J., & Pearce, L. L. (2019). Antidotal Action of Some Gold (I) Complexes toward Phosphine Toxicity. *Chemical Research in Toxicology, 32*(6), 1310-1316.

3.1 INTRODUCTION

Worldwide, ingestion of pesticides is seemingly the most common method of suicide, accounting for approximately one-third of all such deaths [121, 154]. Since the early 1980s, particularly in parts of Asia, phosphine (PH_3) released from pelleted phosphides has become increasingly used as the poison within this genre [4, 10, 155-158], yet there appears to be no antidote currently available. Throughout North America, phosphides (particularly of aluminum and zinc) are legally obtainable from many commercial outlets in pelleted form for use as rodenticides. There are dozens of sublethal occupational exposures annually in the U.S. [159, 160] and occasional domestic accidents leading to fatalities in Canada and the U.S. [161, 162], but of greater public health concern is the possibility that phosphine may be deliberately put to malicious purposes, since the phosphide pellets release the toxic gas simply upon contact with mildly acidic water. A key target for the acute toxic action of phosphine is believed to be the mitochondrion, seemingly by inhibition of cytochrome *c* oxidase (complex IV) [41, 57, 75, 77, 94]. Unfortunately, rigorous verification of this mechanism of action at the biochemical and cellular levels is lacking, representing a barrier to the rational development of possible antidotes. Phosphine, however, is slow acting, relatively stable *in vivo*, and a ligand much used in synthetic chemistry; it follows, therefore, that a scavenging approach employing metal ion complexes designed to bind phosphine ought to significantly ameliorate its toxicity.

In this investigation, we studied a number of compounds that are commercially available and have previously been evaluated for their pharmacological activity and safety, although not as decorporating agents. The essential desired activity we sought was the ability to rapidly bind phosphine with reasonably high affinity, and based on general inorganic principles [18, 163], we proposed that some gold(I) complexes should prove to be good candidate phosphine antidotes.

Phosphine is a “soft” ligand with a marked preference for binding in σ-donor/π-acceptor fashion to “soft” metal ions, typically second- and third-row transition metals in low oxidation states. Gold in its univalent state, Au(I), is the softest metal ion, and given that Au(I) compounds have been widely used to treat rheumatoid arthritis for about a century [102, 103], we gave Au(I) complexes a high priority for investigation as potential phosphine-scavenging agents. Non-life-threatening side effects develop in about one-third of patients given repeated high doses of Au(I) antiarthritics, but these are usually minor and manageable/reversible [100, 101]. Gold salts are about an order of magnitude more expensive than salts of most first-row transition metals, but this cost is still small in comparison to that of the overall purified product.

In addition, we have previously shown that *Galleria mellonella* larvae (caterpillars) can usefully be applied to the screening of antidotes for mitochondrial toxicants, namely, azide, cyanide, and sulfide [131]. Accordingly, we have employed *G. mellonella* larvae to find an exposure level to phosphine gas useful for testing both the prophylactic and therapeutic effects toward phosphine of three antiarthrytic Au(I) compounds, namely auro-bisthiosulfate (AuTS), sodium aurothiomalate (AuTM), and aurothioglucose (AuTG). All of these compounds contain sulfide donors, keeping gold in its reduced univalent state, lowering toxicity, and promoting affinity for phosphine. The outcomes of these experiments with the larvae were then used to guide the development of a protocol for testing the potential antidotes to phosphine in mice.

3.2 RESULTS

3.2.1 *G. mellonella* model

We have previously shown that *G. mellonella* caterpillars provide a reasonable model for screening antidotes to cytochrome *c* oxidase toxicants, such as cyanide, and found that isolated tissue and mitochondria particles are useful in monitoring oxygen turnover activity [131]. Uncoupled, isolated mitochondrial particles were used rather than intact mitochondria or cells because we needed to ensure that our limited dose of aqueous phosphine (minimized to prevent phosphine-electrode interaction) reached the target site. Further, with mitochondrial particles, we can add supplemental cytochrome *c* to the system.

Oxygen consumption was initiated by adding cytochrome *c* (to replace any lost when the mitochondria were lysed) along with the electron donor succinate, and rotenone (complex I inhibitor) to prevent backflow. The respirometric inhibition (decreased oxygen flux, JO_2) of *G. mellonella* mitochondrial particles [131] observed was quite linear ($R^2 = 0.95$) with respect to micromolar phosphine additions as shown in Figure 8.

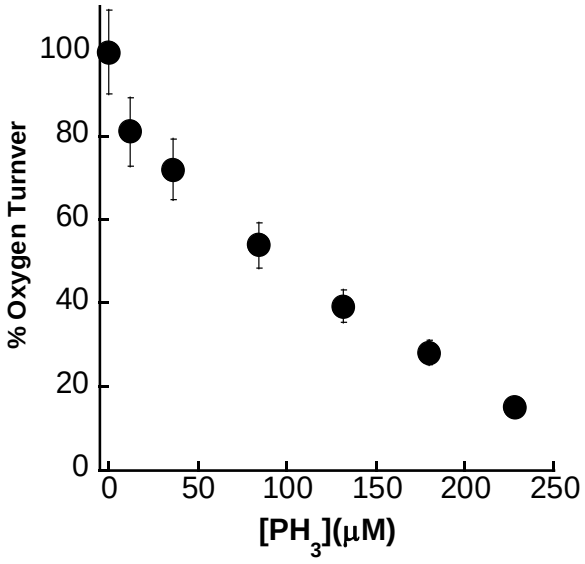

Figure 8. Respirometric response of *G. mellonella* mitochondrial particles titrated with PH_3.

Oxygen consumption was assessed in *G. mellonella* mitochondrial particles diluted in MiR05 Oxygraph solution. The tissue suspension (2.1 mL) was allowed to equilibrate in chamber for ~10 min prior to measuring oxygen consumption. Default Oxygraph settings of block temperature, 25 °C; stir bar speed, 400 rpm; and data recording, 2 s were used. All reagents/substrates quantities are given as final concentrations. Cytochrome *c* (10 μM), succinate (0.5 mM), and rotenone (0.5 μM) were added to the 2.1 mL of respirometric solution containing 100 μL of mitochondrial particles and the oxygen flux recorded over 5 min (JO2 of ~140 pmol/s · mL). Subsequently, PH_3 was added, from a saturated solution, resulting in PH_3 concentrations of 12−230 μM in the respirometer, and the oxygen flux was followed until it was constant (~5 min). Circles represent mean % oxygen turnover normalized to a 100% maximum and bars represent standard error.

Exposure of *G. mellonella* larvae to phosphine in a closed container for 20 min caused ~50% of the larvae to become immobile (paralyzed), and the time (recovery time) until the paralyzed larvae regained their ability to move was then recorded. Any larvae that were not immobilized were recorded as having a recovery time of zero. A dose-response of this adjusted recovery time of the *G. mellonella* larvae exposed to phosphine (12-10,000 ppm·min) was

subsequently determined (Figure 9). An exposure of 4300 (±700) ppm·min phosphine (over a 20 min time span) induced a state of paralysis that lasted ~35 min, a conveniently repeatable response.

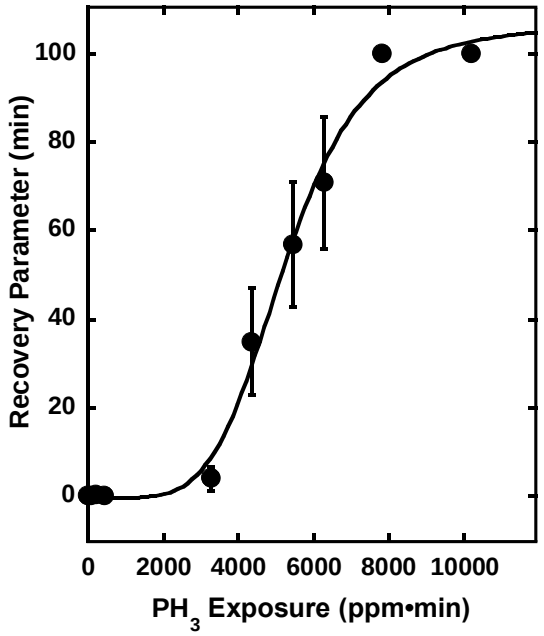

Figure 9. Dose-response data for *G. mellonella* larvae exposed to varying amounts of PH_3.

The larvae were exposed to PH_3 gas generated by the reaction of Ca_3P_2 with 20 mL of 1.2 M H_2SO_4 in a closed chamber (4.8 L volume). In sham controls, the addition of the same amount of acid to a reaction vessel (separated from the larvae) caused no change in the larval behavior. The time from which each larva ceased movement until movement began again (recovery time) was recorded. Each group of larvae (~10) were exposed to PH_3 at 12−10 000 ppm·min. Roughly 60% of control larvae were incapacitated and any larvae that did not knockdown were assigned recovery times of 0 min. The few larvae that had recovery times over 120 min were not scored. Total population (N) = 100 with 10 larvae per exposure group. Circles represent mean recovery time and bars are standard error.

Once a reproducible recovery time for the larvae was obtained, putative antidotes at levels that showed no visible toxicity to the *G. mellonella* larvae (AuTS, 25 mg/kg; AuTM, 1 g/kg; AuTG, 1 g/kg) were administered by injection into the most distal left abdominal proleg 5 min

prior to or 10 minutes after exposure to phosphine gas. When administered prophylactically, all of the gold(I) complexes tested significantly increased survival rates (Figure 10A) and decreased knockdown (Figure 10B) compared to untreated, phosphine-exposed controls (35 (±3.4) min). Prophylactic treatment significantly decreased the mean time until the larvae were recovered (AuTM, 3 (±3) min, $p < 0.0001$; AuTG, 0 min, $p < 0.0001$; AuTS, 2.1 (±0.7) min, $p < 0.0001$, Kruskal-Wallis Chi-square approximation, Figure 10C, Table 2) and decreased the median recovery time for all surviving caterpillars to 0 (Table 2).

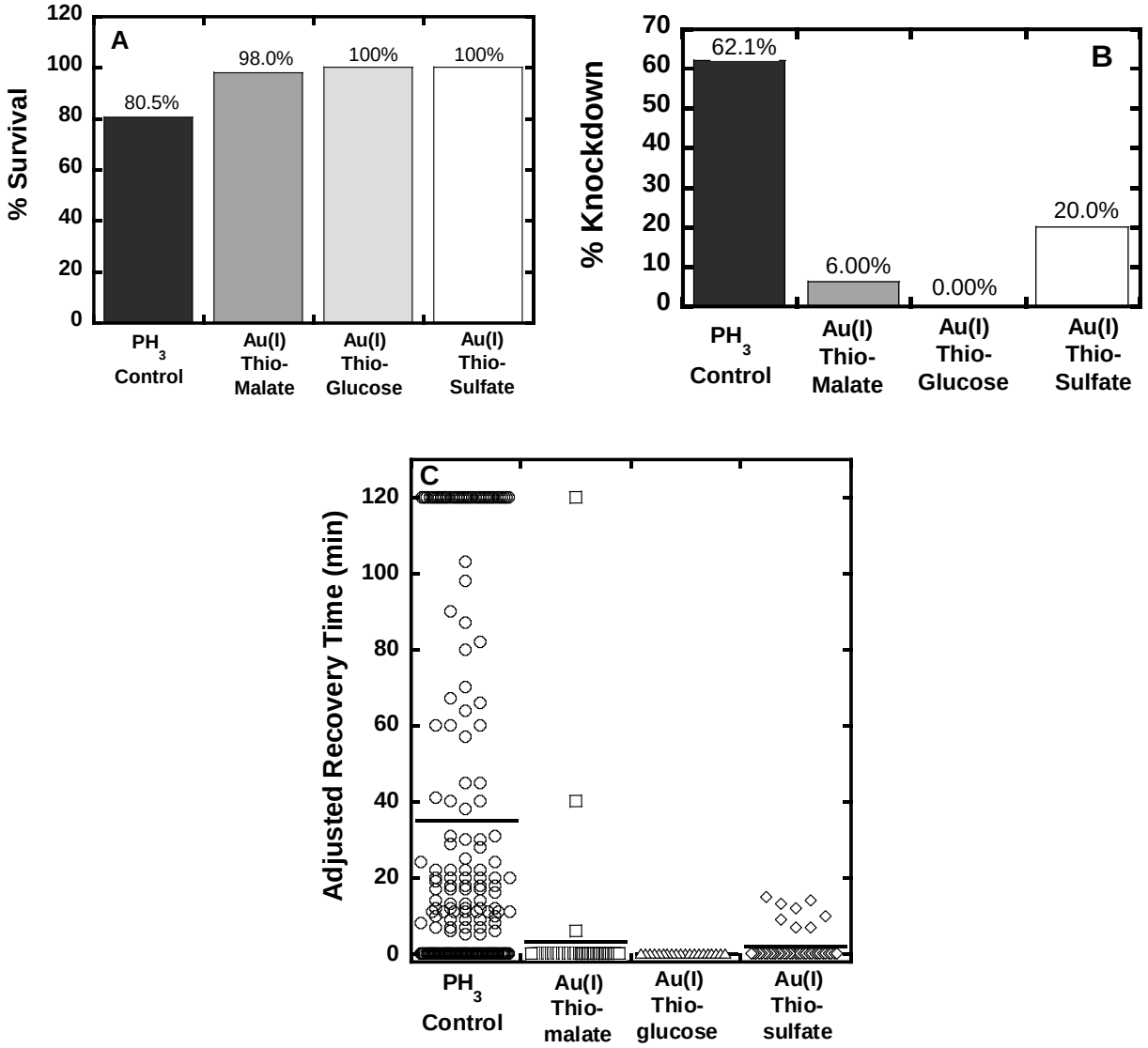

Figure 10. Prophylactic use of Au(I) thiomalate, Au(I) thioglucose, and Au(I) thiosulfate against phosphine toxicity in *G. mellonella* larvae.

Larvae were injected with each of the three putative antidotes (Au(I) thiomalate, 1 g/kg; Au(I) thiogluocse, 1 g/kg; Au(I) thiosulfate, 25 mg/kg) 5 min prior to a PH_3 exposure of 4300 (±700) ppm·min. Roughly 80% of control larvae survived (A) and 60% of control larvae were incapacitated after PH_3 exposure (B). Any larvae that did not knockdown were assigned recovery times of 0 min. The few larvae that had recovery times over 2 h were scored as 120 min. Sample sizes (n larvae): PH_3 control = 190, prophylactic Au(I) thiomalate = 50, prophylactic Au(I) thioglucose = 20, prophylactic Au(I) thiosulfate = 40, therapeutic Au(I) thiomalate = 90, therapeutic Au(I) thioglucose = 30, therapeutic Au(I) thiosulfate = 70. (A) Percent survival for controls and each group with

prophylactic treatment, exposure groups compared to controls with a 2-tailed Fisher's Exact Test: PH_3 control (black bar) = 153/190; Au(I) thiomalate (dark gray bar) = 49/50, $p = 0.0017$; Au(I) thioglucose (light gray bar) = 20/20, $p = 0.028$; Au(I) thiosulfate (white bar) = 40/40, $p = 0.0006$. (B) Knockdown incidence for controls and prophylactic treatment groups, compared with a 2-tailed Fisher's Exact Test: PH_3 control (black bar) = 118/190; Au(I) thiomalate (dark gray bar) = 3/50, $p < 0.0001$, Au(I) thioglucose (light gray bar) = 0/20, $p < 0.0001$, Au(I) thiosulfate (white bar) = 8/40, $p < 0.0001$. (C) Recovery time for PH_3-exposed larvae treated prophylactrically with Au(I) compounds compared to controls including non-survivors (recovery time ≥ 120 min). Bars represent sample mean. Means compared using a Kruskal-Wallis chi-square approximation assuming a nonparametric distribution. Mean recovery for PH_3 controls (circles) = 35 (±3.4) min, Au(I) thiomalate (squares) = 3.3 (±2.5) min, $p < 0.0001$, Au(I) thioglucose (triangles) = 0 (±0) min, $p < 0.0001$, Au(I) thiosulfate (diamonds) = 2.2 (±0.73) min, $p < 0.0001$ Data tabulated in Table 2.

Table 2. Mean and median recovery times for *G. mellonella* larvae treated with Au(I) compounds prophylactically against PH_3 exposure.

Treatment (Prophylactic)	All		Surviving*	
	Mean Recovery Time (±SE) (min)	Median Recovery Time (min)	Mean Recovery Time (±SE) (min)	Median Recovery Time (min)
PH_3 Control	35 (±3.4)	11.5	15 (±1.8)	7.0
1 g/kg Au(I) Thiomalate	3.3 (±2.5)	0	0.94 (±3.4)	0
1 g/kg Au(I) Thioglucose	0	0	0	0
25 mg/kg Au(I) Thiosulfate	2.1 (±0.73)	0	2.2 (±0.73)	0

*Data labeled "surviving" incorporates larvae with recovery times < 120 min.

We calculated an estimated absorbed phosphine concentration for the caterpillars using Equation 6. During a 20 minute phosphine exposure of 4300 ppm · min, the average PH_3 concentration in the exposure chamber is 0.3 mg/L. Larval intake rate was estimated using data reported by Burkett and colleagues [164] and determined to be ~4 μL per minute at 21 °C. Because

the larvae have an open circulatory system, body mass and circulatory volume were assumed to be proportional (0.2 g larvae = 0.2 mL control volume) and D_{Exp} and D_{Abs} presumed to be equivalent. The estimated circulating concentration for phosphine in the caterpillars under our experimental conditions was found to be ~3 μM.

Treatment with Au(I) thiosulfate 10 minutes after phosphine exposure significantly improved survival compared to untreated controls ($p = 0.0066$) (Figure 11A) and treatment with Au(I) thioglucose and Au(I) thiosulfate significantly reduced knockdown rates (Figure 11B, $p = 0.01$ and 0.0004, respectively). All of the tested Au(I) compounds improved recovery times for phosphine-exposed larvae upon therapeutic administration, Au(I) thioglucose and Au(I) thiomalate significantly so (Figure 11C and Table 3, AuTM, 19 (±5) min, $p = 0.89$; AuTG, 17 (±7) min, $p = 0.0057$; AuTS, 14 (±4) min, $p < 0.0001$; controls, 35 (±3.4) min). In surviving larvae, therapeutic treatment with the Au(I) compounds reduced median recovery time; treatment with Au(I) thiosulfate and Au(I) thioglucose reduced the median to 0 (Figure 11C).

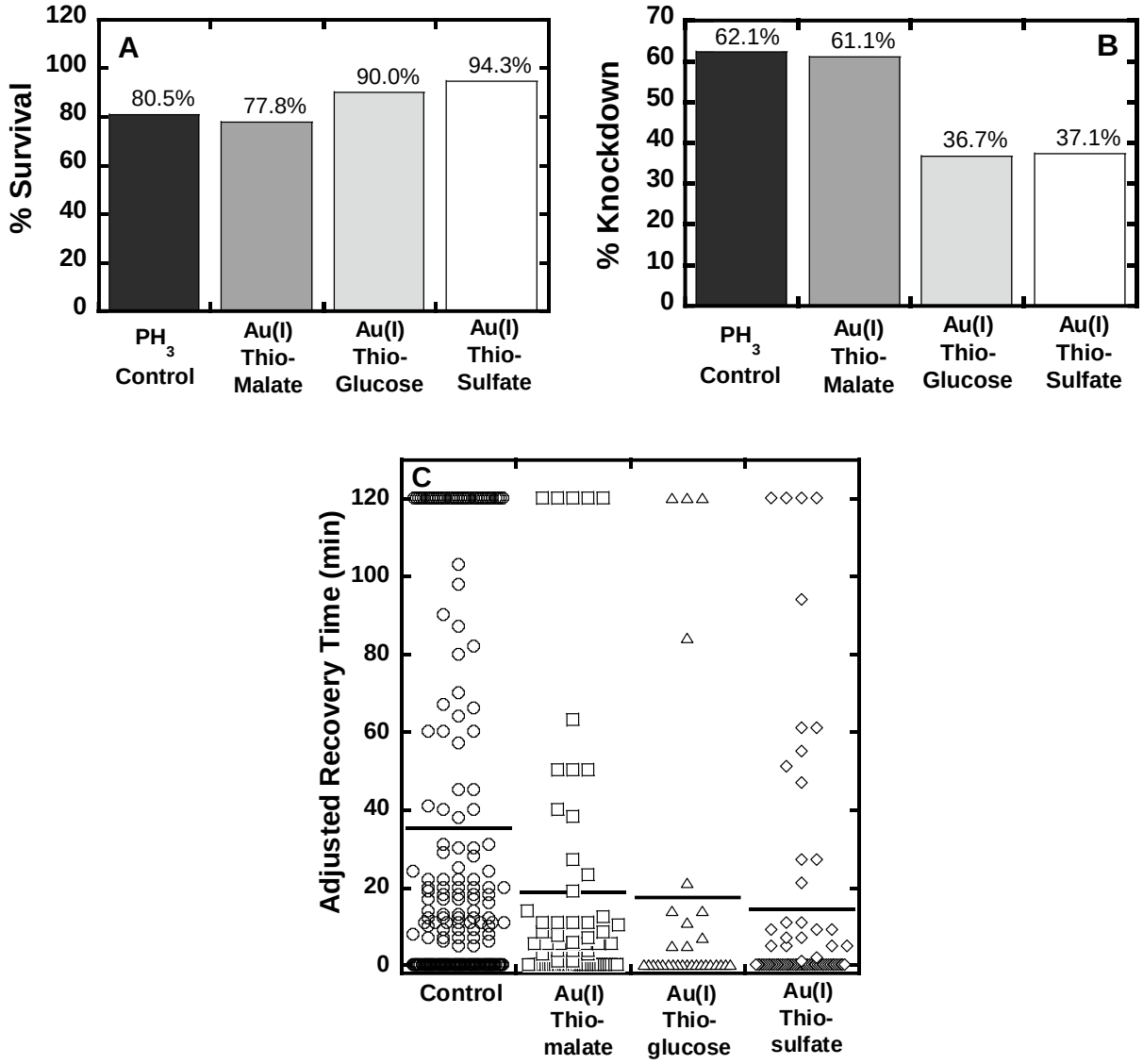

Figure 11. Therapeutic use of Au(I) thiomalate, Au(I) thioglucose, and Au(I) thiosulfate against phosphine toxicity in *G. mellonella* larvae.

Larvae were injected with each of the three putative antidotes (Au(I) thiomalate, 1 g/kg; Au(I) thiogluocse, 1 g/kg; Au(I) thiosulfate, 25 mg/kg) 10 min after a PH_3 exposure of 4300 (±700) ppm·min. Roughly 80% of control larvae survived (A) and 60% of control larvae were incapacitated after PH_3 exposure (B). Any larvae that did not knockdown were assigned recovery times of 0 min. The few larvae that had recovery times over 2 h were scored as 120 min. Sample sizes (n larvae): PH_3 control = 190, therapeutic Au(I) thiomalate = 90, therapeutic Au(I) thioglucose = 30, therapeutic Au(I) thiosulfate = 70. (A) Percent survival for controls and each group with therapeutic treatment, exposure groups compared to controls with a 2-tailed Fisher's Exact Test: PH_3 control (black

bar) = 153/190; Au(I) thiomalate (dark gray bar) = 70/90, $p = 0.64$; Au(I) thioglucose (light gray bar) = 27/30, $p = 0.31$; Au(I) thiosulfate (white bar) = 66/70, $p = 0.0066$. (B) Knockdown incidence for controls and therapeutic treatment groups, compared with a 2-tailed Fisher's Exact Test: PH_3 control (black bar) = 118/190; Au(I) thiomalate (dark gray bar) = 55/90, $p = 0.90$, Au(I) thioglucose (light gray bar) = 11/30, $p = 0.010$, Au(I) thiosulfate (white bar) = 26/70, $p = 0.0004$. (C) Recovery time for PH_3-exposed larvae treated therapeutically with Au(I) compounds compared to controls including non-survivors (recovery time ≥ 120 min). Bars represent sample mean. Means compared using a Kruskal-Wallis chi-square approximation assuming a nonparametric distribution. Mean recovery for PH_3 controls (circles) = 35 (±3.4) min, Au(I) thiomalate (squares) = 19 (±5.3) min, $p = 0.89$, Au(I) thioglucose (triangles) = 17 (±7.0) min, $p = 0.0057$, Au(I) thiosulfate (diamonds) = 14 (±3.8) min, $p < 0.0001$. Data tabulated in Table 3.

Table 3. Mean and median recovery times for *G. mellonella* larvae treated with Au(I) compounds therapeutically after PH_3 exposure.

Treatment (Therapeutic)	All		Surviving*	
	Mean Recovery Time (±SE) (min)	Median Recovery Time (min)	Mean Recovery Time (±SE) (min)	Median Recovery Time (min)
PH_3 Control	35 (±3.4)	11.5	15 (±1.8)	7.0
1 g/kg Au(I) Thiomalate	19 (±5.3)	2.7	14 (±3.7)	1.0
1 g/kg Au(I) Thioglucose	17 (±7.0)	0	6.0 (±3.2)	0
25 mg/kg Au(I) Thiosulfate	14 (±3.8)	0	8.0 (±2.3)	0

*Data labeled "surviving" incorporates larvae with recovery times < 120 min.

Prophylactic treatment with any of the three Au(I) candidates significantly improved larvae survival and recovery times after phosphine exposure compared to untreated controls (Figure 10). Au(I) thiosulfate was the only candidate to significantly improve both survival and recovery time when administered prophylactically (Figure 11).

3.2.2 Enzyme assay

Since cytochrome *c* oxidase is difficult to isolate from *G. mellonella* larvae in large enough amounts for steady-state turnover experiments, it has been shown that minimal differences between enzymes isolated from different species exist [131, 165], and we wanted to confirm the inhibition of mammalian cytochrome *c* oxidase by phosphine, the turnover experiments were performed with enzyme isolated from bovine hearts. For straightforward spectroscopic activity analysis, cytochrome *c* must be added to large excess over cytochrome *c* oxidase. In practice, this means working with isolated cytochrome *c* oxidase or mitochondrial fragments so that cytochrome *c* can gain access to the enzyme. Further, isolated mitochondria have more severe limitations than intact cells, specifically, they must be isolated and utilized very quickly. Optimally functional respiration only persists for up to approximately 1 hour in freshly isolated mitochondria [166, 167]. Mitochondrial fragments, however, can be frozen and stored without loss of complex IV activity [148].

Using methods described by Yonetani and colleagues [168] and Singorgo et al [169], The steady-state turnover of oxygen by bovine cytochrome *c* oxidase was monitored by following the absorbance changes of cytochrome *c*, the oxidase electron donor, after providing a source of electrons for cytochrome *c*, sodium ascorbate (Figure 12A, open circles). Once the steady state was established, phosphine (to 100 μM) was added (at ~100 s), resulting in inhibition of the enzyme. The resulting time course of the inhibition of cytochrome *c* oxidase was fit by a single exponential: $[E]_{active} = 0.87e^{-0.033t} + 0.13$ (Figure 12B). The inactivation rate was proportional to the phosphine concentration with a k_{on} calculated to be 3.3×10^3 $M^{-1} \cdot s^{-1}$ with 13% of the enzyme still active at the phosphine concentration of 100 μM. This residual activity is proportional to the apparent K_i, which was determined to be 13 μM, similar to those previously reported [74]. To test

if the observed amelioration of phosphine toxicity by gold(I) complexes (Figure 10 and Figure 11) could indeed be attributable to antagonism of cytochrome *c* oxidase activity, AuTS (300 μM) was added to the enzyme solution prior to the initiation of steady-state conditions by addition of ascorbate (Figure 12A, closed diamonds). When phosphine (100 μM) was subsequently added, the steady-state turnover was roughly 70% of that observed for the normally functioning enzyme.

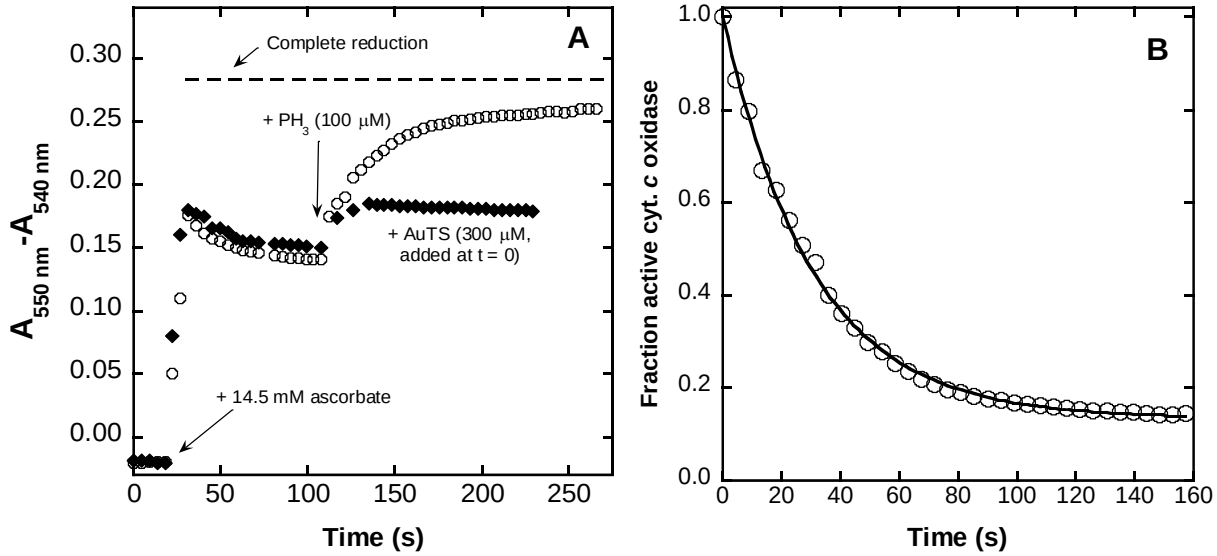

Figure 12. Cytochrome *c* oxidase asteady-state turnover: inhibition by phosphine and rescue by auro-sodium bisthiosulfate hydrate (AuTS).

Cytochrome c oxidase (0.194 μM) turnover was followed by observing the oxidation of reduced cytochrome c (14 μM) monitored spectroscopically at A550 nm − A540 nm (T = 25 °C, 0.1 M sodium phosphate, pH 7.44, 0.02% lauryl maltoside) over time. Turnover was initiated by the addition of 1.45 mM sodium ascorbate. (A) Representative plots for the addition of phosphine (100 μM, open circles) to the active enzyme. Addition of 300 mM AuTS prior to ascorbate initiation of turnover (closed diamonds, symbols have been slightly offset so as to view both data sets) and subsequent addition of 100 μM phosphine. (B) A single exponential fit (solid line) to the fraction of active enzyme vs time (open circles) calculated according to eq 1 (see Experimental Section). All reagents/quantities are given as final concentrations.

3.2.3 Mouse model

After screening the potential antidotes in *G. mellonella* larvae, a preliminary set of similar experiments were then carried out in mice. Swiss-Webster mice were exposed to phosphine gas, produced by the same method as used with the *G. mellonella* larvae, in a closed container for 15-20 min. This dose of phosphine, 3200 (±500) ppm·min, did not cause the mice to "knockdown" but did induce a severely lethargic state (motionless in open field). The mice were then examined by a pole-climbing behavioral assessment (see section 2.3.2). Mice were examined 5 days prior to the phosphine experiments in order to obtain a baseline and then subjected to the pole test starting immediately following their exposure to phosphine.

We estimated an inhaled, absorbed, and circulating dose for phosphine in exposed mice assuming a 40 g mouse with a tidal volume of 0.18 ml and an average respiratory rate of 255 breaths per minute [170]. During phosphine exposure, mouse breathing rate can decrease to about half of normal while tidal volume has been found to double [67]. With this in mind, we calculated a range of exposures from fully inhibited breathing to uninhibited breathing. During a 20 minute phosphine exposure of 3200 ppm·min, the average PH_3 concentration in the exposure chamber is 0.22 mg/L. With Equation 6, we estimated that a 40 g mouse inhales 3-6 μmol of phosphine during the 20 minute exposure. With a K_{ow} of 0.54, 1.6-3.2 μmol is absorbed (Equation 7) and the estimated circulating dose in the blood (estimated 3.5 mL) is 460-920 μM (maximally, under ideal conditions, not accounting for metabolism or excretion).

Pole test scores were not significantly correlated to time point (compared using Kruskal-Wallis rank sum test for nonparametric distribution, control $p = 0.95$, prophylactic $p = 1$, therapeutic $p = 0.98$) so mice were compared using time-independent mean scores. Mice given the AuTS antidote (50 mg/kg, previously determined to cause no change in behavior by pole testing

and chosen based on the mean recovery time in *G. mellonella*) 5 min prior to the phosphine exposure performed as well as mice that had never been exposed to phosphine; prophylactic treatment with AuTS resulted in a significant improvement in average pole test scores compared to controls (p = 0.017, calculated using a Kruskal-Wallis rank sum test). However, when mice were exposed to phosphine and given the AuTS antidote 1 min after the toxicant exposure, the results of the pole test were less impressive with insignificant improvement in performance compared to untreated, phosphine-exposed controls (p = 0.60).

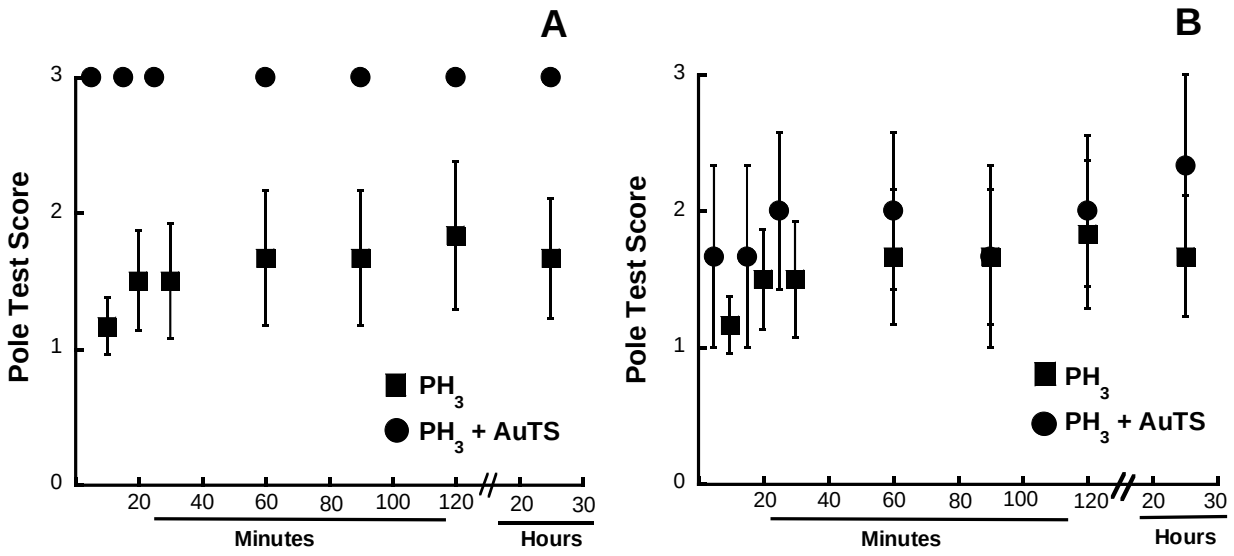

Figure 13. Prophylactic and therapeutic use of aurobisthiosulfate (AuTS) in phosphine exposed mice.

Mice were given 50 mg/kg of AuTS intraperitoneally (closed circles) either 5 min before (A) or 1 min after (B) a PH_3 (closed squares) exposure of 3200 (±500) ppm·min (over a 15 min time period), The mice were examined using a behavioral assessment (pole-climbing test, see section 2.3.2) to evaluate their response to the toxicant and putative antidote (AuTS). Sample sizes (n mice): 6 control, 3 prophylactic treatment, 3 therapeutic treatment. Symbols represent mean pole test scores and bars standard error. Scores were compared using a Kruskal-Wallis chi-square approximation assuming a nonparametric distribution. Time did not significantly impact pole test scores (control p = 0.95, prophylactic p = 1, therapeutic p = 0.98). Prophylactic treatment (A) with AuTS resulted in a significant effect on average pole test scores (p =0.017) while therapeutic treatment (B) did not (p = 0.60).

3.3 DISCUSSION

It is intrinsically clear from the data (Figure 10, Figure 11) that, in the caterpillars, all three of the Au(I) compounds are highly effective antidotes to phosphine. That is, the original concept has been at least circumstantially validated in a biological system; Au(I) complexes are indeed able to detoxify phosphine, presumably through scavenging (coordination) and decorporation. Regarding the trials with mice, the compounds are certainly prophylactically effective (Figure 13A) but when administered after the toxicant, any beneficial effects were much more modest in these assays (Figure 13B).

The acute pharmacokinetics of gold(I) salts are not well documented though much is known about chronic use and metabolism on the scale of hours to days [171-173]. After intramuscular injection, Au(I) salts are well-absorbed and maximum circulating concentrations are established a few hours after exposure [172]. In the absence of acute absorption data in mice, we estimated a best-case (100% blood absorption) circulating concentration of ~1.7 mM Au(I) thiosulfate based on the administered dose, mouse body weight, and estimated blood volume. Compared to the estimated range of circulating phosphine (0.46-0.92 mM), this represents a 1.7-3.7-fold excess of Au(I) thiosulfate to phosphine in the blood. When administered orally to humans, as little as 15% of a dose of Au(I) thiomalate is absorbed to the blood (hours after ingestion) [172]. Assuming Au(I) thiosulfate exhibits similar absorption (albeit at a faster rate), the circulating concentration in our mouse model may reach 0.26 mM, a Au(I)-phosphine ratio between 0.28 and 0.57. These ratios are much lower than that for the larval model, which was estimated to have a 20-fold excess of antidote to phosphine. If the ratio of phosphine-ligand binding is 1:1, Au(I) thiosulfate could reduce the circulating phosphine concentration in mice to 0.2 – 0.4 mM. *In vitro*, a 3-fold excess of Au(I) thiosulfate to phosphine successfully prevented

complex IV inhibition in the isolated enzyme (Figure 12). Our results show that prophylactic administration of candidate Au(I) antidotes is more efficacious than therapeutic injection, likely due in part to "lead time" in establishing a circulating antidote concentration.

This result should not, however, be taken to indicate that the approach will ultimately prove to be of no therapeutic application for two main reasons. First, it is presently unclear exactly why Au(I) complexes seem to be significantly therapeutic in the caterpillars (Figure 11) but not the mice (Figure 13B). The compounds may have significantly different pharmacodynamics/kinetic characteristics in the two organisms, in which case, there may be related structures exhibiting such properties more suitable for therapeutic use in mammals. At this juncture, especially given that there is no antidote for phosphine currently available, any detectable ameliorative effect is encouraging. Second, most human victims reach the clinic having ingested a phosphide salt, and the exposure is ongoing as the phosphide continues to release phosphine gas through hydrolysis in the stomach. Additionally, while phosphides are employed as fumigants in western countries, for indoor control of insects and outdoor control of rodents, it is not clear that their use is so effectively regulated worldwide. The recent increase in the application of drones to crop-dusting operations, particularly in Asia, could conceivably lead to future exposures of larger human populations, either through accident or with malicious intent, not to mention the possibility of release by deliberate detonations. Any individuals thus exposed to particulate phosphides dispersed in air will likely have infiltration of phosphide particles into the esophagus and airways, also adhered to clothing. In all such cases, where slow and continuing release of phosphine gas is to be expected, the availability of effective prophylactics to prevent any further toxic dose exacerbating the condition of the victims could have life-saving consequences. The mechanism(s) through which phosphine exerts its toxicity is (are) seemingly complicated [57, 67, 174] and remain(s) incompletely

delineated [42, 60, 78]. We think it pertinent to consider if the present findings shed any light on these matters. For almost half a century, mitochondria have been [75] and continue to be [59] identified as key targets for disruption by phosphine through inhibition of cytochrome *c* oxidase [3, 74, 76, 77, 82]. In response to sublethal phosphine exposure, the *G. mellonella* larvae used in the current study exhibit dose-dependent (Figure 9) temporary paralysis (knockdown), from which they appear to fully recover. This behavior is analogous to that obtained employing the bona fide cytochrome *c* oxidase inhibitors azide, cyanide, and sulfide [131]. Consequently, while we have not set out to examine this particular question rigorously, our observations concerning the caterpillars do appear to be at least consistent with mechanism of acute phosphine toxicity primarily involving inhibition of cytochrome *c* oxidase. If this is so, then it follows that the different response to the antidotes of phosphine-challenged mice (Figure 13) compared to the caterpillars (Figure 11) is plausibly due to another toxic mechanism operating in the mice, which might not involve reversible inhibition of cytochrome *c* oxidase.

In mammals, acute phosphine/phosphide poisoning is reported to lead to death by cardiopulmonary failure, with microscopically visible injury to myocardial tissue [67, 175]. This shares some similarity with acute cyanide and sulfide toxicity in mammals, where death is also the result of cardiopulmonary collapse, but cyanide and sulfide act more rapidly [176, 177] and principally on the central nervous system stimulating cardiopulmonary function [178, 179]. The measured inhibition constant (K_i = 13 μM) and on-rate (k_{on} = 3.3 × 10^3 $M^{-1}{\cdot}s^{-1}$) for phosphine reacting with isolated cytochrome *c* oxidase (Figure 8) are, respectively, 2 orders of magnitude greater an 3 orders of magnitude slower than the corresponding reaction of the enzyme with cyanide [180], in keeping with the less toxic nature of phosphine compared to cyanide. It follows that lethal doses of inhaled phosphine may require prolonged exposure as recently reported [181-

183], but there remains an observable difference between the behavior of phosphine and the better characterized mitochondrial toxicants in mammals, again suggesting that there could be at least one other toxic mechanism in play, possibly non-mitochondrial. Rahimi et al. [87] have recently shown that phosphine poisoning in rats can be ameliorated through blood transfusion, clearly implicating some component of the blood/vasculature as a target for the toxicant. This finding seems to be in keeping with earlier observations [5, 20] that hemolysis and methemoglobinemia may correlate with severity of outcome in aluminum-phosphide-poisoned human patients. There is a paucity of information regarding the reaction of phosphine with hemoglobin and red blood cells, the available literature being more than 25 years old [69, 184]. Further effort in this area now appears to be warranted.

4.0 SILVER(I) AND COBALT(II) COMPOUNDS AS PHOSPHINE ANTIDOTES: RESULTS FROM MOUSE AND INSECT MODELS

Kimberly K. Garrett, Samantha Carpenter Totoni,

Mikayla Kerr, Jim Peterson*, and Linda Pearce*

Department of Environmental and Occupational Health, Graduate School of Public Health,

The University of Pittsburgh, Pittsburgh, Pennsylvania, 15219, United States

*Corresponding Authors: jimmyp@pitt.edu; lip10@pitt.edu

Currently unpublished

4.1 INTRODUCTION

Phosphine (PH_3) gas released from metal phosphides is a top suicide agent in parts of South Asia and much of the Middle East [41-43] and mishandling of phosphide tablets is responsible for many accidental poisonings in Europe and North America [28, 30, 33, 37, 38, 40, 86]. Metal phosphide pellets are used as agricultural fumigants and are easily accessible in most of the world. Upon reaction with air, water, or an acid, phosphide pellets release phosphine, which inhibits mitochondrial complex IV, cytochrome *c* oxidase [57, 185]. No antidote to phosphine poisoning is commercially available; cases are treated with supportive care with inconsistent success [11, 41]. Because of its rapid generation from phosphide pellets and its potency, phosphine has the potential to be used as a weapon of chemical terrorism. Because of its threat to public health, the development of antidotes to phosphine poisoning that can be used both in individual poisonings and mass-casualty exposures is crucial. In past work, our group has identified gold(I)-based compounds that ameliorate phosphine toxicity in an insect and mouse model [186].

According to inorganic principles, phosphine is a "soft" ligand and should bind preferentially to "soft" metals [17, 18]. Gold(I) is the softest metal and in our previous investigation we demonstrated the antidotal activity of some Au(I) compounds against phosphine poisoning [186]. While Au(I) was successful against phosphine, it is quite expensive. Silver(I) is similar to gold(I) in its softness and its compounds are used in a variety of medical applications [17, 18, 105-107]. It is also less expensive than gold. Thus, we propose a variety of Ag(I) compounds as potential phosphine antidotes. In this work, we assessed the potential ameliorative effects of Ag(I) nitrate, Ag(I) lactate, Ag(I) thiosulfate, Ag(I) sulfadiazine, and bis(metronidazole) silver(I) nitrate against phosphine in an insect model. Additionally, we screened hydroxocobalamin (Cb), $Co(II)N_4$[14], and $Co(II)N_4$[11.3.1], identified as antidotes to other

complex IV inhibitors [15, 16]. We identified the most promising candidate antidotes using the insect model then tested them against phosphine in mice. We also studied the interaction of the candidate antidotes with phosphine *in vitro* to further assess candidate viability.

While a decorporation approach may work against phosphine poisoning, it is important to understand other potential impacts of phosphine to determine additional treatment methods. We studied the impacts of phosphine on red blood cells (RBCs) and hemoglobin (Hb). Hemolysis and methemoglobinemia have been reported in cases of phosphine poisoning [9, 24, 25, 184] but the relationship between blood and phosphine remains undefined. Recent evidence suggests that packed RBCs may help prevent phosphine poisoning in a rat model [87]. Based on this evidence, we hypothesized that phosphine induces methemoglobinemia and hemolysis.

4.2 RESULTS

4.2.1 Therapeutic effects of selected Ag(I) and Co(II) compounds in a *G. mellonella* model

We have previously shown that *G.mellonella* larvae are useful models for screening potential antidotes to cytochrome *c* oxidase inhibitors including cyanide, azide, and phosphine [131, 186]. Larvae were exposed, 10 at a time, to 5740 (±340) ppm·min PH_3 for 20 minutes in a sealed chamber (4.8 L). Phosphine was generated from Ca_3P_2 or AlP as described in section 2.3.1. Ten minutes after exposure to phosphine, ~60% of the larvae became paralyzed in "knockdown." The time it took for them to recover (become mobile) from the moment they became paralyzed was monitored and subsequently designated the recovery time, and larvae that did not knock down

were assigned a recovery time of 0 minutes. Larvae that remained incapacitated for 120 minutes rarely recovered within 24 hours, so recovery values were capped at 120 min.

Candidate Ag(I) antidotes were injected (10 μL) into the hemocel via the leftmost distal proleg immediately after the completion of phosphine exposure. Doses of candidate antidotes were chosen at concentrations that resulted in no visible toxicity (Ag(I) lactate, 10 mg/kg; Ag(I) nitrate, 10 mg/kg; Ag(I) bis(metronidazole) nitrate, 50 mg/kg; Ag(I) thiosulfate, 10 mg/kg; Ag(I) sulfadiazine, 9 mg/kg). The Ag(I) complexes were found to be insoluble in phosphate buffered saline (PBS) due to the precipitation of AgCl (K_{sp}l = 1.77 x 10^{10} at room temperature), thus compounds were dissolved in either 50 mM HEPES buffer (Ag(I) lactate, Ag(I) nitrate, and Ag(I) thiosulfate) or HEPES-10% (v/v) DMSO (Ag(I) bis(metronizdazole) nitrate and Ag(I) sulfadiazine). Presumably, direct injection into the hemocel, and thus the fat bodies of the larvae, helped prevent undue precipitation of AgCl in the larvae.

Ag(I) nitrate, Ag(I) sulfadiazine, Ag(I) thiosulfate, and Ag(I) lactate all significantly improved recovery time in the larvae ($p < 0.05$) (Figure 14C). Larvae treated with Ag(I) thiosulfate and Ag(I) lactate demonstrated the best mean recovery times of 14 (±4) and 10 (±3) min, respectively, compared to phosphine exposed controls given no antidote, 39 (±3) min. For comparison, we previously demonstrated that Au(I) thiosulfate, when given therapeutically, lowered the recovery time of phosphine exposed worms to 15 (±4) min. (Figure 11) [186]. Because the strong electrolyte (fully dissociated in aqueous solution) silver nitrate proved antidotal, if less efficient than the other Ag(I) compounds, the primary importance of the Ag^+ ion, rather than the ligands or anions present, is reinforced. Furthermore, the failure of Ag(I) bis(metronidazole) as a potential antidote is noteworthy because this might be due to the more fully occupied first

coordination sphere of the Ag(I) in this complex and/or its nitrogenous donors compared to the other compounds.

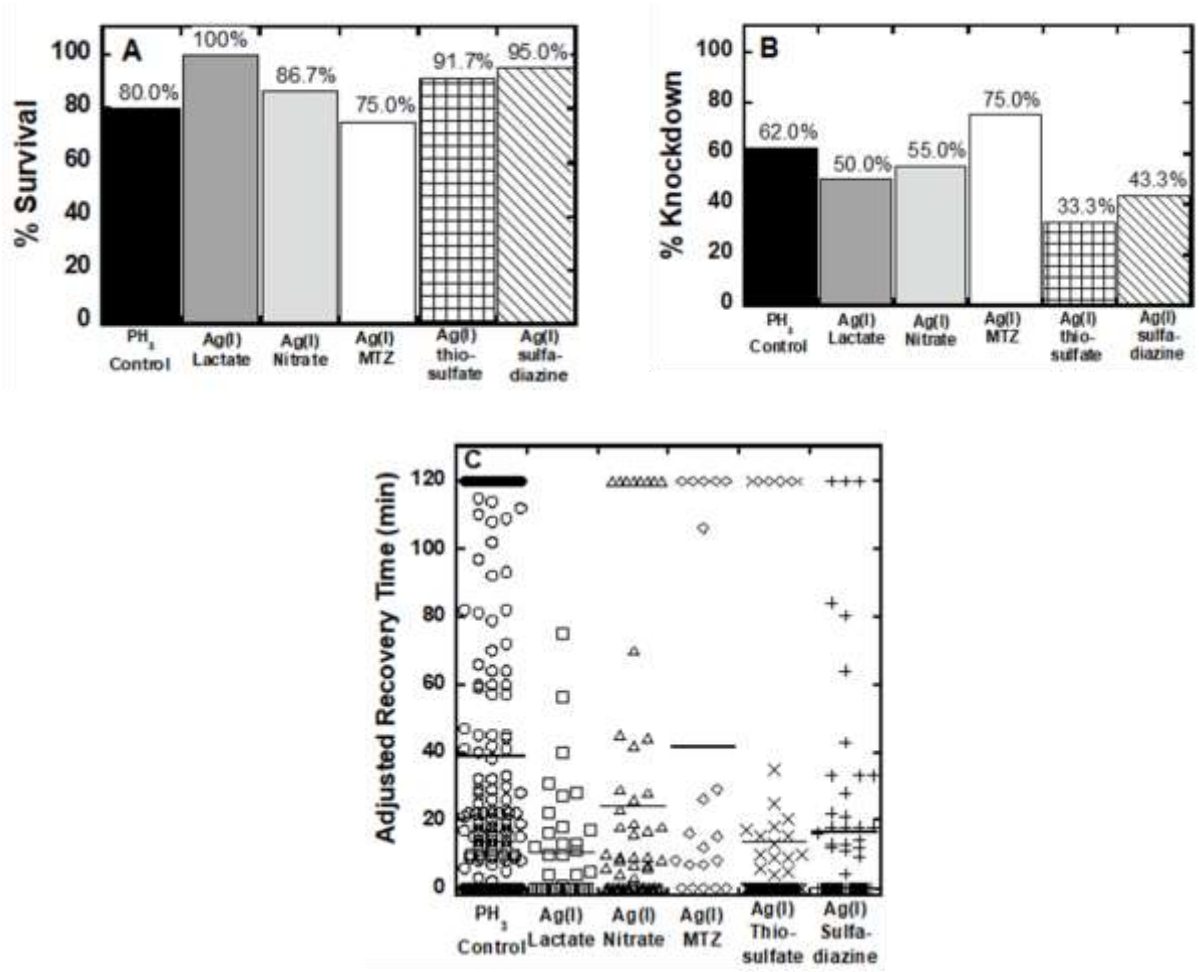

Figure 14. Therapeutic use of Ag(I) lactate, Ag(I) nitrate, Ag(I) bis(metronidazole) nitrate (Ag(I) MTZ)), Ag(I) thiosulfate, and Ag(I) sulfadiazine against PH_3 in *G. mellonella* larvae.

Larvae were injected with the candidate antidotes (Ag(I) lactate, 10 mg/kg; Ag(I) nitrate, 10 mg/kg; Ag(I) bis(metronidazole) nitrate, 50 mg/kg; Ag(I) thiosulfate, 10 mg/kg; Ag(I) sulfadiazine, 9mg/kg) immediately after a PH_3 exposure of 5740 ($\pm$340) ppm·min. Roughly 60% of control larvae were incapacitated after PH_3 exposure (B). Any larvae that did not knockdown were assigned recovery times of 0 min. The few larvae that had recovery times over 2 h were scored as 120 min. Sample sizes (n larvae): PH_3 control = 250, Ag(I) lactate = 40, Ag(I) nitrate = 60, Ag(I) bis(metronidazole) nitrate = 20, Ag(I) thiosuflate = 60, Ag(I) sulfadizaine = 60. (A) Percent survival for

controls and each group with therapeutic treatment, exposure groups compared to controls with a 2-tailed Fisher's Exact Test: PH_3 control (black bar) = 200/250; Ag(I) lactate (dark gray bar) = 40/40, $p = 0.0005$; Ag(I) nitrate (light gray bar) = 52/60, $p = 0.27$; Ag(I) bis(metronidazole) nitrate (white bar) = 15/20, $p = 0.57$, Ag(I) thiosulfate (gridded bar) = 55/60, $p = 0.038$, Ag(I) sulfadiazine (diagonal lined bar) = 57/60, $p = 0.0039$. (B) Knockdown incidence for controls and therapeutic treatment groups, compared with a 2-tailed Fisher's Exact Test: PH_3 control (black bar) = 155/200; Ag(I) lactate (dark gray bar) = 20/40, $p = 0.17$, Ag(I) nitate (light gray bar) = 33/60, $p = 0.38$, Ag(I) bis(metronidazole) nitrate (white bar) = 15/20, $p = 0.34$, Ag(I) thiosulfate (gridded bar) = 20/60, $p < 0.0001$, Ag(I) sulfadiazine (diagonal lined bar) = 26/60, $p = 0.013$. (C) Recovery time for PH_3-exposed larvae treated therapeutically with Ag(I) compounds compared to controls including non-survivors (recovery time ≥ 120 min). Bars represent sample mean. Means were compared using a Kruskal-Wallis chi-square approximation assuming a nonparametric distribution. Mean recovery for PH_3 controls (circles) = 39 (±3.0) min, Ag(I) lactate (squares) = 10 (±2.6) min, $p = 0.0030$, Ag(I) nitrate (triangles) = 24 (±5.2) min, $p = 0.048$, Ag(I) bis(metronidazole) nitrate (diamonds) = 42 (± 12) min, $p = 0.64$, Ag(I) thiosulfate (X marks) = 14 (±4.3) min, $p < 0.0001$, Ag(I) sulfadiazine (plus signs) = 16.6 (±4.0) min, $p = 0.0012$. Data tabulated in Table 4.

Table 4. Mean and median recovery times for *G. mellonella* larvae treated with Ag(I) compounds therapeutically after PH_3 exposure.

Treatment (Therapeutic)	All		Surviving*	
	Mean Recovery Time (±SE) (min)	Median Recovery Time (min)	Mean Recovery Time (±SE) (min)	Median Recovery Time (min)
PH_3 Control	39 (±3.0)	15	18 (±2.0)	7.5
10 mg/kg Ag(I) lactate	10 (±2.6)	0.5	10 (±2.6)	0.5
10 mg/kg Ag(I) nitrate	24 (±5.2)	6	9.3 (±2.1)	0
50 mg/kg Ag(I) bis(metronidazole) nitrate	42 (±12)	14	16 (±6.9)	8.0
10 mg/kg Ag(I) thiosulfate	14 (±4.3)	0	3.8 (±1.0)	0
9 mg/kg Ag(I) sulfadiazine	16 (±4.0)	0	11 (±2.5)	0

*Data labeled "surviving" incorporates larvae with recovery times < 120 min.

Because both Ag(I) and Au(I) thiosulfate (Figure 11, Figure 14) significantly improved recovery times in phosphine-exposed *G. mellonella*, thiosulfate, the counter ion of these Ag(I) complexes, was tested for antidotal activity to ensure the effect was due to the soft metal cation and not the thiosulfate anion [186]. Sodium thiosulfate was found to be less toxic to the larvae than Au(I) or Ag(I) thiosulfate and a dose of 50 mg/kg was selected for these experiments based on the lack of any observed toxicity. Treatment with sodium thiosulfate (50 mg/kg) did not significantly improve recovery times in *G. mellonella* after phosphine exposure (p = 0.39) (Figure 15), confirming that the Ag(I) and Au(I) cationic complexes are responsible for the amelioration of phosphine toxicity [186].

Carrier molecules are often used in drug delivery; they transport small molecules through unfavorable conditions including changes in polarity, pH, and ionic concentration. While DMSO, also used as a carrier molecule, did increase the solubility of some of the Ag(I) compounds (Ag(I)

bis(metronizdazole) nitrate and Ag(I) sulfadiazine) in HEPES buffer, when mixed with PBS, precipitation of AgCl still occurred. As a possible carrier molecule for silver we investigated calix[4]arene sulfonate tetrasodium, part of a diverse group of calix[n]arenes, macrocyclic ligands that contain a hydrophobic cavity which can bind a number of molecules [187, 188]. It was expected, however, that the Ag(I) ions would displace the sodium ions bound to the sulfonate groups (Figure 7). In addition, we found that calix[4]arene sulfonate tetrasodium was not toxic to *G. mellonella* at the desired experimental dose (5 mg/kg, or 0.5x the Ag(I) nitrate dose). The combination of calix[4]arene (5 mg/kg) and a 2-fold excess of Ag(I) nitrate (10 mg/kg), however, was not effective in ameliorating phosphine toxicity and improving recovery times compared to untreated, PH_3-exposed controls (Figure 15).

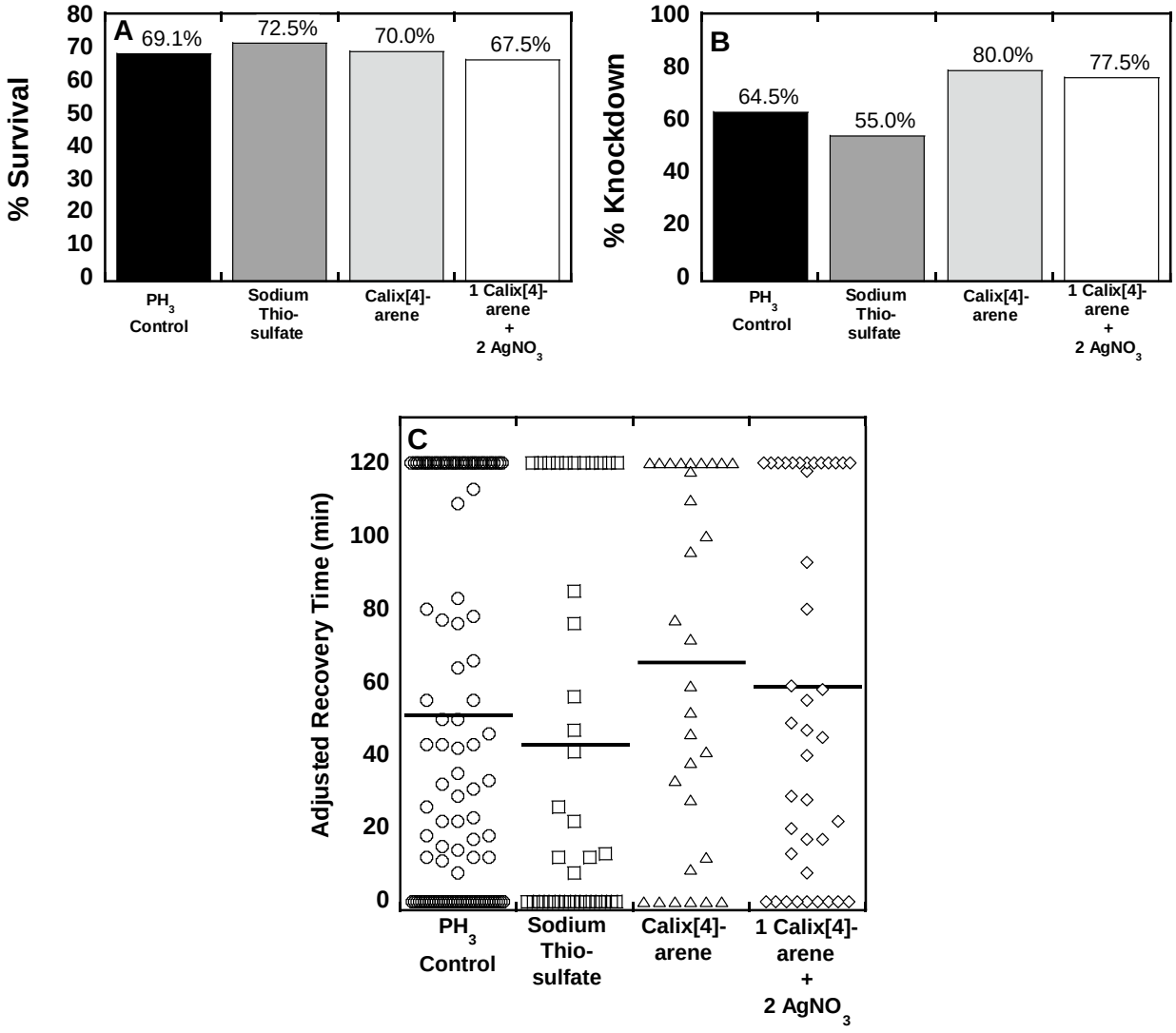

Figure 15. Therapeutic use of sodium thiosulfate, calix[4]arene, and a combination of Ag(I) nitrate with calix[4]arene against PH_3 in *G. mellonella* larvae.

Larvae were injected with the experiment solutions (sodium thiosulfate, 50 mg/kg; tetrasodium calix[4]arene tetrasulfonate, 5 mg/kg; tetrasodium calix[4]arene tetrasoulfonate, 5 mg/kg mixed with $AgNO_3$, 10 mg/kg) immediately after a PH_3 exposure of 5740(±340) ppm·min. The mean time until recovery was measured for each putative antidote vs control (shown as bars). 65% of control larvae were incapacitated after PH_3 exposure. Any larvae that did not knockdown were assigned recovery times of 0 min. Larvae that had recovery times over 2 h were scored as 120 min. Sample sizes (n larvae): PH_3 control = 110, sodium thiosulfate = 40, calix[4]arene = 30, calix[4]arene/$AgNO_3$ = 40. (A) Percent survival for controls and each group with therapeutic treatments, exposure groups were compared to controls with a 2-tailed Fisher's exact test: PH_3 control (black bar) = 76/100, sodium

thiosulfate (dark gray bar) = 29/40, $p = 0.84$, calix[4]arene (light gray bar) = 21/30, $p = 1.0$, calix[4]arene/$AgNO_3$ (white bar) = 27/40, $p = 0.85$. (B) Knockdown incidence for controls and therapeutic treatment grouips, compared with a 2-tailed Fisher's exact test: PH_3 control (black bar) = 71/110, sodium thiosulfate (dark gray bar) = 22/40, $p = 0.34$, calix[4]arene (light gray bar) = 24/30, $p = 0.13$, calix[4]arene/$AgNO_3$ (white bar) = 31/40, $p = 0.17$. (D) Recovery time for PH_3-exposed larvae treated therapeutically with sodium thiosulfate, calix[4]arene, and calix[4]arene/$AgNO_3$ compared to controls including non survivors (recovery time ≥ 120 min). Bars represent sample mean. Means were compared using a Kruska-Wallis chi-square approximation assuming a nonparametric distribution. Mean recovery for PH_3 controls (circles) = 51 (±5.0) min, sodium thiosulfate (squares) = 43 (±8.3) min, $p = 0.32$, calix[4]arene (triangles) = 66 (±9.0) min, $p = 0.20$, calix[4]arene/$AgNO_3$ (diamonds) = 59 (±8.0) min, $p = 0.30$. Data tabulated in Table 5.

Table 5. Mean and median recovery times for *G. mellonella* larvae treated with sodium thiosulfate, calix[4]arene, and a calix[4]arene-$AgNO_3$ mixture therapeutically after PH_3 exposure.

Treatment (Therapeutic)	All		Surviving*	
	Mean Recovery Time (±SE) (min)	Median Recovery Time (min)	Mean Recovery Time (±SE) (min)	Median Recovery Time (min)
PH_3 Control	51 (±5.0)	32	21 (±3.3)	0
50 mg/kg Sodium thiosulfate	43 (±8.3)	12	14 (±4.5)	0
5 mg/kg calix[4]arene	66 (±9.0)	66	42 (±8.7)	38
5 mg/kg calix[4]arene + 10 mg/kg $AgNO_3$	59 (±8.0)	48	30 (±6.2)	20

*Data labeled "surviving" incorporates larvae with recovery times < 120 min.

When the Ag(I) nitrate/calix[4]arene sulfonate tetrasodium solution in HEPES buffer was dissolved in PBS, a precipitate, AgCl, immediately formed (Figure 16A and B). When the calix[4]arene and Ag(I) were incubated overnight, we observed the precipitation of what appeared to be silver oxide (Figure 16C). Samples combined with calix[4]arene reproduced the solubility

problems previously observed with Ag(I) and chloride. Thus, calix[4]arene sulfonate tetrasodium is not a likely candidate for a Ag(I) carrier molecule in its present form.

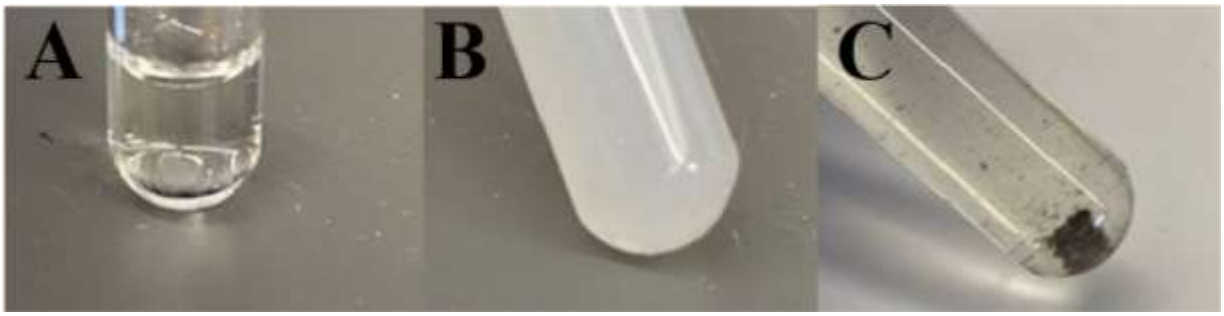

Figure 16. Precipitation of Ag(I) compound from Calix[4]arene sulfonate tetrasodium solution upon addition of PBS.

A solution of 0.3 mM calix[4]arene sulfonate tetrasodium and 3 mM $AgNO_3$ in 50 mM HEPES buffer (pH 7.4) was incubated at room temperature for 30 minutes then diluted in an equal volume of PBS buffer (pH 7.4, final concentration = 0.15 mM calix[4]arene sulfonate tetrasodium and 0.15 mM $AgNO_3$). Images are representative from multiple trials. (A) stock solution after incubation for 30 minutes, before PBS suspension showing no precipitate (B) solution approximately 5 minutes after dilution in PBS showing suspended precipitate, (C) solution 24 hours after dilution in PBS showing dark preceipitate collected at the bottom of test tube.

In addition to the Ag(I) compounds, we also tested some Co(II) complexes that were found to ameliorate both cyanide and azide toxicities [15, 16, 131] at doses that showed no behavioral toxicity: (Hydroxocobalamin (Cb), 82 mg/kg; Co(II)N_4[14], 31 mg/kg; Co(II)N_4[11.3.1], 28 mg/kg). Initially, these experiments were conceived purely as controls, Co(II) being a "harder" metal than Au(I) or Ag(I). The cobalt complexes were injected in a similar fashion to the silver complexes (10 μL into the hemocoel), 5 minutes after phosphine exposure (5740 ±340 ppm·min over a 20 min time span). Surprisingly, Co(II)N_4[11.3.1] treatment was associated with significant improvement in recovery time, 7.4 (±4.1) min vs 39 (±3) min for controls, $p < 0.001$(Kruskal-

Wallis chi-quare approximation) (Figure 17), with only 27% of the larvae becoming incapacitated (compared to 62% of controls, $p = 0.0003$, 2-tailed Fisher's exact test). This antidotal effect is comparable to that observed for the Au(I) and Ag(I) compounds. Neither Cb nor Co(II)N_4[14] showed any significant improvement in recovery time compared to controls. Because Ag(I) lactate and Co(II)N_4[11.3.1] significantly improved recovery times therapeutically for phosphine-exposed larvae, these potential antidotes were subsequently chosen to test against phosphine toxicity in mice.

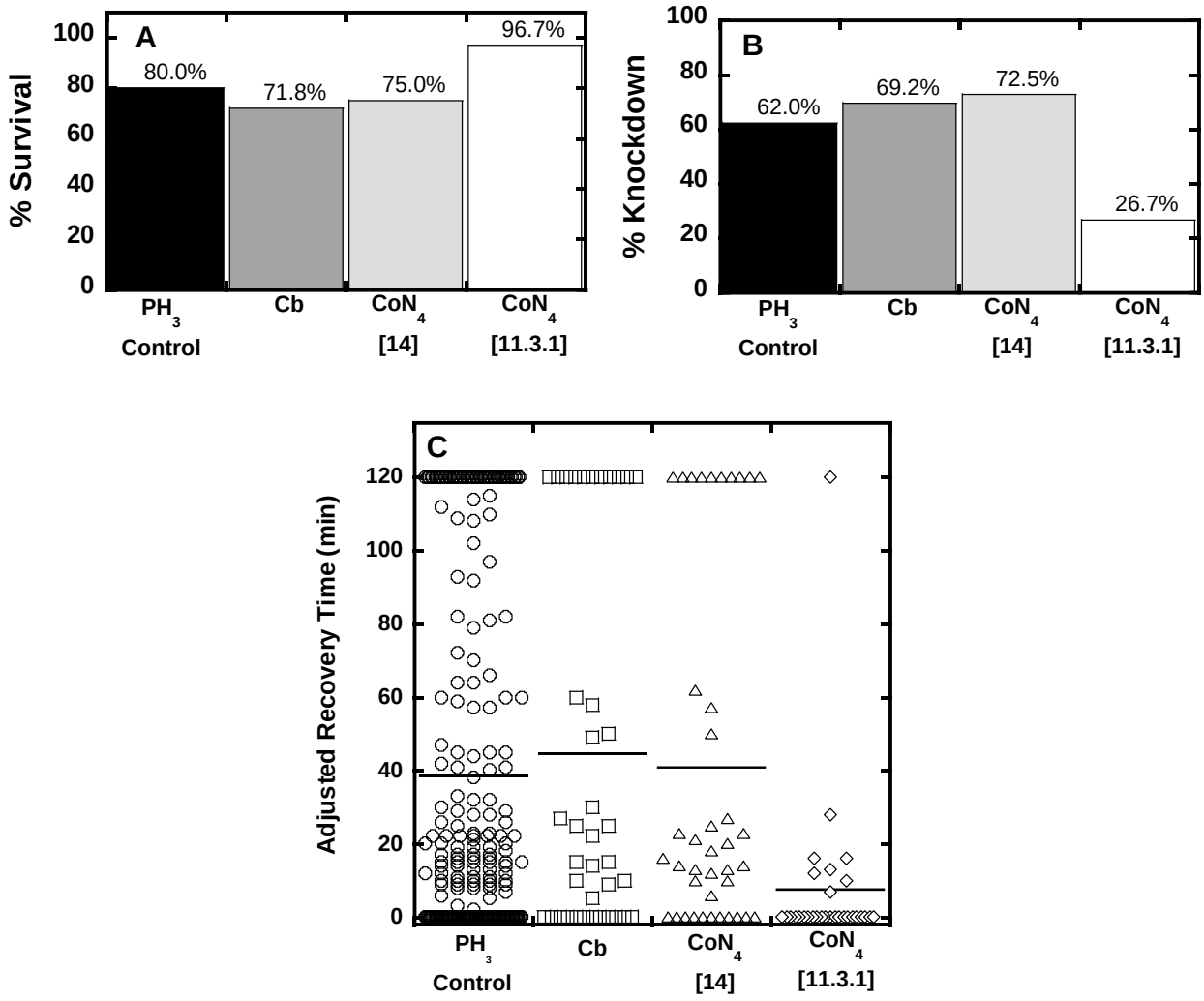

Figure 17. Therapeutic use of hydroxocobalamin (Cb), Co(II)N$_4$[14], and Co(II)N$_4$[11.3.1] against PH$_3$ in *G. mellonella* larvae.

Larvae were injected with the candidate antidotes immediately after a PH$_3$ exposure of 5740 (±340) ppm·min. Roughly 80% of the control larvae were incapacitated after PH$_3$ exposure. Any larvae that did not knockdown were assigned recovery times of 0 min. The few larvae that had recovery times of over 2 h were scored as 120 min. Sample sizes (n larvae): PH$_3$ control = 250, Cb = 39, Co(II)N$_4$[14] = 40, Co(II)N$_4$[11.3.1] = 30. (A) Percent survival for controls and each group with therapeutic treatment, exposure groups compared to controls with a 2-tailed Fisher's Exact Test: PH$_3$ control (black bar) = 200/250; Cb (dark gray bar) = 28/39, p = 0.29; Co(II)N$_4$[14] (light gray bar) = 30/40, p = 0.53; Co(II)N$_4$[11.3.1] (white bar) = 29/30, p = 0.023. (B) Knockdown incidence for controls and therapeutic treatment groups, compared with a 2-tailed Fisher's Exact Test: PH$_3$ control (black bar) = 155/200;

Cb (dark gray bar) = 27/39, $p = 0.48$, Co(II)N_4[14] (light gray bar) = 27/39, $p = 0.22$, Co(II)N_4[11.3.1] (white bar) = 8/30, $p = 0.0003$. (D) Recovery time for PH_3-exposed larvae treated therapeutically with cobalt compounds compared to controls including non-survivors (recovery time ≥ 120 min). Bars represent sample mean. Means were compared using a Kruskal-Wallis chi-square approximation assuming a nonparametric distribution. Mean recovery for PH_3 controls (circles) = 39 (±3.0) min, Cb (squares) = 45 (±8.1) min, $p = 0.34$, Co(II)N_4[14] (triangles) = 41 (±7.7) min, $p = 0.40$, Co(II)N_4[11.3.1] (diamonds) = 7.4 (±4.1) min, $p < 0.0001$. Data tabulated in Table 6.

Table 6. Mean and median recovery times for *G. mellonella* larvae treated with sodium thiosulfate, calix[4]arene, and a calix[4]arene-$AgNO_3$ mixture therapeutically after PH_3 exposure.

Treatment (Therapeutic)	All		Surviving*	
	Mean Recovery Time (±SE) (min)	Median Recovery Time (min)	Mean Recovery Time (±SE) (min)	Median Recovery Time (min)
PH_3 Control	39 (±3.0)	15	18 (±2.0)	7.5
82 mg/kg Cb	45 (±8.1)	22	15 (±3.6)	9.5
31 mg/kg Co(II)N_4[14]	41 (±7.7)	17	15 (±3.1)	13
28 mg/kg Co(II)N_4[11.3.1]	7.4 (±4.1)	0	3.5 (±1.3)	0

*Data labeled "surviving" incorporates larvae with recovery times < 120 min.

4.2.2 Prophylactic and therapeutic effects of Ag(I) lactate and Co(II)N_4[11.3.1] in a mouse model

Swiss-Webster mice were exposed to 3200 (±500) ppm·min PH_3 for 15-20 min in a 4.8 L closed container in a similar fashion to the *G. mellonella* larvae (see section 2.3.2). Mice were tested using a behavioral assay, a modified pole test [131]. Two mice were placed in the container to be exposed to phosphine simultaneously; one served as a control (phosphine exposure alone) and one received the potential antidote. Candidate antidotes were administered via IP injection either 5 minutes before or immediately after phosphine exposure. Pole test scores did not vary

significantly over time (analyzed by Kruskal-Wallis rank sum test with chi-square approximation, control $p = 0.99$, treatment $p = 0.98$). Thus, average pole test scores were compared independent of time. Prophylactic treatment with 7.5 mg/kg Ag(I) lactate did not result in a statistically significant improvement in average pole test scores compared to controls ($p = 0.11$, individual averages compared using a Wilcoxon sign-ranked test for paired data) (Figure 18). We noticed that in two trials, control mice recovered fairly quickly after phosphine exposure while the paired mouse that received Ag(I) lactate remained inhibited. This could mean that the antidote has previously-unidentified toxic effects at the current dose (perhaps due to solubility constraints discussed below). Even with these points removed, prophylactic Ag(I) lactate treatment did not significantly improve average pole test scores compared to controls ($p = 0.063$, Wilcoxon sign-ranked test for paired data).

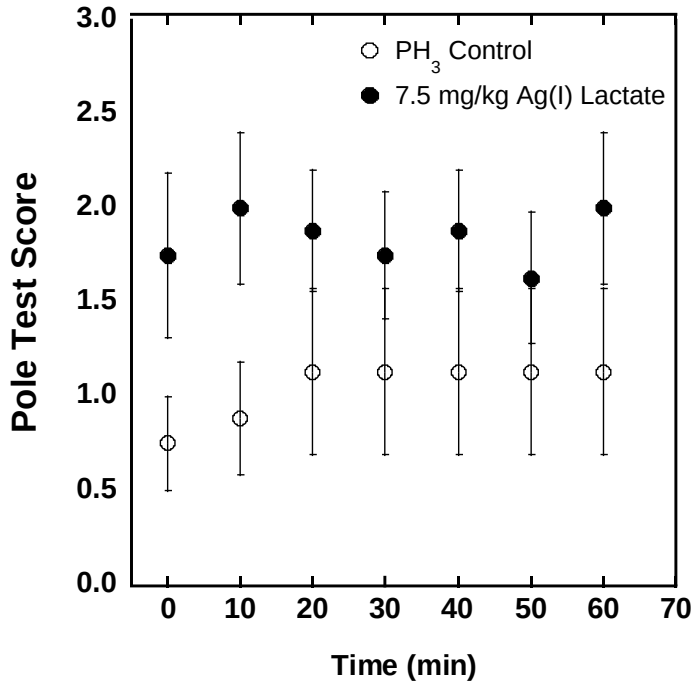

Figure 18. Prophylactic use of silver(I) lactate against PH_3 in mice.

Mice were administered 7.5 mg/kg silver lactate intraperitoneally five minutes before a phosphine exposure of 3200 (±500) ppm·min. The mice were examined using a behavioral assessment (pole-climbing test, see 2.3.2) to evaluate intoxication and recovery. Bars represent standard error. Sample sizes (n mice) = 8 control, 8 7.5 mg/kg Ag(I) lactate treatment. Time-dependent average pole test scores from untreated, PH_3-exposed controls (open circles) and mice that received 7.5 mg/kg (closed circles) Ag(I) lactate 5 minutes before PH_3 exposure. The relationship of pole test score to time was assessed using a Kruskal-Wallis rank sum test with chi-square approximation assuming a nonparametric distribution. Pole test scores did not vary significantly over time (control $p = 0.99$, treatment $p = 0.98$). Time-independent average scores between treatment and control groups were compared using a nonparametric Wilcoxon Rank Sign test for paired data. Prophylactic treatment resulted did not result in signficant improvement in average pole test scores compared to untreated, phosphine-exposed controls ($p = 0.11$).

We did not perform therapeutic experiments with Ag(I) lactate because of solubility concerns. We were unable to store injection stock solutions of Ag(I) lactate (15 mM) in HEPES buffer for longer than ~45 minutes at room temperature before a precipitate formed. Stock

solutions were made fresh for each experiment and 7.5 mg/kg was determined to be near to the NOAEL, the highest dose possible before mice displayed visible discomfort and signs of toxicity. Presumably, the magnitude of the antidotal effect would not be conserved upon therapeutic administration (based on our findings with Au(I) (Figure 13)) unless we are able to administer a higher dose. Also, it should be noted that the observed effect of prophylactic treatment with Ag(I) lactate is less than that observed with Au(I) thiosulfate (Figure 13). As previously noted, Ag(I) compounds have low solubility in chloride solutions and the Ag(I) lactate most likely precipitated after injection into the intraperitoneal space due to the chloride concentration (similar to PBS). While prophylactic Ag(I) lactate indeed improved pole test scores, these constraints limit its usefulness as an antidote. It appears then that we need something like an auxiliary complexing agent to "transport" the Ag(I) ions and prevent them from precipitating before they can react with the toxicant.

In similar experiments, mice were treated with 28 mg/kg $Co(II)N_4$[11.3.1] injected IP 5 minutes prior to or immediately after phosphine exposure (3200 (±500) ppm·min for 15-20 min). The average pole test score for mice treated therapeutically with $Co(II)N_4$[11.3.1] (Figure 19, closed circles) was, with the exception of a single time point, greater than the untreated controls (Figure 19, open squares). Pole test scores did not vary widely over time (control $p = 0.99$, prophylactic $p = 0.99$, therapeutic $p = 0.50$, compared using a Kruskal-Wallis rank sum test). That therapeutic treatment has a higher correlation to time (a p-value of 0.50) is attributed to the magnitude of difference from controls at 0 min (Figure 19). When the 0 minute time point was removed, the relationship between pole test score and time was similar to the other groups ($p = 0.95$). Thus, individual scores were compared as time-independent averages. Neither prophylactic nor therapeutic treatment with $Co(II)N_4$[11.3.1] significantly impacted average pole test scores

compared to phosphine-exposed controls (p = 0.77 and 0.59, respectively, compared using a Wilcoxon sign-ranked test for paired data). Average pole test scores of treated mice were not statistically different from controls when the initial time point (0 min) was excluded (prophylactic p = 0.77, therapeutic p = 0.68, Wilcoxon sign-ranked test for paired data).

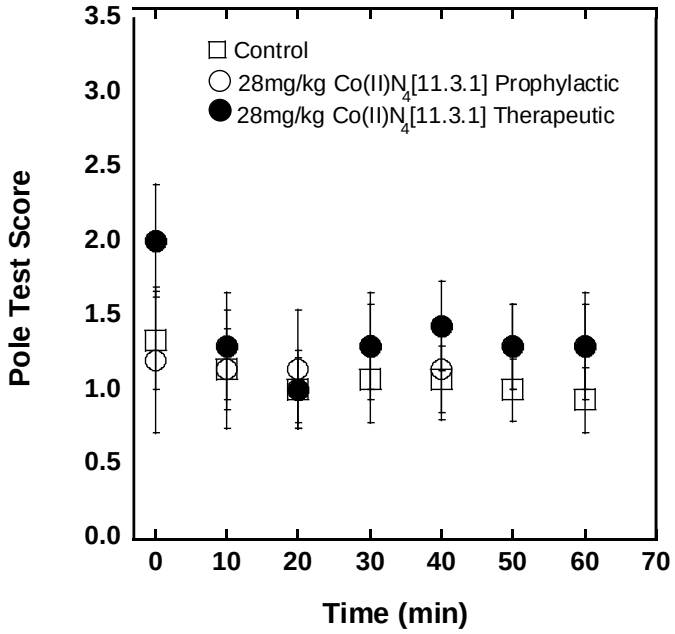

Figure 19. Prophylactic and therapeutic use of Co(II)N$_4$[11.3.1] against PH$_3$ in mice.

Mice were administered 28 mg/kg Co(II)N4[11.3.1] intraperitoneally five minutes before (closed circles) or immediately after (open circles) a phosphine exposure of 3200 (±500) ppm·min. The mice were examined using a behavioral assessment (pole-climbing test, see section 2.3.2) to evaluate intoxication and recovery. Sample sizes (n mice) = 14 control, 7 prophylactic, 7 therapeutic. Pole test scores compared to time were analyzed using a Kruskal-Wallis rank sum test with chi-square approximation assuming a nonparametric distribution. Pole test scores did not change signfiicantly over time (control p = 0.99, prophylactic p = 0.99, therapeutic p = 0.50). Paired pole test scores were assessed using a nonparametric Wilcoxon rank sign test and neither prophylactic nor therapeutic treatment resulted in significant improvement over paired controls (p = 0.77 and 0.59, respectively).

4.2.3 Potential PH_3 –mediated hemolysis and hemoglobin oxidation in mice

Rahimi and colleagues (2018) found that blood transfusions were helpful in ameliorating phosphine toxicity in rats and other researchers have found evidence for hemolysis and methemoglobin production in cases of phosphine poisoning [5, 20, 24, 25, 87]. We investigated whether phosphine might 1) increase the oxidation of hemoglobin (increase metHb levels) and/or 2) cause red blood cell (RBC) lysis. When RBCs are lysed, Hb is released and is easily detected in extracellular media (*i.e.* plasma) using electronic absorption spectroscopy as Hb has a very high extinction coefficient (~100,000 M^{-1} cm^{-1} per heme). Isolated mouse blood was mixed with varying amounts of phosphine, using phosphine-saturated buffer (11.6 mM) along with EDTA to prevent clotting, at concentrations 0.2-5.8 mM phosphine. Following incubation, for times of 15 min to one hour (Table 7) samples were centrifuged and the supernatant of the packed RBCs was monitored spectrophotometrically for the presence of Hb. The amount of Hb in the PH_3-treated samples was primarily oxyHb (415 nm maximum) and was indistinguishable from that of the negative controls (Table 7). MetHb (405 nm maximum) was not detected in the supernatant of the phosphine-exposed samples nor in that of controls. Phosphine-exposed RBCs showed no significant lysis over a 60 minute period, even at 5.8 mM PH_3 concentrations (Table 7). Small amounts of metHb are difficult to detect over a background of large amounts of oxyHb by electronic absorption spectroscopy. MetHb can be easily detected by electron paramagnetic resonance (EPR) spectroscopy where the signals due to metHb emerge from an essentially zero background.

Table 7. Lack of hemolysis in isolated RBCs exposed to PH_3.

Sample	% Hemolysis	±SE
Control (-) diluted in PBS	0.33	0.12
Control (+) diluted in H_2O	100	2.3
0.3 – 5.8 mM PH_3	0.28	0.02
5.8 mM PH_3 (15-60 min)	0.32	0.04

RBCs were isolated from fresh whole mouse blood, suspended in PBS, and exposed to various amounts of aqueous PH_3 to test concentration-dependence and for various lengths of time to test time-dependence. Positive controls were exposed to deionized water and negative controls to isotonic PBS. After exposure, intact RBCs were pelleted and the supernatant was sampled for free oxyhemoglobin using electronic absorption spectroscopy to monitor absorbance at 415 nm. These values were translated into % hemolysis with positive controls as 100%.

In order to establish if any metHb formation occurs latently in phosphine-exposed mice, whole blood was taken from control mice (used in antidote screening experiments after exposure to phosphine, see above) immediately after sacrifice, 60 min after phosphine exposure. Samples were mixed with EDTA to prevent clotting, transferred to quartz EPR tubes, then immediately frozen and stored in liquid nitrogen for later analysis (see section 2.3.6). The only EPR signals arising from Hb are those of metHb (the Fe(III) form inactive in oxygen transport). OxyHb (oxygen-bound) and deoxyHb (Fe(II) form with no oxygen bound) are EPR silent. Thus, unlike electronic absorption spectroscopy, detection of metHb by EPR spectroscopy is over an essentially zero (EPR) background. MetHb can have additional signals due to what is known as the alkaline transition. A water molecule bound to the iron site (metHbH_2O) can lose a proton to form hydroxide (metHbOH) inducing a high- to low-spin transition. Therefore metHb can have both high spin signals (metHbH_2O, S=5/2) and low spin signals (metHbOH, S = 1/2) due to the strong field hydroxo ligand. In reality, the low spin signals are more difficult to observe and generally are

lower in concentration at neutral pH compared to the high spin signals found at 1100 and 3400 ($g_{parallel}$ and $g_{perpendicular}$). EPR samples of the blood of phosphine-exposed mice did not contain notable levels of methemoglobin. These signals were indistinguishable from those from mice that were not exposed to phosphine. A representative EPR spectrum from a phosphine-exposed mouse is shown in Figure 20, where the low field (1100 gauss) signal is denoted by the # symbol. At ~1500 gauss, we can observe a signal due to transferrin (marked by the * symbol), normally found in blood at ~50 μM, for comparison. The amount of metHb quantitates to less than 20 μM (> 1% of the total Hb in blood). In the short term, over the initial 1 hour period after the mice were exposed to phosphine, we can find no evidence for RBC lysis or any metHb formation in freshly drawn blood.

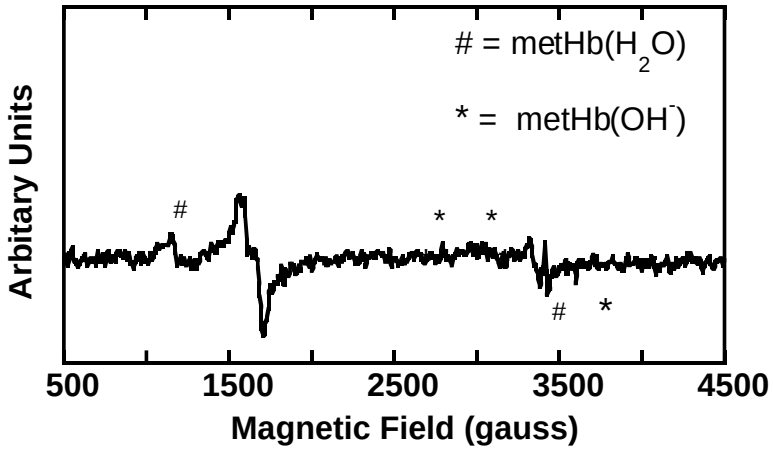

Figure 20. Representative X-band EPR spectra of the blood of PH_3-exposed mice.

Mice were exposed to 3200 (±500) ppm·min for ~20 min (time adjusted for mouse weight). Blood was taken from mice immediatley after sacrifice, 1 hour after the end of exposure. Resulting spectra showed < 1% methemoglobin in the blood of PH_3 – exposed mice. Asterisks and hashtags represent the location of characteristic spectra of methemoglobin species.

4.2.4 Unusual complication of PH_3 exposure in mice

During our experiments in the mouse model, we observed an unreported symptom in some phosphine exposed mice: the development of cataracts at least 30 minutes after the end of phosphine exposure (Figure 21). Affected mice displayed impaired blink reflex response and decreased exploratory behavior. Only 20% of exposed organisms developed these issues and this did not correlate with survival status (Table 8, analyzed with two-sided fisher's exact test). Cataracts did not develop uniformly; some organisms had only one cloudy eye (Figure 21B).

Table 8. Incidence of observed vision impairment in mice after inhalational PH_3 exposure.

(A)		Blink Response	
		+	-
Survival	+	30	8
	-	5	1

(B)		Blink Response	
		+	-
CoN_4[11.3.1] Treatment	+	11	3
	-	11	3

(C)		Blink Response	
		+	-
Ag(I) Lactate Treatment	+	6	2
	-	7	1

Contingency tables show the incidence of vision loss as measured by the eye blink reflex test (see section 2.3.2) in PH_3-exposed mice (3200 (±500) ppm·min PH_3 for a maximum of 20 min, exposure time adjusted for mass, see section 2.3.2) compared using a two-tailed Fisher's exact test and grouped by (A) survival (p = 1.0) and treatment: (B) 28 mg/kg CoN_4[11.3.1] administered 5 minutes before or immediately after PH_3 exposure (p = 1.0), (C) 7.5 mg/kg Ag(I) lactate administered 5 minutes before PH_3 exposure (p = 1.0). No significant relationships were observed between survival, treatment, and incidence of vision impairment or cataracts.

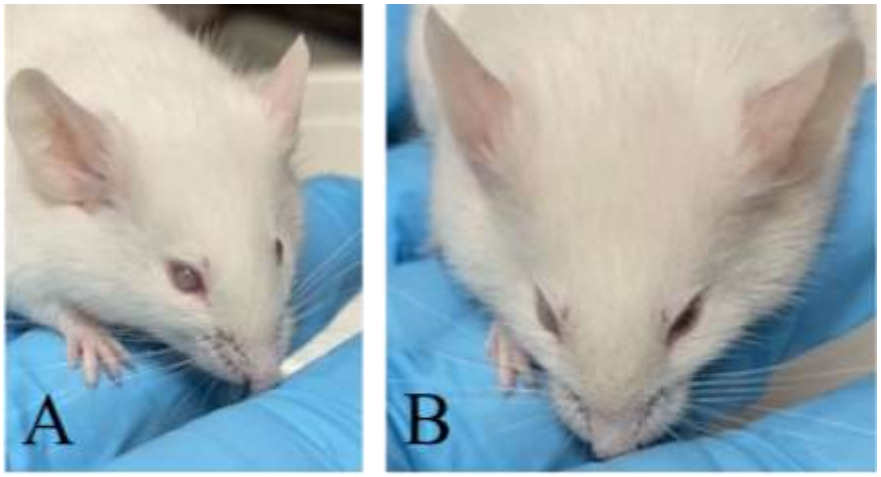

Figure 21. Cataract development in phosphine-exposed mice.

Mice were exposed to 3200 (±500) ppm·min PH_3 for a maximum of 20 min (exposure time adjusted for weight) in a 4.8 L chamber as described in section 2.3.2. Mice were monitored for PH_3 toxicity for 1-2 hours after PH_3 exposure. Vision loss developed in 20% of mice at least 30 minutes after the end of PH_3 exposure and were not correlated to treatment status or survival.

4.2.5 Reduction of Co(III)N_4[11.3.1] by PH_3

Because phosphine is known to be a strong reductant [7], we hypothesized that it reduces Co(III)N_4[11.3.1] to Co(II)N_4[11.3.1]. Co(III)N_4[11.3.1] (1 mM) in 500 mM sodium phosphate buffer (pH 7.4) was titrated with increasing amounts of aqueous phosphine under anaerobic conditions at 21 °C while monitoring the absorbance changes between 300 and 700 nm using electronic absorption spectroscopy. As previously described, Co(II)N_4[11.3.1] has a characteristic spectrum with a peak at 460 nm while Co(III)N_4[11.3.1] is very weak in the same range. When 1/2 of an equivalent of phosphine was added to Co(III)N_4[11.3.1], the resulting spectrum is indistinguishable from that of Co(II)N_4[11.3.1] (Figure 22A, dotted trace) [98]. A plot of the absorbance values at 460 nm upon addition of phosphine shows that the reaction has reached > 90% completion at this same ratio (Figure 22B, dotted line). This shows that phosphine reduces

Co(III)N_4[11.3.1] to Co(II)N_4[11.3.1] through a two-electron reduction similar to the reduction of the oxidized cobalt complex by sodium ascorbate [98].

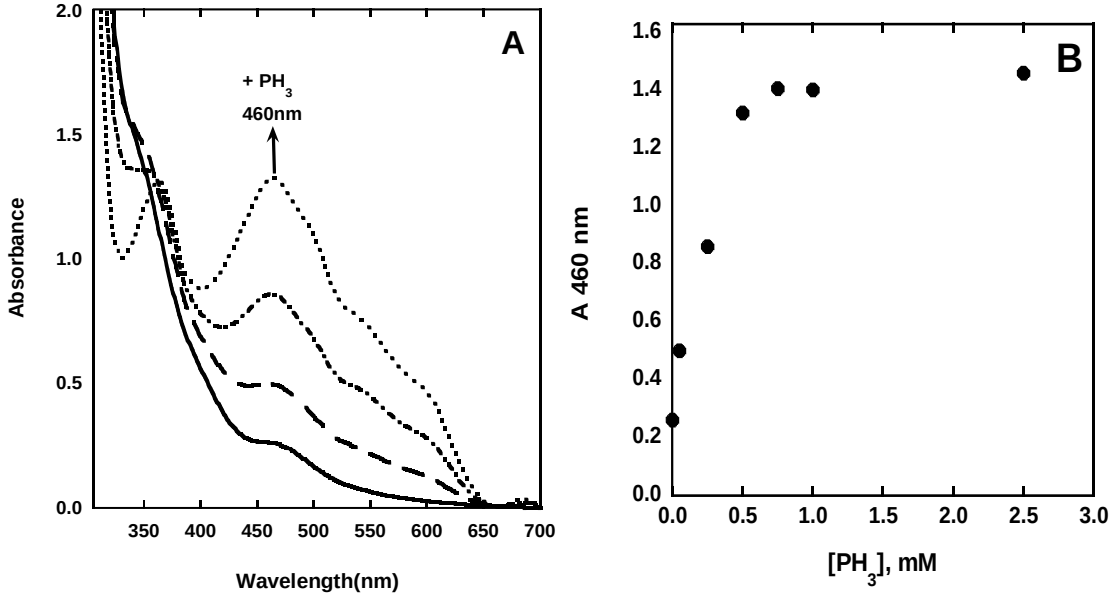

Figure 22. Anaerobic titration of Co(III)N_4[11.3.1] with PH_3.

Increasing amounts of aqueous PH_3 were added to Co(III)N_4[11.3.1] (1 mM) in 500 mM sodium phosphate buffer (pH 7.4) under anaerobic conditions. (A) Electronic absorption spectra of the reduction of Co(III)N_4[11.3.1] by PH_3. 1 mM Co(III)N_4[11.3.1] (thick solid trace) with additions of 0.05 mM PH_3 (dashed trace), 0.25 mM PH_3 (dot-dash trace), and 0.5 mM PH_3. (B) Absorbance values at 460 nm upon addition of PH_3 to 1 mM Co(III)N_4[11.3.1].

4.2.6 H_2O_2 production in the oxygen consumption reaction of Co(II)N_4[11.3.1] and PH_3

The well-known reduction of oxygen to water by metal catalysts (including cytochrome *c* oxidase) often includes the production of H_2O_2 as an intermediate. In our previous examination of the oxygen consumption of Co(II)N_4[11.3.1] in the presence of ascorbate, we detected the presence of 1-2 μM H_2O_2 [15]. This was consistent with our proposed mechanism for this activity based on other metal complexes [15].

The reaction between Co(II)N_4[11.3.1] and phosphine was carried out under several different reaction conditions and the solutions were examined for the production of H_2O_2 using the Amplex® UltraRed probe (see 2.3.4). Hydrogen peroxide concentrations were quantified using a standard curve (Figure 23B). The reaction between Co(II)N_4[11.3.1] and phosphine indeed produces H_2O_2, and the concentration of H_2O_2 increased as a ratio of phosphine to Co(II)N_4[11.3.1] (Figure 23A). At a ratio of ~10 to 20 PH_3/Co(II)N_4[11.3.1], the production of H_2O_2 reached a maximum of ~1.5 μM (Figure 23A). In the respirometric experiments, roughly 150 μM oxygen reacts (Figure 26); if H_2O_2 was the end product, one would expect to see at least half that amount produced (Equation 10C). Because the observed concentration of H_2O_2 was much less than 75 μM this possibility is likely excluded and H_2O_2 is probably an intermediate in the conversion of oxygen to water. In addition, a report also notes that phosphine does not react with H_2O_2 [52].Since the concentration of H_2O_2 was observed to increase with the increasing ratio of PH_3 to cobalt complex, this suggests the first step in this mechanism (Equation 10A) is faster than the reduction of H_2O_2 to water.

$$PH_3 + 2\ Co^{3+} + H_2O \rightarrow\ H_3PO + 2\ Co^{2+} + 2\ H^+ \qquad (A)$$

$$2\ Co^{2+} + 2\ O_2 \rightarrow 2\ Co^{3+} + 2\ O_2^- \qquad (B)$$

$$2\ O_2^- + 2\ H^+ \xrightarrow{Co^{3+}} O_2 + H_2O_2 \qquad (C)$$

$$H_2O_2 + PH_3 \xrightarrow{Co^{3+}} H_3PO + H_2O \qquad (D)$$

Equation 10. Potential rapid reduction of oxygen to water mediated by CoN_4[11.3.1] (written as $Co^{2+/3+}$) with phosphine as a source of electrons.

Representative scheme of the oxygen consumption of CoN_4[11.3.1] upon reduction. Note: The Co^{3+} in equations (C) and (D) is a catalyst.

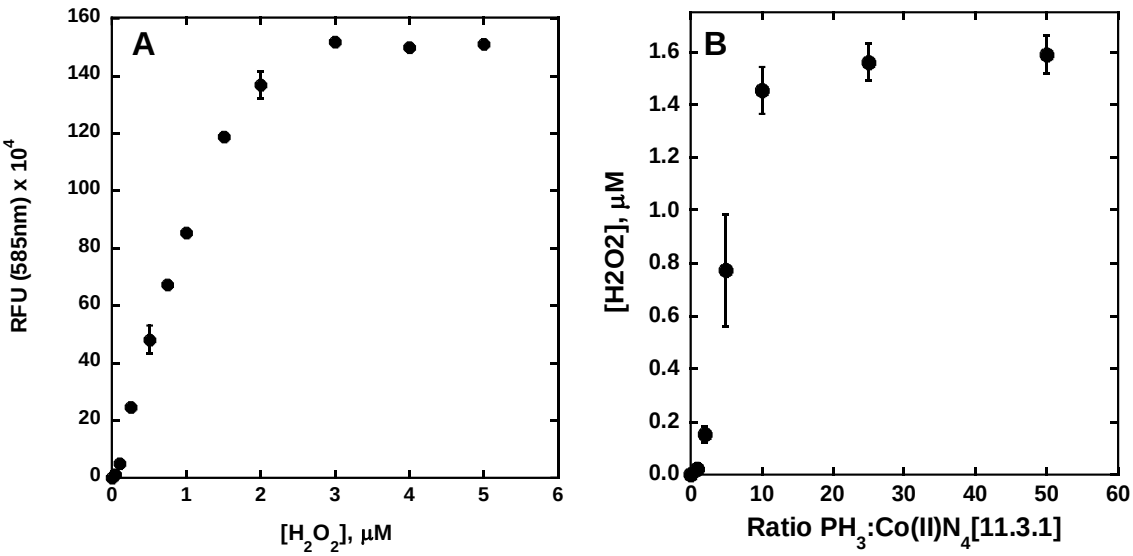

Figure 23. H_2O_2 production during the oxygen consumption reaction of Co(II)N_4[11.3.1], O_2 and phosphine. (A) Standard curve using Amplex® UltraRed/horseradish peroxidase assay used to determine H_2O_2 as described in section 2.3.4. (B) Co(II)N_4[11.3.1] (0.12 µM–5 mM) in 50 mM sodium phosphate buffer, pH 7.4, was incubated with increasing amounts of phosphine (5-11 mM) under aerobic conditions at 21 °C for 30 min and H_2O_2 concentration determined by Amplex® UltraRed/horseradish peroxidase assay and comparison to the standard curve (A).

4.2.7 Binding of phosphine to Co(II)N_4[11.3.1]

As Co(II) is an intermediate cation on the Pearson's scale of hard-soft cations [99], we did not expect strong binding between the cobalt complex and phosphine. Still, any interaction between the Co(II) complex and phosphine is notable. Since phosphine reacts with oxygen to form oxy-phosphorous compounds that ultimately lead to phosphate and Co(II)N_4[11.3.1] is also oxidized to Co(III) in the presence of oxygen, the reaction of these two compounds was examined anaerobically. Aqueous phosphine solutions were prepared through the reaction of AlP with deoxygenated PBS (pH 7.4) in septa-sealed vials with minimal headspace and transfers of

solutions were performed using gastight syringes. Titrations were performed by adding increasing amounts of aqueous phosphine to constant concentrations of Co(II)N_4[11.3.1] in PBS buffer (pH 7.4) with minimal headspace and solutions were monitored using electronic absorption spectroscopy from 300-700nm. Co(II)N_4[11.3.1] has a characteristic peak at 460 nm that can be used to identify it in solution. A new peak in the spectrum appeared at 425 nm upon addition of at least a 50-fold excess of phosphine (Figure 24A) and the peak at 460 nm due to Co(II)N_4[11.3.1] was considerably diminished upon the addition of a 100-fold excess of phosphine. The reaction, monitored at 425 nm, does not appear to reach an end point even with the addition of a 200-fold excess of phosphine (Figure 24B). The phosphine concentration cannot be increased much more as its solubility is limited to ~11 mM in aqueous solution and Co(II)N_4[11.3.1] has a low extinction coefficient, thus increasing the difficulty of the measurements. We can, however, fit the electronic absorption data (Figure 24B) using Equation 9 (see Methods) using nonlinear least squares analysis and thus estimate a binding constant. Using the absorption coefficients for the Co(II)N4[11.3.1] compound at 425 nm, the calculated concentration of the cobalt complex, the fact that phosphine has no absorption at that wavelength and the method of Hargrove et al [152], the binding of phosphine to the cobalt complex was investigated by fitting the changes in absorption (Equation 9). Because we could not reach an endpoint in the titration, this was floated in the calculation and the binding equilibria was found to be 0.08 (±0.02). This equilibrium constant, below zero, is indicative of low binding of phosphine to the cobalt complex.

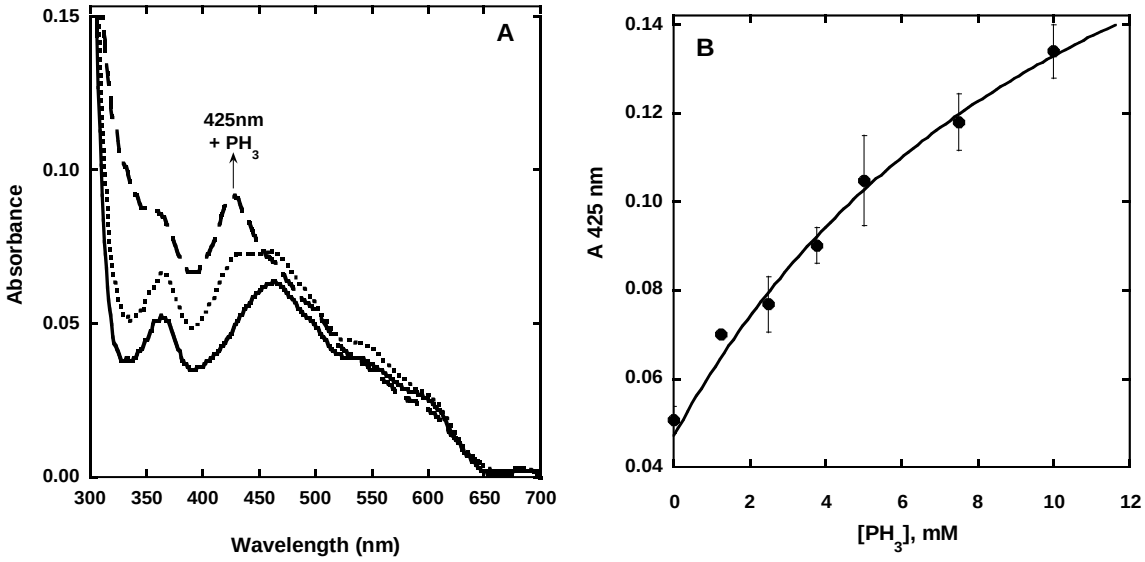

Figure 24. Spectroscopic analysis of the interaction between phosphine and Co(II)N4[11.3.1] under anaerobic conditions.

(A) Electronic absorption spectra of Co(II)N4[11.3.1] alone (solid trace) and with a 50-fold excess of PH3 (dotted trace) and a 100-fold excess of PH_3 (dashed trace) under anaerobic conditions. (B) Absorbance values at 425 nm plotted against increasing phosphine concentration added to Co(II)N4[11.3.1] (0.5 mM) under anaerobic conditions. The K_{eq} of 0.08 ±0.02 was determined from this data using a nonlinear least-squares fit (solid trace, $R^2 = 0.99$) (Equation 9).

Since phosphine is a good reductant, one would not expect Co(II)N_4[11.3.1] to be oxidized to Co(III) in the presence of phosphine, but it may further reduce Co(II)N_4[11.3.1] to Co(I). Co(II)N_4[11.3.1] has an electronic configuration of d^7; it has an odd electron and the surrounding ligands can be thought of as strong field and has an S=1/2, low spin, EPR signal with a crossover of ~3080 gauss (Figure 25). When a large excess of phosphine was added to Co(II)N_4[11.3.1], a shift in the signal was observed with the crossover now appearing at 3030 gauss and some small changes found in the nuclear hyperfine (due to the cobalt nuclear spin, S=7/2). Double integration of the signal indicated that there was little loss of intensity, suggesting that while the signal may be a combination of the original signal plus that of a Co(II)N_4[11.3.1]-phosphine adduct, the

compound is still primarily Co(II) and has not changed its oxidation state. The calculated equilibrium for the binding of phosphine to the cobalt complex (see above) would indicate that at the ratio of phosphine/cobalt in Figure 25, only ~2/3 of the cobalt complex would be bound to phosphine perhaps resulting in a slight shoulder observed at 3000 gauss (due to residual unbound CoN_4[11.3.1]. Subtraction (of the unbound complex) from the phosphine –cobalt EPR signal and subsequent simulation of the signal resulted in a slight improvement of the EPR signal.

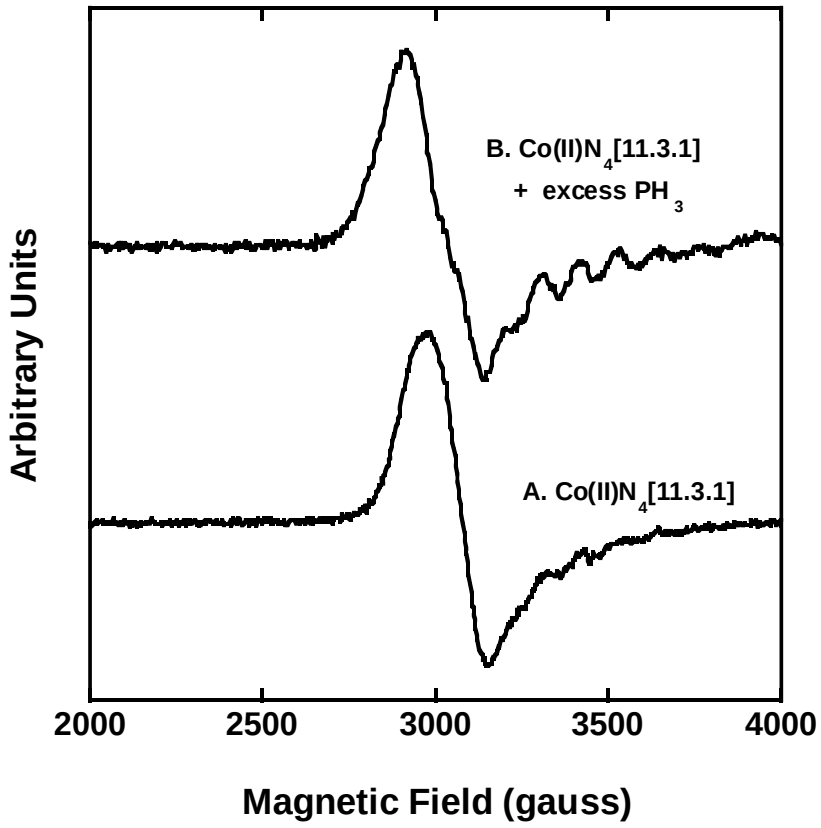

Figure 25. X-band EPR spectra (at 20 K) of Co(II)N_4[11.3.1] with phosphine.

(A) Co(II)N_4[11.3.1] (1 mM) prepared under anaerobic conditions at room temperature in 50 mM sodium phosphate buffer (pH 7.4) and 10% glycerol. (B) Co(II)N_4[11.3.1] (1 mM, 50 mM sodium phosphate buffer, pH 7.4) plus a 50-fold excess of PH_3 (prepared under anaerobic conditions at room temperature). Samples were frozen immediately and stored in liquid nitrogen immediately after preparation for later analysis. EPR conditions: Power = 63.2 μW, modulation amplitude = 9.8 G

4.2.7.1 Rapid oxygen consumption of PH_3 and $Co(II)N_4$[11.3.1]

As previously shown in our laboratory, $Co(II)N_4$[11.3.1] is only slowly oxidized by oxygen with a rate constant of ~0.5 M^{-1} s^{-1} at 25 °C [98] and this oxygen consumption can be followed using an oxygen electrode (Figure 26, dotted trace). Phosphine also reacts quite slowly with oxygen (Figure 26, dashed trace). When a reductant, such as ascorbate, is added to $Co(II)N_4$[11.3.1] the oxygen consumption becomes quite rapid [15]. We previously suggested, as other authors have [189], that, similar to many transition metals, $Co(II)N_4$[11.3.1] can mediate an oxygen consumption process in the presence of reductant (see Equation 10). When $Co(II)N_4$[11.3.1] was added to a solution of phosphine, the rate of oxygen consumption increased dramatically (Figure 26, solid trace) and thus it seems plausible that phosphine may act in a fashion similar to ascorbate in these oxygen consumption reactions.

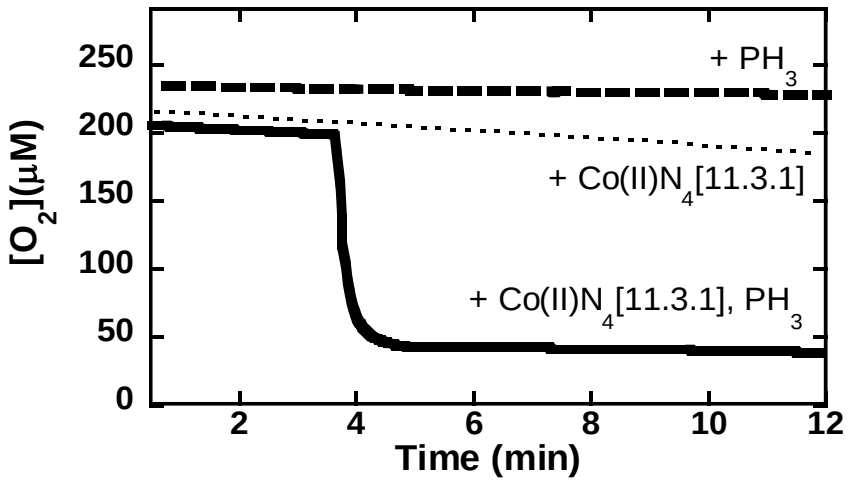

Figure 26. High-resolution respirometry showing oxygen consumption of $Co(II)N_4$[11.3.1] in the presence of PH_3.

All reactions were carried out in 500 mM sodium phosphate buffer, pH 7.4, 21 °C, in air saturated solutions. Dotted trace:$Co(II)N_4$[11.3.1] (150 μM) and representative traces are shown. Dashed trace: PH_3, 90 μM. Solid trace:PH_3 (90 μM) added to a solution of CoN4[11.3.1](150 mM) at 3.5 min. All concentration are final.

4.3 DISCUSSION

4.3.1 Ameliorative effects of Ag(I) and Co(II/III) complexes

Earlier work (Section 3.0**Error! Reference source not found.**, [186]) demonstrated that Au(I) compounds were very good antidotes for phosphine in the *G. mellonella* caterpillars and the present work now demonstrates that some Ag(I) compounds (see Figure 14) are similarly effective. Ag(I), as Au(I), likely ameliorates phosphine toxicity through a decorporation mechanism. Ag(I) lactate reduced the average recovery time in phosphine-exposed *G. mellonella* larvae more effectively than Au(I) thiosulfate by ~5 minutes but in mice prophylactic treatment with Au(I) thiosulfate was far more effective than Ag(I) lactate. Ag(I) lactate's diminished ameliorative effect in mice (Figure 18) is almost certainly due to the precipitation of AgCl. The solubility of these Ag(I) compounds (in distilled water, pH 7, 20-25°C) vary widely [107, 122, 190-192]. For example, $AgNO_3$ has a molar solubility of 14.4 M [192] while Ag(I) sulfadiazine has a molar solubility value of 3.2×10^{-6} M [191]. In our experiments, antidote effectiveness did not correlate with molar solubility; Ag(I) lactate (solubility 0.4 M [190]) and silver sulfadiazine were more effective than $AgNO_3$, which might suggest an inverse relationship with solubility but Ag(I) metronidazole nitrate was not effective despite modest solubility [107]. Because silver ions are not soluble due to the high levels of chloride found in the vasculature, a "carrier" compound could be used, such as a calix[n]arene. The tetrasodium calix[4]arene tetrasulfonate does appear to be relatively non-toxic, at least in the caterpillars, but its sodium ions do not appear to be displaced by Ag(I) ions (Figure 16). Thus, to potentially employ the calix[4]arene as a carrier, the tetra Ag(I) compound could be synthesized and tested, a future project. Other Ag(I) carrier compounds, such as Ag(I) Schiff-base complexes, might also be a potential area to be investigated. Finally, while

none of the compounds we investigated were of much therapeutic value in the mice, it can be argued that in cases of poisoning by the slow release, *i.e.* ingestion, of phosphine from phosphides such as AlP, the Au(I) and perhaps future Ag(I)/carrier compounds may be of value in possible treatment protocols.

As described above (section 3.2.1), we estimated the circulating phosphine concentration in the mouse model to be 460-920 μM. Even if the full dose of Ag(I) lactate was immediately absorbed, the circulating concentration would reach a Ag(I) – phosphine ratio of 0.44-0.87. If one Ag(I) binds 2 phosphine ligands, Ag(I) lactate may be a practically effective antidote but these estimates are calculated for ideal conditions. Our findings in mice suggest that Ag(I) precipitates and little of the administered dose is absorbed *in vivo*. Again, solubility constraints limit the practicality of Ag(I)-based antidotes.

Unexpectedly, a significant therapeutic effect of Co(II)N_4[11.3.1], a compound being investigated for its antidotal effects on cyanide and azide poisoning, was observed for phosphine exposed larvae (Figure 17). Although this effect was not observed in the mouse model (Figure 19), the fact that Co(II)N_4[11.3.1] was effective against phosphine in any capacity is notable. CoN_4[11.3.1] does not bind phosphine to any appreciable extent (Figure 24), although perhaps even a very small decrease in phosphine levels in organisms may be beneficial. Phosphine, however, could be oxidized in a two electron process by Co(III)N_4[11.3.1] (Figure 22), presumably converting phosphine to phosphinous acid (H_3PO), see Equation 11.

$$PH_3 + 2\ Co(III)N_4[11.3.1] + H_2O \rightarrow 2\ Co(II)N_4[11.3.1] + H_3PO + 2H^+$$

Equation 11. Reduction of Co(III)N_4[11.3.1] by phosphine under anaerobic conditions.

Another way to discuss the efficacy of candidate antidotes in mice is to compare the distribution of pole test scores 10 minutes after the end of phosphine exposure, a time point at which differences between groups are consistently observed (Figure 13, Figure 18, and Figure 19) as displayed in Figure 27. Prophylactic treatment with Au(I), identified as the most effective antidote overall, stands out with no variation in pole test scores compared to controls, which had scores distributed between 0 and 2 (Figure 27A). When compared using a paired Wilcoxin sign-ranked test for a nonparametric distribution, 10-minute pole test scores for mice treated prophylactically with Au(I) thiosulfate are significantly improved from those of controls ($p = 0.02$) while those of therapeutically-treated mice are not ($p = 0.67$). When generalized, pole test scores of mice treated prophylactically with Ag(I) lactate were slightly improved at 10 minutes ($p = 0.05$, unpaired Wilcoxon sign-rank test) but this significance did not hold upon comparison of paired mice ($p = 0.07$). Overall, there was no difference in the distribution of pole test scores at 10 minutes for mice treated with CoN_4[11.3.1] either prophylactically or therapeutically compared to controls, which is in keeping with the lack of efficacy overall in the mouse model (Figure 27C).

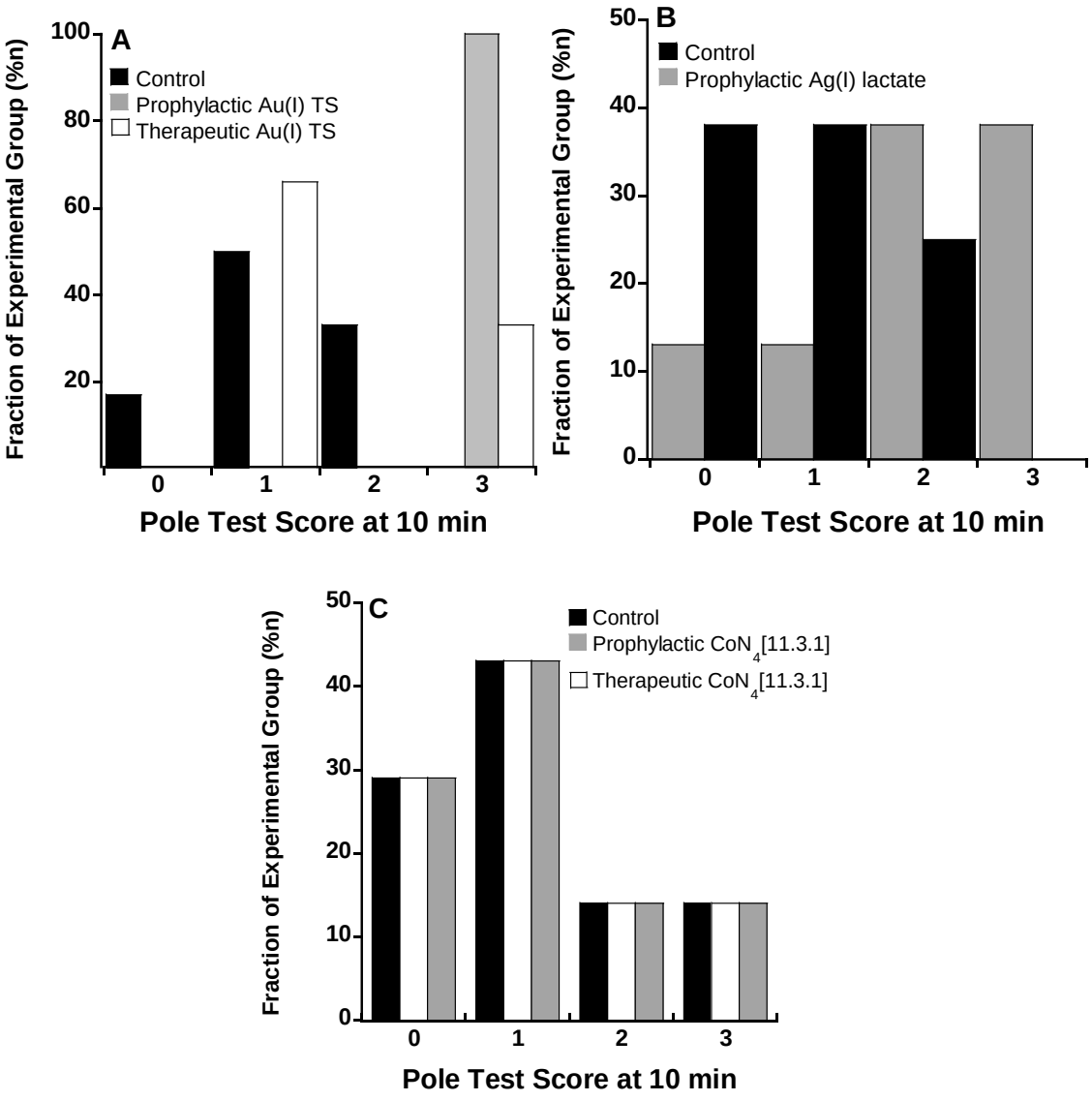

Figure 27. Pole test score distributuion 10 minutes after the end of phosphine exposure for controls and mice treated with candidate antidotes.

Distribution of pole test scores 10 minutes after the end of exposure for phosphine-exposed mice treated with candidate antidotes . Scores are normalized as a fraction of the experimental group size (n mice) Antidotes were administered intraperitoneally five minutes before or immediately after a phosphine exposure of 3200 (±500) ppm·min. The mice were examined using a behavioral assessment (pole-climbing test, see 2.3.2) to evaluate intoxication and recovery. (A) Distribution of pole test scores of mice treated with 50 mg/kg Au(I) thiosulfate before (gray bar) or after (white bars) phosphine exposure compared to controls (black bars). Sample sizes (n mice) = 6 control, 3 prophylactic, 3 therapeutic. At the 10 minute time point, mice treated prophylactically with Au(I)

thisoulfate had significantly improved pole test scores compared to controls (p = 0.02, Wilcoxin sign-rank test for paired data). (B) Distribution of pole test scores of mice treated with 7.5 mg/kg five minutes before phosphine exposure (gray bars) compared to untreated controls (black bars) 10 minutes after the end of exposure. Sample sizes (n mice) = 8 control, 8 prophylactic. Ag(I) lactate treatment did not significantly improve pole test scores at the 10 minute time point (p = 0.07, Wilcoxon sign-ranked test for paired data). (C) Distribution of 10-minute pole test scores of mice treated with 28 mg/kg CoN_4[11.3.1] five minutes before (gray bars) or immediately after (white bars) phosphine expousre compared to untreated controls (black bars). Sample sizes (n mice) = 14 control, 7 prophylactic, 7 therapeutic. Treatment did not result in any change in pole test scores compared to controls.

The comparison of 10-minute pole test scores reflects the overall effectiveness of each candidate antidote. This, along with the fact that prophylactic treatment is most effective, shows that the ameliorative reaction between phosphine and the candidate antidote must occur fairly quickly *in vivo*. Certainly, a decorporating agent that precipitates before circulation (Ag(I) lactate) would not be effective under these conditions. Our group has previously demonstrated that CoN_4[11.31], like many transition metal complexes, can catalyze the reduction of oxygen using ascorbate as a reductant [15]. The reduction reaction in Equation 11, coupled with the increase in oxygen turnover (Figure 26) driven by in the presence of phosphine suggests that phosphine can indeed participate (like ascorbate) in the turnover of oxygen to water, with superoxide/hydrogen peroxide intermediates, as shown in Equation 10. While this plausible mechanism of clearing phosphine might not be as rapid as the decorporation mechanism(s) of Au(I) (and potentially Ag(I)), it may represent another approach toward phosphine antidotes.

CoN_4[11.3.1] is highly soluble and rapidly absorbed into the blood after injection [14, 15]. We have previously detected Co(III)N_4[11.3.1] in the urine of mice 40 minutes after injection of 26 mg/kg [15], suggesting rapid circulation and metabolism. If 100% of the dose is absorbed, we would expect a circulating concentration of 0.67 mM in mouse blood. With our estimated

phosphine concentration, this represents an antidote-phosphine ratio between 0.73 and 1.5. Our data suggests that the cobalt compound does not bind phosphine at these levels but it may facilitate phosphine oxidation. Phosphine likely reduces Co(III)N_4[11.3.1] to Co(II)N_4[11.3.1] through a 2-electron process (Equation 11) which requires a ratio of 2 PH_3 to 1 Co(III)N_4[11.3.1]. The circulating level of phosphine is likely reduced by CoN_4[11.3.1] under our reported experimental conditions but the cobalt complex may be more effective in at least a 2-fold excess. Co(II)N_4[11.3.1] was more effective in the caterpillars than in mice. The ratio of antidote to phosphine in the larvae is estimated to be over 10.

Neither hydroxocobalamin nor CoN_4[14] treatment resulted in any amelioration of phosphine poisoning (Figure 17). The interaction of oxygen with the cobalt complex may be the crucial step in this process. We previously observed that oxidation of Co(II)N_4[11.3.1] by oxygen had a second order rate constant of 0.5 (±0.02) $M^{-1}s^{-1}$ [98] and the rate constant for the oxidation of CoN_4[14] is estimated to be a least an order of magnitude slower (unpublished data) offering a partial explanation as to why CoN_4[14] does not work (Figure 17). Clearly, the exact mechanism by which CoN_4[11.3.1] protects against phosphine toxicity should be further explored.

As described in Equation 2, phosphine is oxidized to phosphoric acid through a series of intermediates including phosphinous acid. If Co(II)N_4[11.3.1] induces this reaction, it produces phosphinous acid. If phosphinous acid were responsible for phosphine poisoning (as suggested by Nath and colleagues [57]), we would expect Co(II)N_4[11.3.1] to not necessarily be ineffective but rather to increase toxicity. Our findings do not support the hypothesis of Nath and colleagues [57] and suggest that phosphine itself is the primary toxic agent.

4.3.2 Impacts on blood & other findings

We found no association between acute phosphine exposure and methemoglobinemia or hemolysis. Even when RBCs were suspended and incubated in aqueous phosphine, we found no evidence for the formation of methemoglobin or extensive hemolysis compared to unexposed controls. This suggests that methemoglobinemia and hemolysis observed in some human cases of phosphine poisoning may not be caused by any direct interaction of phosphine with RBCs but by some secondary effect. In our studies, intact mice were exposed to gaseous phosphine via inhalation while in most, if not all case reports, patients were reported to develop methemoglobinemia after ingestion of metal phosphide tablets. It has been speculated that these symptoms are the result of the absorption of unhydrolyzed AlP particles into the blood stream and subsequent hydrolysis and reaction with RBCs [4, 10, 23, 24, 69, 175, 184]. This seems unlikely as in our *vitro* study phosphine solutions were added directly to RBCs with phosphine levels of millimolar concentrations (Table 7). Phosphine solutions, prepared under 100% phosphine gas, are saturated at ~11 mM so it is difficult to understand how ingestion of phosphides, followed by hydrolysis to phosphine, would give rise to higher concentrations than that in the bloodstream. Although ingestion may give rise to phosphine concentrations in the body at higher levels than those caused by inhalation of the gas.

As of this writing, there do not seem to be any reports of blindness or cataracts in the phosphine literature. Cataract development is typically the result of long-term illness (e.g. diabetes), aging, ultraviolet rays in sunlight and/or chronic chemical exposures [146, 193, 194]. Cataracts were not associated with either antidotal treatments (Ag(I) lactate or Co(II)N_4[11.3.1]) or survival in phosphine exposed mice (see Table 8). Cataracts have not been previously linked to phosphine, metal phosphides, or their metal oxide products either but they are associated with

oxidative damage [146, 194]. The lens of the eye is hypoxic with oxygen levels from ~1-5% [195]. The concentration of mitochondria varies throughout the lens [193] and they are certainly important in maintaining the low oxygen tension found there. Since phosphine inhibits cytochrome *c* oxidase, it can be easily envisioned that this might disturb the lens' oxygen environment and generate oxidative damage leading to cataracts. Because of this symptom's novelty, further study is warranted.

5.0 CONCLUSIONS

5.1 DECORPORATION APPROACH

We have demonstrated that some Au(I) and Ag(I) compounds are effective antidotes to phosphine poisoning in both an insect and a mouse model. In keeping with a decorporation mechanism, we observed that antidote effectiveness diminished between prophylactic and therapeutic administration. Presumably, prophylactic treatment was more effective because the decorporating agent was circulating before phosphine exposure, allowing it to bind the toxicant throughout exposure thereby and reducing the effective toxic dose. While these putative antidotes may be of limited therapeutic use in cases of poisoning with gaseous phosphine (PH_3), they could perhaps be effectively applied in cases of ingested metal phosphide poisoning, which accounts for the majority of phosphine poisoning worldwide [27, 42, 43]. When metal phosphides are ingested, the reaction with hydrochloric acid in the stomach is ongoing and patients undergo continuous exposure to phosphine over a series of hours [41, 59]. In fact, medical staff are encouraged to take measures to avoid secondhand phosphine exposure themselves as the gas can be exhaled by the patient long after ingestion [2, 41, 97]. In such a situation, a decorporating antidote nominally regarded as "prophylactic" could scavenge phosphine from this ongoing reaction and prevent cumulative exposure, even if administered after ingestion. Since phosphine's scope of toxicity is not fully delineated, antidotes that prevent cumulative exposure and reduce circulating phosphine are advantageous.

We found that Ag(I) lactate was a promising candidate phosphine antidote in *G. mellonella* larvae but was less effective in mice. This work is currently limited by Ag(I)'s low solubility both

under physiologic conditions and in stock solution. Our preliminary trial with tetrasodium calix[4]arene tetrasulfonate was unsuccessful (Figure 15) but other carrier molecules, perhaps prepared as argentum salts, may prove efficacious. Clearly, some synthetic development is required to find suitable Ag(I) compounds for administration *in vivo*. The possibility of using Ag(I) lactate (or other insoluble Ag(I) formulations) orally in cases of ingested metal phosphides, however, should not be completely dismissed without further testing.

5.2 PHOSPHINE'S IMPACTS ON THE VASCULATURE

Even the most promising candidate antidotes demonstrated reduced efficacy in the mouse model compared to the larvae. This may be due to key differences in organismal vasculature and circulation. *G. mellonella* larvae lack a complex vascular system and instead have an open circulatory system and mitochondria-rich fat body [131, 196]. In the larval stage, *G. mellonella* do not have an active oxygen carrier and instead respire through diffusion [131]. In insects, phosphine's impacts are likely primarily mitochondrial and it follows that additional toxic effects in mammal models could be vasculature-associated. We initially hypothesized that the difference was due to erythrocyte damage, specifically hemolysis and methemoglobinemia, but our evidence shows that neither is a primary consequence of phosphine exposure. However, according to recent research [87], blood transfusions appear to be ameliorative. While phosphine does not directly induce methemoglobinemia or hemolysis (section 4.2.3), perhaps it interacts with some other major blood component. Serum albumin is highly concentrated in the blood but is an unlikely alternate target for rapid reaction as evidenced by the late onset of cardiac-dependent lethality, which occurs hours to days after exposure. This timescale of cardiovascular effects suggest that

they are not due to a rapid biochemical modification of one blood component, rather an ongoing more cellular-based signaling mechanism finally leading to cardiac failure. Multi-organ congestion has been reported alongside cardiac failure in cases of phosphine poisoning [4, 8, 60]. This is not particularly surprising as congestion is closely associated with acute heart failure. This, combined with reports of hypotension [1, 78, 197], could suggest that PH_3 toxicity results in damage to or dysfunction of the vascular endothelium [198]. In a 2016 review of phosphine toxicity, Farahani and colleagues indeed highlight vascular wall damage as an important contribution to the overall outcome of phosphine poisoning [49]. The effects of phosphine poisoning may be diverse and wide-ranging.

5.3 INSIGHTS INTO PHOSPHINE BIOCHEMISTRY

Our findings suggest that the effective candidate antidotes work by lowering circulating levels of phosphine. The Au(I) and Ag(I) compounds do this through decorporation/scavenging the PH_3 ligand and CoN_4[11.3.1] likely induces the oxidation of PH_3 to H_3PO. Under physiologic conditions, H_3PO is transient and the reaction quickly proceeds through a series of benign intermediates to phosphoric acid (see Equation 2). Consequently, it appears that PH_3 is the toxic agent; if H_3PO were an actual toxic species (as suggested by Nath and colleagues [57]), CoN_4[11.3.1] should have exacerbated (or at least have no effect on) the measured toxicity, whereas it was significantly antidotal in the larvae and mildly so in the mice.

In vivo, the putative antidotes demonstrated the highest efficacy when administered prior to the onset of PH_3 exposure; they were less effective when given therapeutically. Essentially, at times longer than 20 minutes from the start of exposure, any protective benefits of the antidotes

were minimal. In context of the putative antidotal activity (reduction of circulating PH_3), this demonstrates that the toxic activity and decomposition of phosphine *in vivo* is rapid. This is further supported by comparative observations between the animal models. The putative antidotes were more effective in *G. mellonella* than in mice which, as discussed, is likely due to its open circulatory system. In addition, PH_3 likely reacts and decomposes more slowly in the insect model because of its body composition. The larval fat body is a lipid and mitochondria-rich organ contained in the hemocoel that performs a variety of biological functions including metabolism [130, 196]. Since larval circulation is passive and the respiratory organs are contained in lipids, it may take more time for phosphine to react and degrade in the caterpillars than in mammals, which have vastly different (and more polar) physiology. Notably, Ag(I) lactate was quite effective therapeutically against phosphine in the caterpillar model (Figure 14) but less impressive when administered prophylactically in mice (Figure 18). Ag(I) likely did not precipitate to AgCl as quickly (if at all) when administered in *G. mellonella* larvae due to the lipid-rich environment of the hemocoel. Thus, the Ag^+ ion remained available to scavenge the PH_3 ligand as an active antidote.

We observed cataract development in some phosphine-exposed mice. This outcome was not associated with any treatment or survival outcome (section 4.2.4). Cataracts are not a previously reported consequence of phosphine toxicity in humans or animals. Acute cataract development is associated with oxidative damage [193, 194]. In our research, cataracts did not develop uniformly and some animals only developed them in one eye (as shown in Figure 21). If cataracts were the result of systemic phosphine poisoning alone, they would likely have developed in both eyes. This suggests that some outside stimulus in combination with phosphine toxicity may lead to cataract formation. This effect could be explained by photochemistry; light is a main source

of radical oxygen species and the eye is obviously quite photosensitive. Perhaps light from a laboratory source induced a photolysis reaction in the eye of phosphine-poisoned mice. Mice demonstrated decreased activity after phosphine exposure; perhaps that the mice that developed only one cataract remained positioned with only one eye facing the light source. Much study remains to explain this observed phenomenon but we recommended that animals exposed to phosphine under experimental conditions be observed for impaired visual response and cataract development.

Because phosphine activity and oxidation is fast, death at later time points must be due to secondary consequences or derivatives of PH_3 (unlikely any oxidation intermediates, as described above). Perhaps along with mitochondrial inhibition, PH_3 induces a signaling cascade responsible for cardiac failure hours to days after exposure. Identifying the nature of this post-acute toxic mechanism is a critical barrier to designing effective antidotes and antidotal measures to phosphine. To delineate the complex mechanism of phosphine toxicity is beyond the scope of this work but we have demonstrated that phosphine inhibits complex IV, can induce redox chemistry, and does not directly induce hemolysis or methemoglobinemia. Thus, we join the many authors that stress the importance of mitochondrial dysfunction and oxidative stress to phosphine poisoning [26, 42, 59].

5.4 FUTURE DIRECTIONS

While our results are currently limited to animal models, we predict that our most promising candidate, gold(I) thiosulfate, will be a practically useful antidote to human exposure to phosphine. We calculated an estimated dose and cost for use in humans after occupational

exposure to phosphine based on available exposure data and regulatory limits using Equation 6 and Equation 7. For this exercise, we assume that Au(I) thiosulfate, when administered orally, distributes similarly to Au(I) thiomalate as reported by Mascarenhas and colleagues [172] (15% of dose reaches bloodstream) and the phosphine intake rate is 4.25 L/min [199] and blood volume is 5 L. We also assume that circulating Au(I) thiosulfate must be in at least a 2-fold excess to phosphine for decorporation. For a 10 minute exposure to 7.2 ppm PH_3 (AEGL3, Table 1), the estimated dose is 38 mg Au(I) thiosulfate, which would cost $11 [119]. For a 5 minute exposure to 700 ppm, the ambient concentration estimate in a fatal phosphine exposure onboard a grain freighter [64], the dose would be 740 mg and cost $98. Of course, these estimates do not include temporal data for antidote uptake or the cost of medical-grade reagents, but these calculations support further study into Au(I) thiosulfate's potential as an antidote to acute phosphine poisoning for mass-exposure events.

Much remains to be learned about phosphine's toxicity mechanism and we can certainly make recommendations on how to proceed with mechanistic research. For example, we have demonstrated that acute phosphine exposure does not induce methemoglobinemia or hemolysis and do not think they should be regarded as direct or primary effects of phosphine poisoning. Phosphine's toxicity mechanism is clearly complex and deserves detailed and focused study. However, mechanism determination falls outside of the bounds of our current project. In the absence of detailed mechanistic information, we will continue to investigate potential antidotes to phosphine poisoning that reduce the circulating concentration. We have identified a variety of promising candidate antidotes and demonstrated their effectiveness under two administration conditions (a few minutes before or after phosphine exposure through non-IV injection). These conditions should be expanded to determine the temporal limits of effectiveness (e.g. how late is

too late for therapeutic administration?) and possibility for multiple injections. Since CoN_4[11.3.1] is rapidly metabolized in mice [15], perhaps a combination of prophylactic and therapeutic doses could be administered. Ag(I) compounds should be studied with oral administration to overcome the solubility barriers in IP injection. Candidate antidote identification should continue and be expanded to include compounds that might catalyze phosphine oxidation in the blood.

APPENDIX A.SUPPLEMENTAL MATERIALS

Raw data for the recovery assessment of *Galleria mellonella* larvae after exposures of phosphine (Table 9) along with the prophylactic and therapeutic administration of putative antidotes Au(I) complexes auro-bisthiosulfate (AuTS), sodium aurothiomalate (AuTM), and aurothioglucose (AuTG).

Table 9. Dose-response recovery times of *G. mellonella* larvae in response to increasing phosphine exposures as shown in Figure 9.

i	[PH_3] ppm•min	Recovery T (min)		i	[PH_3] ppm•min	Recovery T (min)
1	12.2	0		51	4362.5	0
2	12.2	0		52	4362.5	0
3	12.2	0		53	4362.5	7
4	12.2	0		54	4362.5	14
5	12.2	0		55	4362.5	17
6	12.2	0		56	4362.5	22
7	12.2	0		57	4362.5	29
8	12.2	0		58	4362.5	60
9	12.2	0		59	4362.5	100
10	12.2	0		60	4362.5	100
11	73.1	0		61	5447	0
12	73.1	0		62	5447	0
13	73.1	0		63	5447	16
14	73.1	0		64	5447	22
15	73.1	0		65	5447	41
16	73.1	0		66	5447	90
17	73.1	0		67	5447	100
18	73.1	0		68	5447	100
19	73.1	0		69	5447	100
20	73.1	0		70	5447	100
21	219.3	0		71	6287.8	0
22	219.3	0		72	6287.8	0
23	219.3	0		73	6287.8	8
24	219.3	0		74	6287.8	100
25	219.3	0		75	6287.8	100
26	219.3	0		76	6287.8	100
27	219.3	0		77	6287.8	100
28	219.3	0		78	6287.8	100
29	219.3	0		79	6287.8	100
30	219.3	4		80	6287.8	100
31	438.7	0		81	7835.4	100
32	438.7	0		82	7835.4	100
33	438.7	0		83	7835.4	100
34	438.7	0		84	7835.4	100
35	438.7	0		85	7835.4	100
36	438.7	0		86	7835.4	100
37	438.7	0		87	7835.4	100
38	438.7	0		88	7835.4	100
39	438.7	0		89	7835.4	100
40	438.7	0		90	7835.4	100
41	3265.8	0		91	10187.3	100
42	3265.8	0		92	10187.3	100
43	3265.8	0		93	10187.3	100
44	3265.8	0		94	10187.3	100
45	3265.8	0		95	10187.3	100
46	3265.8	0		96	10187.3	100
47	3265.8	0		97	10187.3	100
48	3265.8	0		98	10187.3	100
49	3265.8	20		99	10187.3	100
50	3265.8	20		100	10187.3	100

Table 10. Dose-response recovery times *of G. mellonella* larvae in response to prophylactic and therapeutic treatment with Au(I) complexes auro-bisthiosulfate (AuTS, (25 mg/kg), sodium aurothiomalate (AuTM, 1 g/kg), and aurothioglucose (AuTG, 1 g/kg).

No Treatment Control	PBS Injection Control	AuTM Injection Control (1000ppm)	AuTG Injection Control (1000ppm)	AuTS Injection Control (25ppm)	PH_3 4300 (±700) ppm●min	Prophylactic PBS	Post Exposure PBS	Prophylactic AuTM (1000ppm)	Prophylactic AuTG (1000ppm)	Prophylactic AuTS (25ppm)	Post Exposure AuTM (1000ppm)	Post Exposure AuTG (1000ppm)	Post Exposure AuTS (25ppm)	H_2SO_4 Control
0	0	0	0	0	0	0	0	0	0	0	0	0	0	0
0	0	0	0	0	0	0	0	0	0	0	0	0	0	0
0	0	0	0	0	0	0	0	0	0	0	0	0	0	0
0	0	0	0	0	0	0	0	0	0	0	0	0	0	0
0	0	0	0	0	0	0	0	0	0	0	0	0	0	0
0	0	0	0	0	0	0	0	0	0	0	0	0	0	0
0	0	0	0	0	0	0	0	0	0	0	0	0	0	0
0	0	0	0	0	0	0	0	0	0	0	0	0	0	0
0	0	0	0	0	0	0	0	0	0	0	0	0	0	0
0	0	0	0	0	0	0	0	0	0	0	0	0	0	0
0	0	0	0	0	0	0	0	0	0	0	0	0	0	
0	0	0	0	0	0	0	0	0	0	0	0	0	0	
0	0	0	0	0	0	0	0	0	0	0	0	0	0	
0	0	0	0	0	0	0	0	0	0	0	0	0	0	
0	0	0	0	0	0	0	0	0	0	0	0	0	0	
0	0	0	0	0	0	0	0	0	0	0	0	0	0	
0	0	0	0	0	0	0	0	0	0	0	0	0	0	
0	0	0	0	0	0	0	0	0	0	0	0	0	0	
0	0	0	0	0	0	0	0	0	0	0	0	0	0	
0	0	0	0	0	0	0	0	0	0	0	0	5	0	
0	0	0	0	0	0	0	0	0		0	0	5	0	
0	0	0	0	0	0	0	0	0		0	0	7	0	
0	0	0	0	0	0	0	0	0		0	0	11	0	
0	0	0	0	0	0	6	0	0		0	0	14	0	
0	0	0	0	0	0	8	0	0		0	0	14	0	
0	0	0	0	0	0	9	0	0		0	0	21	0	
0	0	0	0	0	0	9	0	0		0	0	84	0	
0	0	0	0	0	0	10	0	0		0	0	120	0	
0	0	0	0	0	0	10	0	0		0	0	120	0	
0	0	0	0	0	0	10	0	0		0	0	120	0	
0	0	0	0	0	0	11	0	0		0	0		0	
0	0	0	0	0	0	12	0	0		0	0		0	
0	0	0	0	0	0	12	0	0		7	0		0	
0	0	0	0	0	0	13	0	0		7	0		0	
0	0	0	0	0	0	13	0	0		9	0		0	
0	0	0	0	0	0	16	0	0		10	2		0	
0	0	0	0	0	0	17	0	0		12	2		0	
0	0	0	0	0	0	24	0	0		13	5		0	
0	0	0	0	0	0	35	6	0		14	5		0	
0	0	0	0	0	0	40	6	0		15	7		0	
0	0	0		0	0	51	8	0			7		0	
0	0	0		0	0	79	8	0			7		0	
0	0	0		0	0	120	8	0			10		0	
0	0	0		0	0	120	8	0			10		0	
0	0	0		0	0	120	8	0			10		1	
0	0	0		0	0	120	8	0			10		2	
0	0	0		0	0	120	10	0			10		5	
0	0	0		0	0	120	0	6			10		5	
0	0	0		0	0	120	0	40			10		5	
0	0	0		0	0	120	10	120			11		5	
0	0	0		0	0		11				13		7	
0	0	0		0	0		11				14		7	
0	0	0		0	0		13				16		9	
0	0	0		0	0		14				16		9	
0	0	0		0	0		19				19		9	
0	0	0			0		20				20		11	
0	0	0			0		23				20		11	
0	0	0			0		23				20		21	
0	0	0			0		31				20		27	
0	0	0			0		34				23		27	
0	0	0			0		86				26		47	
0	0	0			5		115				35		51	
0	0	0			5		120				43		55	
0	0	0			6		120				50		61	
0	0	0			6		120				71		61	
0	0	0			7		120				74		94	
0	0	0			7		120				93		120	
0	0	0			7		120				93		120	
0	0	0			7		120				93		120	
0	0	0			8		120				117		120	
0	0	0			8		120				120			
0	0	0			9		120				120			
0	0	0			9		120				120			
0	0	0			9		120				120			

No Treatment Control	PBS Injection Control	AuTM Injection Control (1000ppm)	AuTG Injection Control (1000ppm)	AuTS Injection Control (25ppm)	PH_3 4300 (±700) ppm●min	Prophylactic PBS	Post Exposure PBS	Prophylactic AuTM (1000ppm)	Prophylactic AuTG (1000ppm)	Prophylactic AuTS (25ppm)	Post Exposure AuTM (1000ppm)	Post Exposure AuTG (1000ppm)	Post Exposure AuTS (25ppm)	H_2SO_4 Control
0	0	0			9		120				120			
0	0	0			10		120				120			
0	0	0			10		120				120			
0	0	0			11		120				120			
0	0	0			11		120				120			
0	0	0			11		120				120			
0	0	0			11		120				120			
0	0				11		120				120			
0	0				11		120				120			
0	0				11		120				120			
0	0				12		120				120			
0	0				12		120				120			
0	0				12		120				120			
0	0				12		120				120			
0	0				13		120				120			
0	0				14		120				120			
0	0				14		120				120			
0	0				16		3							
0	0				17		5							
0	0				17		7							
0	0				17		19							
0	0				18		0							
0	0				19		0							
0	0				20		0							
0	0				20		0							
0	0				20		0							
0	0				22		120							
0	0				22									
0	0				22									
0	0				24									
0	0				25									
0	0				29									
0	0				30									
0	0				30									
0	0				31									
0	0				31									
0	0				38									
0	0				40									
0	0				40									
0	0				41									
0	0				45									
0	0				45									
0	0				57									
0	0				60									
0	0				60									
0	0				60									
0	0				64									
0	0				66									
0	0				67									
0	0				70									
0	0				80									
0	0				82									
0	0				87									
0	0				90									
0	0				98									
0	0				103									
0	0				120									
0	0				120									
0	0				120									
0	0				120									
0	0				120									
0	0				120									
0	0				120									
0	0				120									
0	0				120									
0	0				120									
0	0				120									
0	0				120									
0	0				120									
0	0				120									
0	0				120									
0	0				120									
0	0				120									
0	0				120									

No Treatment Control	PBS Injection Control	AuTM Injection Control (1000ppm)	AuTG Injection Control (1000ppm)	AuTS Injection Control (25ppm)	PH_3 4300 (±700) ppm•min	Prophylactic PBS	Post Exposure PBS	Prophylactic AuTM (1000ppm)	Prophylactic AuTG (1000ppm)	Prophylactic AuTS (25ppm)	Post Exposure AuTM (1000ppm)	Post Exposure AuTG (1000ppm)	Post Exposure AuTS (25ppm)	H_2SO_4 Control
0	0				120									
0	0				120									
0	0				120									
0	0				120									
0	0				120									
0	0				120									
0	0				120									
0	0				120									
0	0				120									
0	0				120									
0	0				120									
0	0				120									
0	0				120									
0	0				0									
0	0				0									
0	0				0									
0	0				18									
0	0				18									
0	0				18									
0	0				20									
0	0				22									
0	0				28									
0	10				120									
0	0				0									
0	0				0									
0	0				0									
0	0				0									
0	0				11									
0	0				20									
0	0				20									
0	0				24									
0	0				120									
0	0				120									
0	0				12									
0	0				13									
0	0				17									
0	0				0									
0	0				0									
0	0				0									
0	0				0									
0	0				120									
0	0				120									
0	0				120									
0	0													
0	0													
0	0													
0	0													
0	0													
0	0													
0	0													
0	0													
0	0													
0	0													
0														
0														
0														
0														
0														
0														
0														
0														
0														
0														
0														
0														
0														
0														
0														
0														
0														
0														
0														
0														

Raw data for the pole climbing assessment of phosphine intoxicated mice (see METHODS for details) establishing prophylactic and therapeutic responses using auro-bisthiosulfate (AuTS, 50 mg/kg) (see Figure 13).

Table 11. Raw data of the responses of phosphine-intoxicated male mice and the putative antidote AuTS as determined by a pole-climbing test (as shown in Figure 13).

		Pole Test Score at Time Point					
	Time (min)	10	20	30	60	90	120
- 5 min	mouse 1	3	3	3	3	3	3
	mouse 2	3	3	3	3	3	3
	mouse 3	3	3	3	3	3	3
+ 1 min	mouse 4	3	3	3	3	3	3
	mouse 5	1	1	2	2	1	2
	mouse 6	1	1	1	1	1	1
controls	mouse 7	2	2	3	3	3	3
	mouse 8	1	1	1	1	1	1
	mouse 9	1	3	3	3	3	3
	moue 10	1	1	1	1	1	1
	mouse 11	2	2	1	2	2	3
	mouse 12	0	0	0	0	0	0

Table 12. Dose-response recovery times of *G. mellonella* larvae in response to prophylactic and therapeutic treatment with Ag(I) complexes as shown in Figure 14.

No Treatment Control	PH_3 Control	HEPES Control	HEPES + 10% DMSO Control	10 mg/kg Ag(I) Lactate Control	10 mg/kg Ag(I) Nitrate Control	50 mg/kg Ag(I) bis(metronidazole) nitrate Control	10 mg/kg Ag(I) Thiosulfate Control	9 mg/kg Ag(I) sulfadiazine Control	10 mg/kg Ag(I) Lactate Treatment	10 mg/kg Ag(I) Nitrate Treatment	50 mg/kg Ag(I) bis(metronidazole) nitrate Treatment	10 mg/kg Ag(I) Thiosulfate Treatment	9 mg/kg Ag(I) sulfadiazine Treatment
0	0	0	0	4	0	0	0	0	0	0	0	0	0
0	0	0	0	11	0	0	0	0	0	0	0	0	0
0	0	0	0	30	0	0	0	0	0	0	0	0	0
0	0	0	0	0	0	0	0	0	0	0	0	0	0
0	0	0	0	0	0	0	0	0	0	0	0	0	0
0	0	0	0	0	0	0	0	0	0	0	7	0	0
0	0	0	0	0	0	0	0	0	0	0	7	0	0
0	0	0	0	0	0	0	0	0	0	0	8	10	12
0	0	0	0	0	0	0	0	0	0	0	8	120	22
0	0	0	0	0	0	0	0	0	0	0	12	120	33
0	0	0	0	0	0	0	0	0	0	0	15	0	0
0	0	0	0	0	0	0	0	0	0	0	16	0	0
0	0	0	0	0	0	0	0	0	0	0	26	0	0
0	0	0	0	0	0	0	0	0	0	0	29	0	0
0	0	0	0	0	0	0	0	0	0	0	106	0	0
0	0	0	0	0	0	0	0	0	0	0	120	0	0
0	0	0	0	0	0	0	0	0	0	0	120	0	13
0	0	0	0	0	0	0	0	0	0	0	120	5	43
0	0	0	0	0	0	0	0	0	0	0	120	6	80
0	0	0	0	0	0	0	0	0	0	0	120	120	84
0	0	0	0	0	0		0	0	1	0		15	21
0	0	0	0	0	0		0	0	4	0		15	33
0	0	0	0	0	0		0	0	4	0		20	120
0	0	0	0	0	0		0	0	5	0		120	0
0	0	0	0	0	0		0	0	10	0		0	0
0	0	0	0	0	0		0	0	10	0		0	0
0	0	0	0	0	0		0	0	11	0		0	0
0	0	0	0	0	0		0	0	12	3		0	0
0	0	0	0	0	0		0	0	13	4		0	0
0	0	0	0	0	0		0	0	13	6		0	0
0	0	0	0	0	0		0	9	16	6		10	18
0	0	0	0	0	0		0	13	17	7		13	18
0	0	0	0	0	0		0	14	18	7		25	18
0	0	0	0	0	0		0	28	22	8		35	18
0	0	0	0	0	0		0	33	27	8		0	120
0	0	0	0	0	0		0	64	28	9		0	0
0	0	0	0	0	0		0	0	31	9		0	0
0	0	0	0	0	0		0	0	40	9		0	0
0	0	0	0	0	0		0	0	56	10		0	0
0	0	0	0	0	0		0	0	75	16		0	4
0	0	0	0		0		17		9	11			
0	0	0	0		0		18		17	12			
0	0	0	0		0		18		120	16			
0	0	0	0		0		19		0	120			
0	0	0	0		0		23		0	0			
0	0	0	0		0		26		0	0			
0	0	0	0		5		28		0	0			
0	0	0	0		5		29		0	0			
0	0	0	0		10		42		0	0			
0	0	0	120		120		44		0	0			
0	0	0	0		45		4						
0	0	0	0		70		9						
0	0	0	0		120		18						
0	0	0	0		120		0						
0	0	0	0		120		0						
0	0	0	0		120		0						
0	0	0	0		120		0						

0	0	0	0	120	0
0	0	0	0	120	0
0	0	0	0	120	0
0	0	0			
0	0	0			
0	0	0			
0	0	0			
0	0	0			
0	0	0			
0	0	0			
0	0	0			
0	0	0			
0	0	0			
0	0	0			
0	0	0			
0	0	0			
0	0	0			
0	0	0			
0	0	0			
0	0	0			
0	0	0			
0	0	0			
0	0	0			
0	0	0			
0	0	0			
0	0	0			
0	0	0			
0	0	0			
0	2	0			
0	3	0			
0	5	0			
0	6	0			
0	7	0			
0	8	0			
0	8	0			
0	8	0			
0	9	0			
0	9	0			
0	9	0			
0	9	0			
0	10	0			
0	10	0			
0	10	0			
0	10	0			
0	10	0			
0	11	0			
0	11	0			
0	11	0			
0	12	0			
0	12	0			
0	12	0			
0	13	0			
0	13	0			
0	14	0			
0	14	0			
0	14	0			
0	15	0			
0	15	0			
0	15	0			
0	15	0			
0	15	0			
0	16	0			
0	16	0			
0	16	0			

0	17	0
0	17	0
0	18	0
0	19	0
0	19	0
0	19	0
0	20	0
0	21	0
0	22	0
0	22	0
0	22	0
0	22	0
0	22	0
0	22	0
0	22	1
0	23	4
0	23	5
0	25	5
0	26	5
0	26	9
0	28	10
0	28	10
0	29	27
0	29	34
0	30	120
0	32	120
0	33	120
0	38	120
0	40	120
0	41	
0	41	
0	44	
0	45	
0	45	
0	47	
0	57	
0	57	
0	59	
0	60	
0	60	
0	60	
0	64	
0	64	
0	66	
0	70	
0	72	
0	79	
0	81	
0	82	
0	82	
0	92	
0	93	
0	97	
0	102	
0	108	
0	109	
0	110	
0	112	
0	114	
0	115	
0	120	
0	120	
0	120	
0	120	

0	120
0	120
0	120
0	120
0	120
0	120
0	120
0	120
0	120
0	120
0	120
0	120
0	120
0	120
0	120
0	120
0	120
0	120
0	120
0	120
0	120
0	120
0	120
0	120
0	120
0	120
0	120
0	120
0	120
0	120
0	120
0	120
0	120
0	120
0	120
0	17
0	20
0	20
0	45
0	120
0	0
0	0
0	0
0	0
0	0
0	15
0	32
0	120
0	120
0	120
0	120
0	120
0	120
0	120
0	120
0	9
0	17
0	42
0	120
0	120
0	0
0	0
0	0
0	0

0	0
0	
0	
0	
0	
0	
0	
0	
0	
0	
0	
0	
0	
0	
0	
0	
0	
0	
0	
0	
0	
0	
0	
0	
0	
0	
0	
0	
0	
0	
0	
0	
0	
0	
0	
0	
0	
0	
0	
0	
0	
0	
0	
0	
0	
0	
0	
0	
0	
0	
0	
0	
0	
0	
0	
0	
0	
0	
120	
120	
120	

Table 13. Dose-response recovery times of *G. mellonella* larvae in response to therapeutic treatment with Sodium Thiosulfate, Calix[4]arene sulfonate tetrasodium, and a 1:2 Calix[4]arene and Ag(I) Nitrate mixture as shown in Figure 15.

No Treatment Control	PH_3 Control	HEPES Control	50 mg/kg Sodium Thiosulfate Control	5 mg/kg Calix[4]arene Control	5 mg/kg Calix[4]arene + 10 mg/kg Ag(I) Nitrate Treatment	50 mg/kg Sodium Thiosulfate Treatment	5 mg/kg Calix[4]arene Treatment	5 mg/kg Calix[4]arene + 10 mg/kg Ag(I) Nitrate Treatment
0	0	0	0	0	0	0	0	0
0	0	0	0	0	0	0	0	0
0	0	0	0	0	0	0	0	0
0	0	0	0	0	0	0	0	0
0	0	0	0	0	0	0	0	0
0	0	0	0	0	0	0	0	0
0	0	0	0	0	0	0	9	0
0	0	0	0	0	0	0	12	0
0	0	0	0	0	0	0	28	0
0	0	0	0	0	0	0	33	8
0	0	0	0	0	0	0	38	13
0	0	0	0	0	0	0	41	17
0	0	0	0	0	0	0	46	17
0	0	0	0	0	0	0	52	20
0	0	0	0	0	0	0	59	22
0	0	0	0	0	0	0	72	28
0	0	0	0	0	0	0	77	29
0	0	0	0	0	0	0	96	40
0	0	0	2	0	0	8	100	45
0	0	0	14	0	0	12	110	47
0	0	0		0	0	12	118	49
0	0	0		0	0	13	120	55
0	0	0		0	0	22	120	58
0	0	0		0	0	26	120	59
0	0	0		0	0	41	120	80
0	0	0		0	0	47	120	93
0	0	0		0	0	56	120	118
0	0	0		0	0	76	120	120
0	0	0		0	0	85	120	120
0	0	0		0	0	120	120	120
	0			0	0	120		120
	0			0	0	120		120
	0			0	0	120		120
	0			0	0	120		120
	0			0	0	120		120
	0			0	0	120		120
	0			0	0	120		120
	0			0	0	120		120
	0			0	0	120		120
	8			0	0	120		120
	11			0	0			
	12			0	0			
	12			0	0			
	12			0	0			
	14			0	0			
	15			0	0			
	17			0	0			
	18			0	0			
	18			0	0			
	22			0	0			

22
23
26
29
31
32
33
35
42
43
43
43
46
50
50
55
55
64
66
76
77
78
80
83
109
113
120
120
120
120
120
120
120
120
120
120
120
120
120
120
120
120
120
120
120
120
120
120
120
120
120
120
120
120
120
120
120
120
120
120

Table 14. Dose-response recovery times of *G. mellonella* larvae in response to therapeutic treatment Hydroxocobalamin, Co(II)N$_4$[14], and Co(II)N$_4$[11.3.1] as shown in Figure 17.*

PBS Control	82 mg/kg Hydroxocobalamin Control	31 mg/kg CoN$_4$[14] Control	28 mg/kg CoN$_4$ [11.3.1] Control	82 mg/kg Hydroxocobalamin Treatment	31 mg/kg CoN$_4$[14] Treatment	28 mg/kg CoN$_4$ [11.3.1] Treatment
0	0	0	0	0	0	0
0	0	0	0	0	0	0
0	0	0	0	0	0	0
0	0	0	0	0	0	0
0	0	0	0	0	0	0
0	0	0	0	0	0	0
0	0	0	0	0	0	0
0	0	0	0	0	0	0
0	0	0	0	0	0	0
0	0	0	0	0	0	0
3	0	0		0	0	0
0	0	0		0	6	0
0	0	0		5	10	0
0	0	0		9	10	0
0	0	0		10	12	0
0	0	0		10	13	0
0	0	0		14	13	0
0	0	0		15	14	0
0	0	0		15	14	0
0	0	1		22	16	0
0	0	0		25	18	0
0	0	0		25	20	0
0	0	0		27	21	7
0	0	0		30	23	10
0	0	0		49	23	12
0	0	0		50	25	13
0	0	0		58	27	16
0	0	0		60	50	16
0	0	0		120	57	28
0	0	0		120	62	120
0	0	0		120	120	
0	0	0		120	120	
0	0	0		120	120	
0	0	0		120	120	
0	0	0		120	120	
0	0	0		120	120	
0	0	0		120	120	
0	0	0		120	120	
0	0	0		120	120	
0	0	0			120	
0	0					
0	0					
0	0					
0	0					
0	0					
0	0					
0	0					
0	0					
0	0					
0	0					
0						
0						
0						
0						
0						

0
0
0
0
0
0
0
0
0
0
0
0
0
0
0
0
0
0
0
0
0
0
0
0
0
0
0
0
0
0
0
0
0
0
0
0
0
0
0
0
0
0
0
0
0
0
0
0
0
0
0
0
0
0

*Experiments were performed along with those with Ag(I) compounds and these groups were compared to untreated and PH_3 exposed groups listed in Table 12.

Table 15. Raw data of the responses of phosphine-intoxicated mice and those treated with 7.5 mg/kg Ag(I) lactate 5 minutes before exposure, as determined by a pole-climbing test, data shown in Figure 18.

	Time (min)	Pole Test Score at Time Point								Time (min)	Pole Test Score at Time Point						
		0	10	20	30	40	50	60			0	10	20	30	40	50	60
7.5 mg/kg Ag(I) Lactate Treatment, Prophylactic	M 1	3	3	3	3	3	3	3	Paired Control	M 9	1	1	1	1	1	1	1
	M 2	3	3	3	3	3	3	3		M 10	1	1	3	3	3	3	3
	M 3	1	1	1	1	1	1	1		M 11	1	2	1	1	1	1	1
	M 4	0	0	1	1	1	1	1		M 12	0	0	0	0	0	0	0
	M 5	3	3	2	2	2	2	3		M 13	0	0	0	0	0	0	0
	M 6	2	2	2	2	2	1	1		M 14	2	1	1	1	1	1	1
	M 7	1	2	2	1	2	1	1		M 15	0	0	0	0	0	0	0
	M 8	1	2	1	1	1	1	3		M 16	1	2	3	3	3	3	3

Table 16. Raw data of the responses of phosphine-intoxicated mice and those treated with 28 mg/kg $Co(II)N_4$[11.3.1] 5 minutes before or immediately after PH_3 exposure, as determined by a pole-climbing test, data shown in Figure 19.

	Time (min)	**Pole Test Score at Time Point**								**Time (min)**	**Pole Test Score at Time Point**						
		0	**10**	**20**	**30**	**40**	**50**	**60**			**0**	**10**	**20**	**30**	**40**	**50**	**60**
28 mg/kg $Co(II)N_4$[11.3.1] Prophylactic	M 1	0	0	0	0	0	1	1	**Paired Controls**	M 15	0	0	0	0	0	0	0
	M 2	3	3	3	3	3	3	3		M 16	2	2	2	2	2	1	1
	M 3	1	0	0	1	1	1	1		M 19	0	0	0	0	0	0	0
	M 4		1	1	1	1	1	1		M 20		1	1	1	1	1	1
	M 5		2	2	2	1	1	1		M 21		3	2	3	3	2	2
	M 6	1	1	1	1	1	1	1		M 24	0	1	1	1	1	1	0
	M 7	1	1	1	1	1	1	1		M 25	1	1	1	1	1	1	1
28 mg/kg $Co(II)N_4$[11.3.1] Therapeutic	M 8	3	1	1	1	1	1	1		M 17	3	3	3	2	1	1	1
	M 9	1	2	1	1	1	1	0		M 18	3	1	1	1	1	1	1
	M 10	3	1	1	1	2	1	2		M 22	1	0	0	0	1	1	1
	M 11	3	3	2	3	3	3	3		M 23	3	2	2	3	2	3	3
	M 12	2	1	1	1	1	1	1		M 26	1	0	0	0	0	1	1
	M 13	1	1	1	1	1	1	1		M 27	1	1	1	1	1	1	1
	M 14	1	0	0	1	1	1	1		M 28	1	1	0	0	1	0	0

APPENDIX B.ADDITIONAL PUBLICATION

A Cobalt Schiff-base Complex as a Putative Therapeutic for Azide Poisoning

Hirunwut Praekunatham, Kimberly K. Garrett, Yookyung Bae,

Andrea A. Cronican, Kristin L. Frawley, Linda L. Pearce* and Jim Peterson*

Department of Environmental and Occupational Health, Graduate School of Public Health,

The University of Pittsburgh, Pittsburgh, PA 15261

*Corresponding Authors: jimmyp@pitt.edu lip10@pitt.edu

Reprinted with permissions from, Praekunatham, H., Garrett, K. K., Bae, Y., Cronican, A. A., Frawley, K. L., Pearce, L. L., & Peterson, J. (2019). A Cobalt Schiff-Base Complex as a Putative Therapeutic for Azide Poisoning. *Chemical research in toxicology*, *33*(2), 333-342.

INTRODUCTION

Most azide poisonings are either accidental or suicide attempts, but there also seem to have been at least half a dozen reported instances of malicious injury to others caused by spiking beverages with azide in Japan [200] and the U.S. [201-203]. The symptoms of acute azide (N_3^-) intoxication are similar to those induced by cyanide (CN^-) [204, 205], and, analogous to cyanide, azide is known to be an inhibitor of the mitochondrial electron transport system, specifically at cytochrome *c* oxidase (complex IV) [206-208]. Unlike cyanide, however, there is no antidote for azide poisoning, either approved or off-label, currently available. Given the similarity in action of these two toxicants, conventional remedies for cyanide poisoning, such as nitrite/thiosulfate or hydroxocobalamin, might reasonably be expected to be of benefits for treating azide toxicity. Curiously, however, it seems that no cyanide antidote has so far been shown to produce any substantial or convincing amelioration of azide toxicity [209, 210].

Recently, we have demonstrated a cobalt containing Schiff-base macrocyclic compound, Co(II)-2,12-dimethyl-3,7,11,17-tetraazabicyclo[11.3.1]heptadeca-1(17)2,11,13,15-pentaenyl dibromide ($Co(II)N_4$[11.3.1]), to be an effective cyanide scavenger in mice [14, 15]. Here, we explore whether CoN_4[11.3.1] might also be an efficacious antidote toward azide toxicity by virtue of its anionic ligand-binding (scavenging) capability. The kinetics of the reaction between azide anion and the complex have been investigated at physiologically relevant pH and temperature by stopped-flow spectrophotometry. The possible interference that oxygen may have on the azide-scavenging reaction has also been examined. Lastly, as a proof-of-principle exercise, the potential utility of CoN_4[11.3.1] as an antidotal therapeutic for azide poisoning has been briefly investigated in sublethally intoxicated mice.

EXPERIMENTAL SECTION

Chemicals

All reagents were ACS grade, or better, used without further purification, and, unless stated to the contrary, obtained from Fisher or Sigma-Aldrich. Sodium dithionite (87% minimum by assay) was purchased from EMD Chemicals Inc. Argon gas (99.998%) and oxygen gas (99.997%) were acquired from Matheson Inc. Phosphate buffer (0.1 M) was prepared by mixing an appropriate volume of 0.1 M sodium phosphate monobasic (NaH_2PO_4) and 0.1 M sodium phosphate dibasic (NaH_2PO_4) to make buffers at the desired pH, ranging from 6 to 8.5. To prepare NaN_3 solutions, weighed quantities of the salt were dissolved in 0.1 M phosphate buffer at the desired pH in septum-sealed vials with minimal headspace. To maintain ionic strength when required, sodium nitrate was added to phosphate buffer. Deoxygenated solutions were prepared under argon using either an Omni-Lab glovebox (Vacuum Atmospheres) operating at <0.3 ppm O_2 or a Schlenk line.

Synthesis of Co(II)N_4[11.3.1]

Co(II)N_4[11.3.1] (cobalt(II)2,12-dimethyl-3,7,11,17-tetraazabicyclo-[11.3.1]-heptadeca-1(17)-2,11,13,15-pentaenyl dibromide) was prepared by the method of Long and Busch [211], as adapted by Lacy et al [212]. Briefly, $CoBr_2$ (1.35 g, 6.17 mmol) and 2,6-diacetylpyridine (1.00 g, 6.13 mmol) were dissolved in 20 mL of deoxygenated ethanol at room temperature under argon, followed by the addition of 0.5 mL of water, and then, over the course of several min, degassed 3,3'-diaminodipropylamine (0.857 mL, 6.13 mmol) was added dropwise. The initial blue-green color of the $CoBr_2$ and 2,6-diacetylpyridine mixture gradually turned to dark red upon addition of the amine. Next, a small amount of glacial acetic (1 μL) was introduced before stirring at 50 °C

for 12 h. Upon cooling, the reaction mixture was transferred to a glovebox (argon atmosphere, <0.5 ppm of O_2, ~4 ppm H_2O) and filtered through a fritted-glass funnel to obtain a pure solid. The product was washed with ethyl acetate and left to dry over phosphorous pentoxide for 24 hr. Elemental analysis (Atlantic Microlab): calculated for $C_{15}H_{22}N_4Br_2Co$, 33.76% C, 4.65% H, 11.74% N, 33.50% Br; found 37.66% C, 4.67% H, 11.62% N, 22.16% Br.

Azide binding equilibria

Azide-binding stoichiometry and equilibria were studied under either aerobic or anaerobic (under argon) conditions in capped (septum-sealed, with head volumes minimized) vessels. Transfers were made with gastight syringes and careful mixing to ensure the complete dissolution of sodium azide. Small aliquots of concentrated azide solutions were titrated into larger volumes of relatively dilute solutions of Co(II/III)N_4[11.3.1] (in freshly made 0.1 M phosphate-buffer, pH 7.4) at 25 °C. The method of continuous variation, also known as Job's method [213-215], was used to determine the stoichiometry of azide binding. Briefly, the total concentrations of azide plus Co(II/III)N_4[11.3.1] were held constant, but the relative proportions of azide and Co(II/III)N_4[11.3.1] were varied, while absorbance changes were monitored at 460 nm. [In fact, because these particular measurements involved weak chromophores, we adopted a small modification of the basic method in which absorption difference spectra were recorded; specifically, complex plus azide (sample) minus azide-free complex (reference). This approach necessitates the slight procedural complication of having to make a fresh blank (reference) containing the same total concentration of the cobalt compound as was present in the sample for each individual point on the Job plot.] The change in absorbance of the Co(II/III)N_4[11.3.1](N_3) compound (normalized) is plotted (ordinate) versus the volume fraction of Co(II), Co(III), or

Cu(II), X_A= [A]/([A]+[B]) (abscissa). The maximum change in absorbance is found at an X_A value corresponding to the binding stoichiometry of the complex formed: 0.5 for a 1:1 binding of Co(II/III)N_4[11.3.1] and azide, and 0.33 for a 1:2 ratio of Co(II/III)N_4[11.3.1] and azide. When a signal was present, the quantitative EPR data (see below) were employed to calculate estimates for association constants.

Animals, exposure, and blood collection

Animal procedures were approved by the University of Pittsburgh Institutional Animal Care and Use Committee (Protocol No. 16088947), and veterinary care was provided by the Division of Laboratory Animal Research of the University of Pittsburgh. Mice, 12-16 week old male Swiss-Webster (CFW) weighing 30-40 g, were purchased from Taconic (Hudson, NY) and were housed four per cage. Upon arrival, the mice were allowed to adapt to their new environment for 2 weeks with access to food and water *ad libitum* prior to experiments. A series of trials determining the level of sodium azide that caused a reproducible impairment of the mice without death was performed, administering solutions (toxicant and control saline) through ~0.1 mL intraperitoneal (ip) injections. All solutions were prepared by dilution into sterilized saline in septum-sealed vials, and gastight syringes were used for all transfers. Groups of at least six mice were tested for each experimental point.

Righting-recovery testing

Following the administration of toxicant, the time required for recovery of righting ability in mice was determined adopting the procedure of Cambal et al [176, 216], a simpler variation of the righting-reflex method described by Crankshaw et al [217]. After injection (ip) of sodium azide

(26 mg/kg), mice were placed in a dark but transparent plastic tube (Kaytee CritterTrail, available from pet stores) in supine position. The time from the toxicant injection until the mice flipped from the supine to prone position in the plastic tube was taken as the end point (righting-recovery time).

Stopped-flow kinetics

The rapid kinetic experiments were carried out in both multiple (photodiode array, PDA) and single wavelength absorbance (photomultiplier tube, PMT) modes using an SX.18MV-R stopped-flow spectrophotometer, manufactured by Applied Photophysics Ltd. The reaction temperature was controlled using an Isotemp 2100 thermostat (Fisher Scientific). At least three data sets were collected for each set of kinetic conditions and subsequently averaged. Upon changing any reagent concentration, the stopped-flow instrument was flushed out at least five times before data were recorded to ensure that the previous reagents remaining in the reaction chamber were completely removed before the next set of reactions started. Pseudo-first-order conditions were employed to obtain the observed rates, k_{obs}. Rate constants (k) were determined from the slope of the linear relationship between k_{obs} and the flooding reagent. All kinetic data were analyzed and modeled using Pro-K and SX.18MV software programs, supplied by the manufacturer. Stopped-flow experiments with oxygen employed phosphate buffer solutions saturated with 99% oxygen (exposed to 1 atm oxygen for 2 h) resulting in solutions with oxygen concentrations of 1 mM [189]. Anaerobic experiments were performed in buffers flushed with argon and drive syringes were filled with reagents in the glovebox. The stopped-flow syringe assembly was fitted with an argon-flushed manifold to prevent any inadvertent leakage of air around the pistons (plungers).

Electron paramagnetic resonance (EPR) spectroscopy

X-band (9 GHz) EPR spectra were recorded on a Bruker ESP 300 spectrometer equipped with an ESR 910 flow cryostat (oxford Instruments) for ultralow-temperature measurements at Carnegie Mellon University. SpinCount software used to analyze the EPR spectra was provided by Professor Michael Hendrich, Carnegie Mellon University. Quantification of EPR signals was performed by simulating the spectra using known (or determined) parameters for each sample in question. Simulations employed a least-squares fitting method to match the line shape and signal intensity of a selected spectrum. Simulated spectra were expressed in terms of an absolute intensity scale, which could then be related to sample concentration through comparison with a Cu(II) (EDTA) spin standard of known concentration. EPR samples were prepared by combining buffered solutions of Co(II/III)N_4[11.3.1] and sodium azide in the requisite stoichiometric ratios, loading the samples into quartz EPR tubes and freezing in liquid nitrogen for subsequent analysis within 10 min of mixing. Anaerobic samples were prepared in the glovebox.

Other instrumentation

Electron absorption spectra were recorded using Shimadzu UV-1650PC and UV-2501PC spectrophotometers. The concentrations of oxygen solutions in sodium phosphate buffer, pH 7.4, were generally calculated from Henry's law. In a limited number of cases, the oxygen concentration was verified by measurement with a Clark-type electrode housed in an Oxygraph O2k polarographic instrument (Oroboros, Innsbruck, Austria). Infrared (IR) spectroscopy was performed using a Nicolet 6700 FT-IR spectrometer. Samples for solution IR were prepared and loaded into a liquid transmission cell in an anaerobic glovebox (<0.5 ppm O_2 in argon). Solid

samples for IR spectroscopy in the attenuated total reflectance (ATR) mode were also prepared anaerobically in the glovebox by drying solutions onto microscope slides over P_2O_5.

Data analysis

Data obtained from titrations and animal experiments were analyzed using KaleidaGraph software v. 4.5.1. Statistical significance was determined by a *p*-value < 0.05. Data are reported as means ± standard deviation (SD).

RESULTS

Azide binding to CoN_4[11.3.1]

The addition of Co(II)N_4[11.3.1] to mouse blood was previously shown to result in its reduction to the Co(II) form [15]. We, therefore, studied the stoichiometry and determined the equilibrium constant for the binding of azide to Co(II)N_4[11.3.1]. The electronic absorption spectrum of Co(II)N_4[11.3.1] exhibits a broad band in the visible region with a maximum at 460 nm (Figure 28, solid trace) and no readily detectible features in the 750-110 nm range (not shown). This type of spectrum is suggestive of some combination of nitrogen and oxygen donors in roughly octahedral geometry, as would be provided by the near square-planar arrangement of four aza groups in the macrocycle plus two axial aquo ligands. Following the anaerobic addition of excess sodium azide (0.1 M phosphate buffer, pH 7.4), the absorption maximum shifts to ~475 nm with slight loss of intensity (Figure 28, broken trace). These spectra are consistent with the observed transitions being largely d-d in origin, and, importantly, their similarity is not suggestive of much change in net ligand geometry around the central Co(II) ion upon binding azide. When excess azide was added to Co(II)N_4[11.3.1] in the presence of oxygen, the spectrum obtained displayed significantly reduced absorption intensity throughout most of the visible region (Figure 28, dotte-dashed trace) in keeping with the typically weak d-d spectra of Co(III) compounds. The absorption spectrum of azide-free Co(III)N_4[11.3.1], demonstrating a similar lack of distinct features in the visible region, is shown for comparison (Figure 28, dotted trace). The five-fold more intense band at 350 nm in the azide adduct, formed under aerobic conditions (Figure 28, dot-dashed trace) is presumably more charge-transfer (ligand-to-metal) in nature than the visible region bands in these spectra. Overall, these data suggest that in the presence of oxygen, the binding of azide to Co(II)N_4[11.3.1] results in oxidation of the cobalt to a Co(III) form. The conversions of an ititally

Co(II) species to a Co(III)-containing azide adduct under aerobic conditions was subsequently confirmed by EPR measurements (see further).

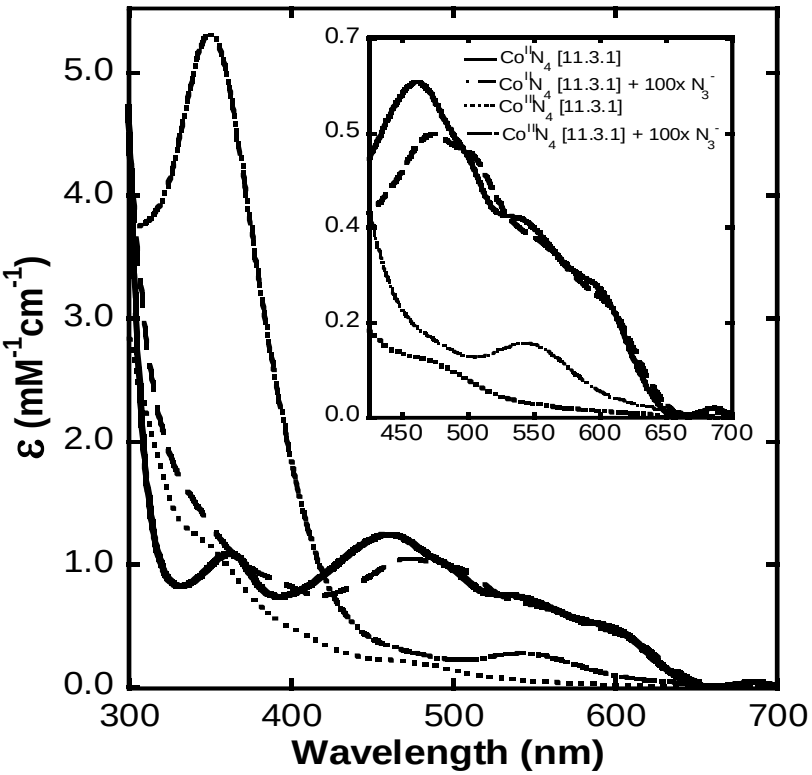

Figure 28. Electronic absorption spectra of CoN_4[11.3.1] and azide adducts in 0.1 M phosphate buffer, pH 7.4. Co(II)N_4[11.3.1] (0.5 mM, solid line), addition of 100-fold excess sodium azide (50 mM) under anaerobic conditions (dashed line). Co(III)N_4[11.3.1] (0.5 mM, dotted line), addition of 100-fold excess sodium azide (50 mM) under aerobic conditons (dot-dashed line). Inset: Enlarged spectra of Co(II)N_4[11.3.1] and Co(III)N_4[11.3.1], both ±100-fold excess sodium azide. Spectra were recorded in 1.00 cm path length cuvettes at 25 °C versus buffer blanks**.**

While the electronic spectral changes indicated that azide bound to Co(II)N_4[11.3.1], the stoichiometry remained unresolved. Job's method has been used for over a century to determine molecular associations such as acid-base equilibria, transition metal coordination, host-guest association, etc. Briefly, the mole fraction of a single component of a two-component system can

be plotted versus some physical property, commonly absorbance, which linearly relates to the formation of a complex. This presentation is often called a Job plot [213-215]. As a positive control, we applied a minor variation of the method to a system containing similarly weak chromophores to the cobalt complexes we intended to investigate further. Formation of the Cu(II)EDTA complex was monitored by absorption difference spectroscopy monitoring the peak-to-trough changes at 723 and 500 nm (

Figure 29A). This well-known 1:1 complex gave a maximal absorption difference at the volume fraction of 0.5, confirming the expected 1 Cu(II):1 EDTA stoichiometry. In addition, the well-defined apex of the plot (rather than something more curved in the vicinity of the maximum) indicates a large binding constant [213]. When the same approach was applied to the anaerobic binding of azide to $Co(II)N_4$[11.3.1] (monitoring the change in absorbance at 460 nm), the maximum was poorly determined, presumably due to an indifferent association constant in conjunction with small changes in absorbance (Figure 28, inset). Thus, the binding stoichiometry was inconclusively defined (Figure29B). In an analogous experiment was carried out in the presence of oxygen, the resulting Job plot was found to exhibit a maximum at a volume fraction of 0.6 (Figure29C). This result best fits a 1:1 stoichiometry.

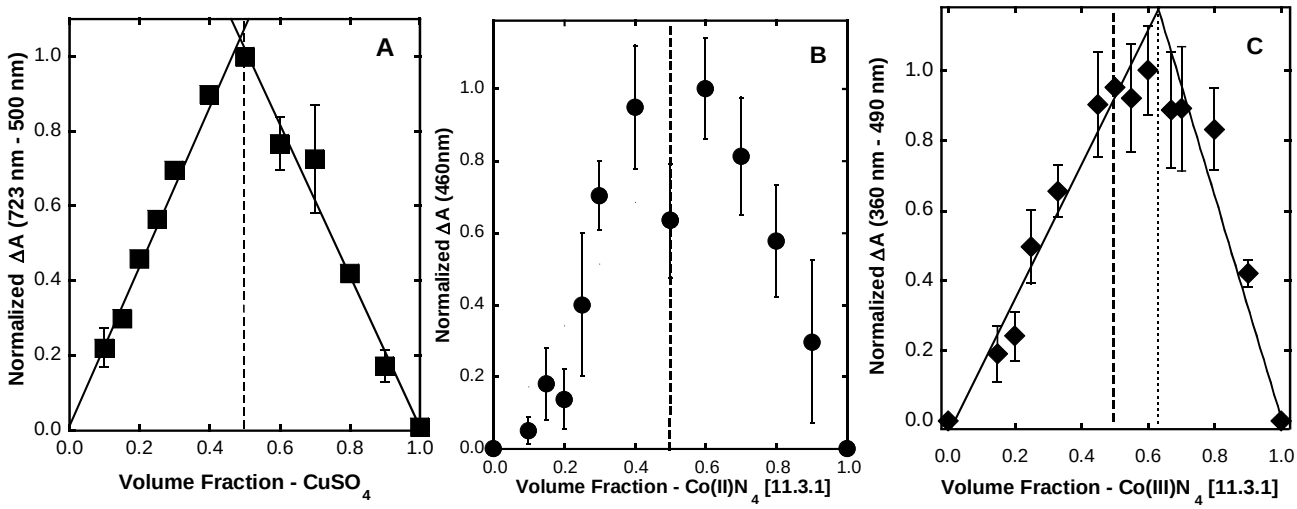

Figure 29. Job plots of Cu(II)SO_4/EDTA, Co(II)N_4[11.3.1]/sodium azide, and Co(III)N_4[11.3.1]/sodium azide using the method of continuous variations.

(A) Cu(II)SO_4 (5 mM) added to Na_2EDTA (5 mM) in 0.025 M acetate buffer, pH 4.7, at the ratios indicated. (B). Co(II)N_4[11.3.1] (0.5 mM) added to sodium azide (0.5 mM) in the presence of 5 mM sodium ascorbate in 0.1 M sodium phosphate, pH 7.4, under aerobic conditions at the ratios indicated. (C) Co(III)N_4[11.3.1] (0.5 mM) added to sodium azide (0.5 mM) in sodium phosphate, pH 7.4, under aerobic conditions at the ratios indicated. The intersection of linear fits to the data represent the volume fraction (X_A=[A]/([A]+[B])) of host corresponding to its binding ratio with the ligand. Dashed lines indicate 1:! Ratio of ligand to complex (see section 0 for details).

To verify the binding of a single azide anion to the reduced cobalt complex, an approach using IR spectroscopy was adopted, taking advantage of both a transmission window in the IR spectrum of solvent water and the absence of any bands arising from the CoN_4[11.3.1] macrocycle in that region of the spectrum where some characteristic azide transitions (asymmetric stretches) are to be found (2000-2200 cm^{-1}) [218]. All measurements shown were performed on samples of the reduced complex prepared/loaded anaerobically (Figure 30). The aqueous solution IR spectrum of Co(II)N_4[11.3.1] in the presence of a substoichiometric amount of azide, 0.5:1, showed only a single transition at 2036 cm^{-1} in the accessible range (Figure 30A, solid trace), indicating a single

azide anion bound to the cobalt complex. Increasing the relative quantity of azide in the sample (3:1, azide:Co(II)N_4[11.3.1]) resulted in the single peak becoming broadened and shifting to 2048 cm^{-1} (indicated by the dashed line). E conclude that only one azide anion is bound to Co(II)N_4[11.3.1] in aqueous solution and interpret the dot-dash trace (Figure 30A) to be a superimposition of the signals due to Co(II)N_4[11.3.1](N_3^{--}) and free azide. When prepared as slowly dried solid films, the IR spectra show that two transitions are now observable in this region of the spectrum located at 2134 and 2008 cm^{-1} (Figure 30B). All these signals have been confirmed to be associated with the azide/azido anion/ligand by obtaining spectra for the ^{15}N-substituted analogs in which they shifted to lower energies (not shown). As the ratio of azide to Co(II)N_4[11.3.1] in samples was increased from 0.5-1 (solid trace) to 1:1 (dotted trace) to 3:1 (dot-dash trace), the intensity of the 2008 cm^{-1} band decreased relative to the 2134 cm^{-1} band, and the underlying spectrum of free azide (now located at 2105 cm^{-1} in the solid films) started to become evident (position of maximum indicated by vertical broken line). The simplest interpretation of these findings is that the 2008 cm^{-1} band is associated with the Co(II)N_4[11.3.1](N_3^{-}) species in the solid and the 2134 cm^{-1} band arises from a diazido adduct or some bridged species. Further unambiguous clarification of this matter would require experiments with isotopically scrambled ligands (like ^{14}N-^{14}N-$^{15}N^{-}$) but, fortunately, this is not necessary for present purposes. Clearly, in comparison with the solution spectra (Figure 30A), the IR spectra of the solid films (Figure 30B) (i) indicate that loss of solvent leads to change in (axial) coordination of the cobalt ion; (ii) provide an example of what the spectrum can be expected to look like with more than one azido ligand bound; and thereby (iii) give reassurance that, in aqueous solution, the Co(II) compound only binds a single azido ligand.

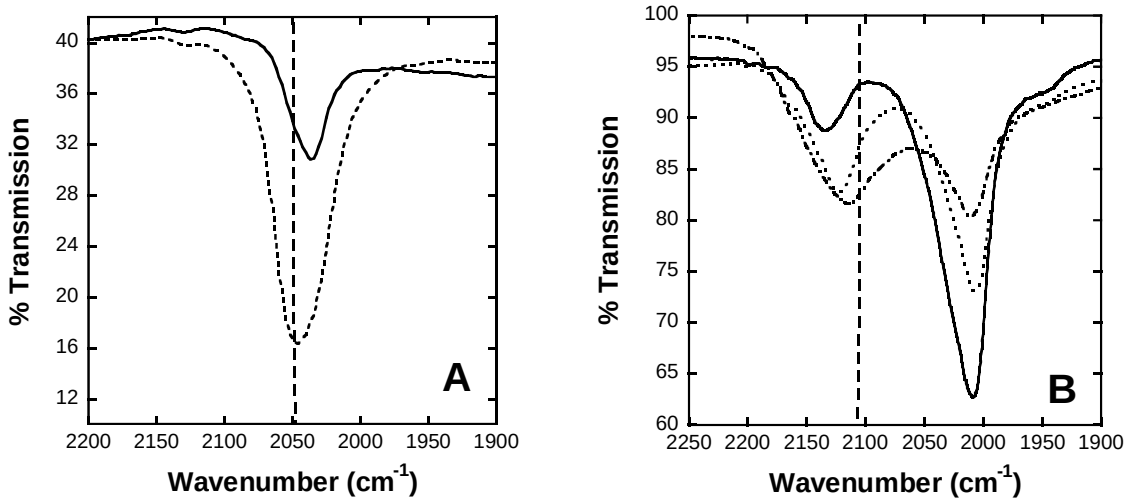

Figure 30. FT-IR spectra of Co(II)N_4[11.3.1] titrated with sodium azide.

(A) Transmission spectra of aqueous samples, 0.025 mm path lengths, containing 100 mM Co(II)N_4[11.3.1] and sodium azide at 50 mM (solid trace) or 300 mM (dotted trace). (B) ATR spectra of solid samples prepared as dried films on glass slides containing azide:cobalt(II) in the following ratios: 0.5:1 (solid trace); 1:! (dotted trace); 3:1 (dot-dashed trace). The frequencies of uncomplexed azide (sodium salt) transitions are indicated by the vertical dashed lines.

Co(II)N_4[11.3.1] has an EPR spectrum typical of S = ½ Co(II) complexes (d^7) having an axis of symmetry with $g_{\parallel} < g_{\perp}$ and exhibiting signals near 3300 G (Figure 31A). We can observe a series of features on top of the main signal (crossover at 3085 G) consisting of eight hyperfine lines resulting from the interaction of the unpaired electron (d^7) with the ^{59}Co nucleus (I = 7/2). Following the addition of increasing amounts of azide to the initial sample, a new EPR signal begins to become apparent (Figure 31B, C, and D) finally resulting in a spectrum with the main crossover feature at 3121 gauss (Figure 31E), a small (36 gauss) but highly reproducible shift.

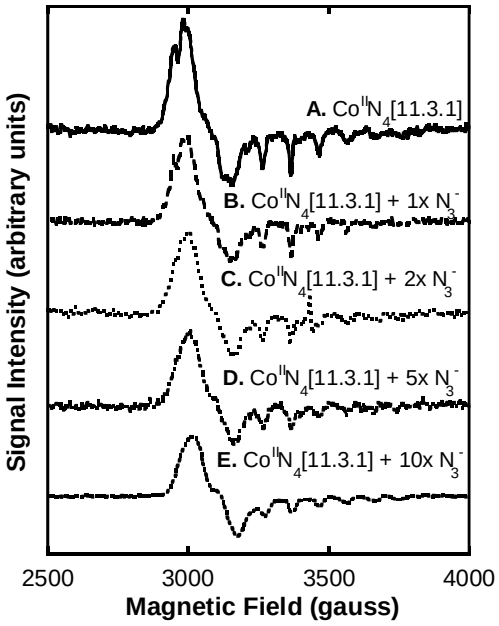

Figure 31. X-band EPR spectra at 20 K of Co(II)N$_4$[11.3.1] titrated with sodium azide.

Samples were prepared anaerobically at room temperature before freezing in liquid nitrogen. (A) Co(II)N$_4$[11.3.1] (0.063 mM) control; (B-E) with increasing amounts of sodium azide (5-100-fold excess) over the cobalt complex concentration. EPR sconditions: 9.8 G modulation amplitude, 63.2 μW microwave power.

In agreement with the electronic spectral findings (Figure 28), the subtlety of these EPR changes suggest that approximately octahedral ligand geometry is maintained around the central Co(II) ion upon azide binding. Even when a 100-fold excess of azide was added to Co(II)N$_4$[11.3.1], the EPR signal obtained did not significantly change from that observed with a 10-fold excess of sodium azide (Figure 31E). When this sample was exposed to oxygen, the signal disappeared, demonstrating the formation of an EPR-silent Co(III)N$_4$[11.3.1[azide compound (data not shown). The concentrations of the Co(III)N$_4$[11.3.1] sample and the fully formed Co(II)N$_4$[11.3.1](N$_3^-$) were determined by double integration of the signals with reference to a Cu(II)EDTA standard using the program SpinCount and found to be within 90% of the calculated

concentrations, that is, 63 μM. The concentrations of the azide-free and azide-bound signals could be determined by combining the two EPR and Co(II)N_4[11.3.1] signals arising from the fully formed Co(II)N_4[11.3.1](N_3^-) and Co(II)N_4[11.3.1] in the samples and matching to the intermediary spectra (Figure 31B, C, and D). This procedure enabled us to quantify concentrations of the Co(II) species present without any interference from small amounts of Co(III), thereby overcoming a significant interference that prevented using electron absorption data to evaluate the azide binding constant. The equilibrium constant (*K*) was determined using the following equation:

$$K = \frac{[Co^{II}N_4[11.3.1](N_3^-)]}{[Co^{II}N_4[11.3.1]][NaN_3]}$$

The concentrations of both cobalt complexes were determined by EPR, and the free azide concentration was calculated by subtracting the amount of bound azide bound from the initial (total) concentration. The equilibrium (association) constant, *K*, for azide binding to Co(II)N_4[11.3.1] was then calculated to be ~10^4 (M^{-1}). This is likely to be an overestimate compared to the value under standard conditions because of the manner in which the EPR samples were prepared (i.e., frozen in liquid N_2). The IR spectra lacked the necessary resolution (Figure 30A), and the visible region absorbance changes were too small (Figure 28 and

Figure 29B) for entirely satisfactory determinations of the association constant. Nevertheless, rough estimates of the ratios of azide to Co(II)N_4[11.3.1] at which the reactions could be judged to be ~50% (or ~90%) complete in the experiments with unfrozen solutions suggest that estimates for the association constant should be in the range of 10^2-10^3 (M^{-1}) with respect to ambient temperatures.

As the oxidation of Co(II) to Co(III) decreases the lability of the cobalt compound and its ability to exchange ligands, a titration of Co(II)N_4[11.3.1] with azide in the presence of oxygen was carried out and analyzed using the Hill equation. A Hill plot of this titration data (log Y = n log [azide] – n log K_A, where Y represents the fractional saturation) resulted in a Hill coefficient (n) of 1.92 (Figure 32). The Hill coefficient of ~2 suggests that there is some type of cooperativity occurring during this reaction, involving at least two processes to which the electronic spectral changes are sensitive. Since the titration monitored the extent of oxygen-dependent oxidation in response to azide addition, the simplest interpretation of the cooperativity is that the binding of an axial ligand to Co(II)N_4[11.3.1] activates the complex to react with oxygen.

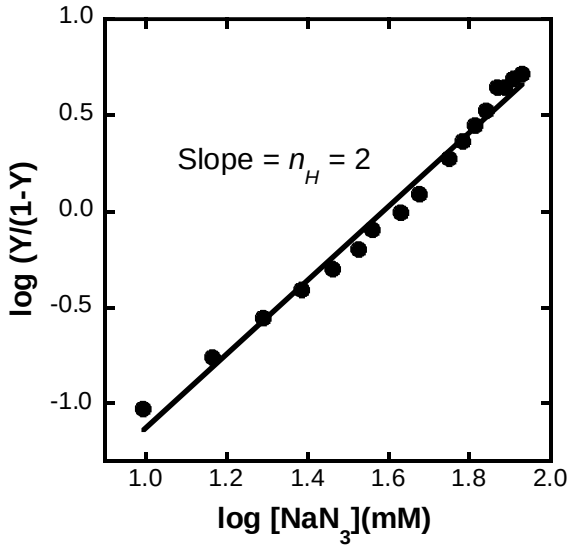

Figure 32. Hill plot of the titration of 0.5 mM Co(II)N_4[11.3.1] with sodium azide following absorbance changes at 360 nm.

The solid line represents a linear least-squares fit of the Hill equation (log Y = n log [azide] – n log K_A, where Y represents the fractional saturation determined from the absorbance data) with n = 1.92.

Kinetics of reaction of azide with Co(II)N_4[11.3.1]

The kinetics of association between azide and the reduced cobalt complex were studied under anaerobic conditions (pH 7.4, 0.1 M sodium phosphate) by following the absorbance changes at 460 nm (absorption maximum of Co(II)N_4[11.3.1]) using stopped-flow spectrophotometry at 25 and 37 °C. The results were indicative of three phases: I (fast, Figure 33A); II (intermediate, Figure 33B), and III (slow, not shown).

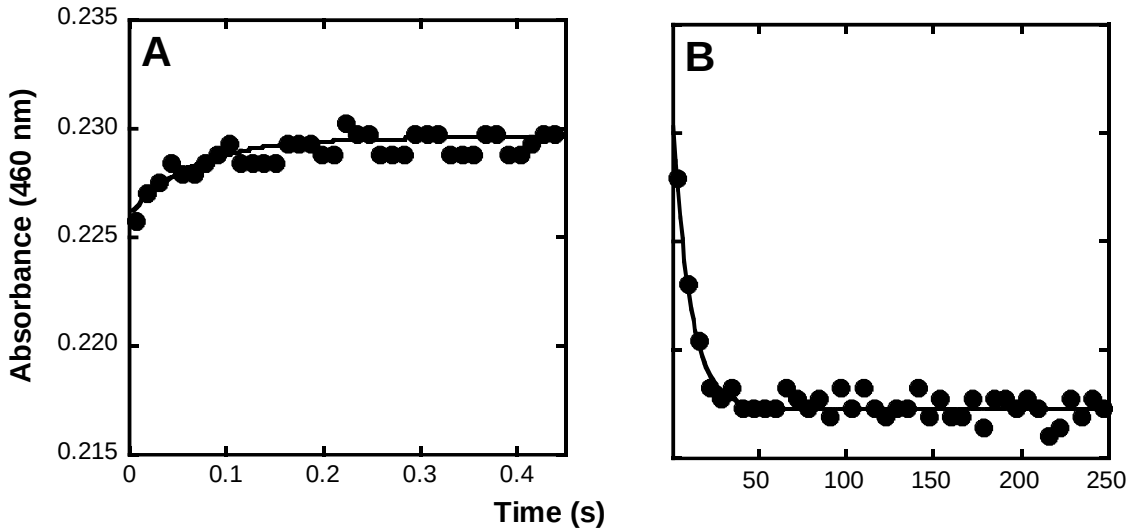

Figure 33. Representative stopped flow kinetics of the reaction of Co(II)N_4[11.3.1] with sodium azide under pseudo-first order conditions.

The reaction was followed anaerobically at 460 nm under the following conditions: 0.3 mM Co(II)N_4[11.3.1], 15 mM (50-fold excess) NaN_3, 0.1 M phosphate buffer, pH 7.4, 25 °C. The absorption at 460 nm was shown to (A) first increase over a one second time frame and then (B) decrease afterward over a 500 s runtime. Symbols represent the collected data with solid lines showing the single exponential fits to the data. All concentrations given are those obtained after mixing.

We first consider phase II that accounted for ~70% of the absorbance change at 460 nm and, therefore, represents the major process observed. Phase II was observed to be linear with respect to both the concentration of azide and the concentration of the cobalt complex (

Figure 34A,B). Second-order rate constants (designated k_2) of 29 (±4) M^{-1} s^{-1} at 25 °C and 70 (±10) M^{-1} s^{-1} at 37 °C were determined for this phase. To verify the lack of any significant pH dependence of the reaction around neutrality, additional experiments at pH values of 6.4 (

Figure 34A, open circle) and 8.5 (

Figure 34, open square) were undertaken and the resulting rates were found to be identical to that observed at pH 7.4 (

Figure 34, solid circles). As the pK_a for azide is 4.72, greater than 97% of the total azide in solution is in the anionic form (N_3^-) at pH values above 6.4. Thus, as expected, the kinetic results are consistent with the unprotonated azide ion being the reacting species.

The fast phase I coincided with a small absorbance increase at 460 nm and was dependent on both the azide concentration and the square of the cobalt compound concentration (Figure 34

C, D). This initial phase was also independent of pH between 6.4 (Figure 34C, open circles) and 8.5 (Figure 34C, open squares) confirming the azide anion to be the attacking species. Phase I and II represent two distinct pathways to the final product, but because phase I is associated with relatively small absorbance changes and occurred partly in the instrument dead time, it was difficult to monitor and we did not attempt a thorough examination of this phase. The rate constant for phase II (above) provides the information of primary concern to the current study, namely, the lower limit of the rate at which Co(II)N_4[11.3.1] binds azide.

The slow phase III also exhibited a small decrease in absorbance at 460 nm (only a few percent change compared to phase II). Interestingly, this fnal phase was linearly dependent on the square root of the azide concentration (Figure 34E)

When the reaction between azide and Co(II)N_4[11.3.1] was carried out aerobically, the presence of oxygen appeared to have no impact on phases I or II. Phase III was masked by the relatively slow oxidation reactions described below, so it is unclear if it was affected.

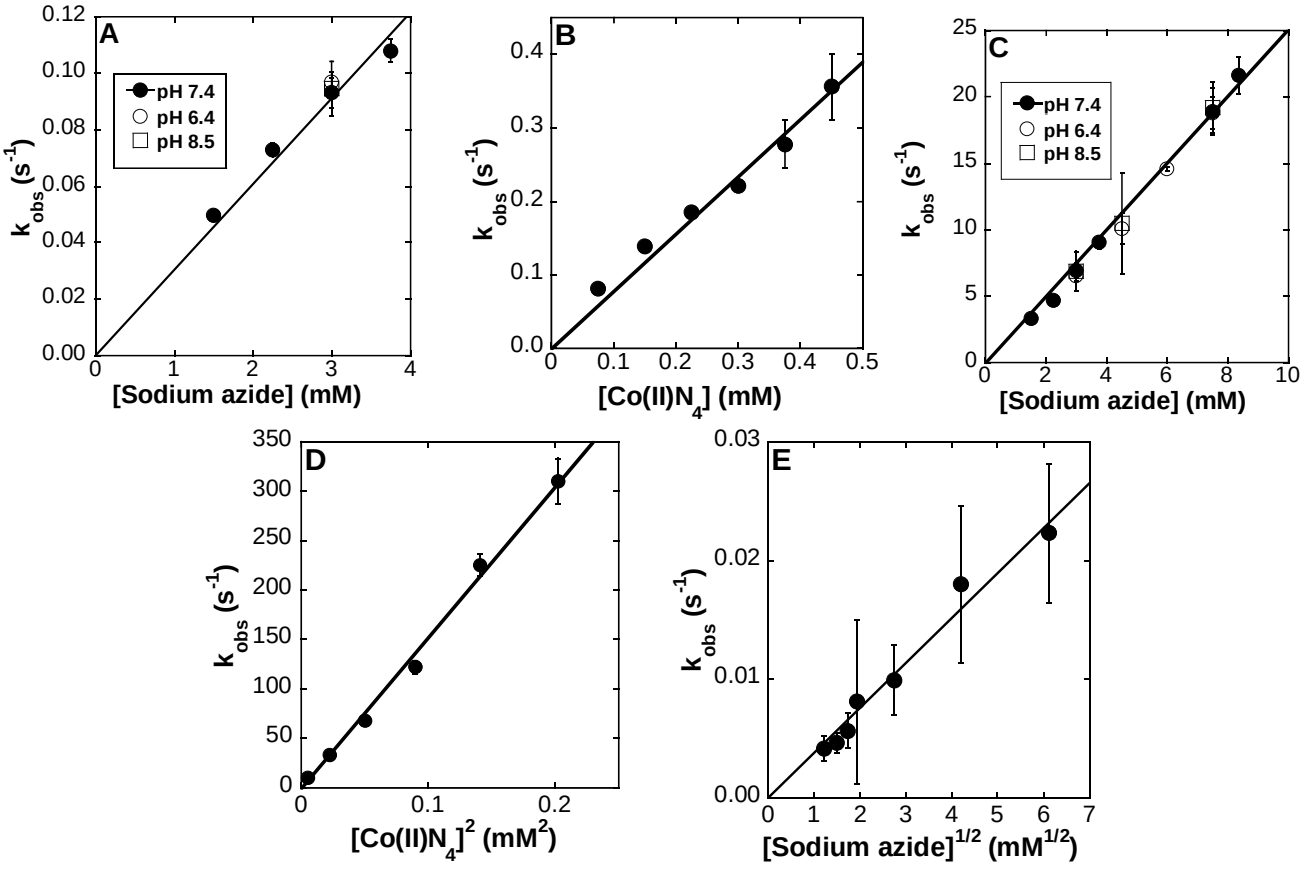

Figure 34. Stopped-flow kinetics of the reaction of sodium azide with Co(II)N_4[11.3.1] under pseudo-first order conditions at 25 °C.

Three phases (fast, k_1; intermediate, k_2; and slow, k_3) were followed anaerobically under pseudo first-order conditions at 460 nm in 0.1 M potassum phosphate buffer (pH 6.4, 7.4, or 8.5) at 25 °C with excess sodium azide (1.5-15 mM) and Co(II)N_4[11.3.1] (0.1-0.5 mM). The observed rates were then plotted versus either the azide concentrations or the Co(II)N_4[11.3.1] concentrations. All concentrations given are those obtained after mixing.

Plots shown are (A) intermediate phase, k_2, varying azide with Co(II)N_4[11.3.1] = 0.15 mM, (B) intermediate phase, k_2, varying Co(II)N_4[11.3.1], with azide = 15 mM, (C) fast phase, k_v varying azide concentration with Co(II)N_4[11.3.1] = 0.15 mM (D) fast phase, k_1, varying Co(II)N_4[11.3.1] concentration with azide = 15 mM, and (E) slow phase varying azide in the presence of 0.15 mM Co(II)N_4[11.3.1].

The oxidation of Co(II)N_4[11.3.1](N_3^-) to Co(III)N_4[11.3.1](N_3^-) in the presence of excess oxygen (pseudo first-order conditions) exhibited biphasic kinetics. Both phases were oxygen dependent (Figure 35 A,B), but the faster phase was linearly dependent on the square of the oxygen concentration (Figure 35A) with calculated rate constants of 3.0 (±0.1) × 10^4 M^{-2} s^{-1} and 130 (±13) M^{-1} s^{-1}. In contrast, the reaction of azide-free Co(II)N_4[11.3.1] with oxygen was significantly slower, 0.5 (±0.1) M^{-1} s^{-1}, with only one significant phase observed [98]. Both oxidation processes appear to be somewhat complicated and warrant further study. Most importantly, however, with regard to the present investigation, the oxidation of the cobalt-azide complex is at least two orders of magnitude faster than the oxidation of the azide-free cobalt complex.

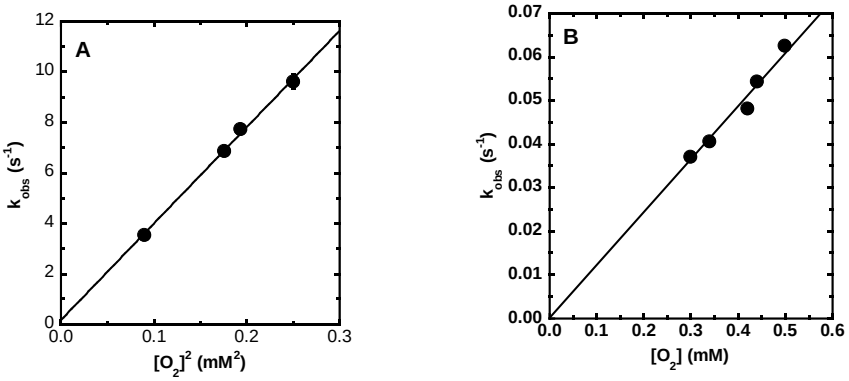

Figure 35. Stopped flow kinetics of the reaction of oxygen with Co(II)N_4[11.3.1](N_3^-) under pseudo-first order conditions at 25 °C.

Saturated oxygen buffer (0.1 M sodium phosphate, pH 7.4) and oxygen saturated buffer diluted into argon saturated buffer were rapidly mixed with Co(II)N_4[11.3.1](N_3^-) (0.05 mM after mixing with a 100-fold ecess of sodium azide) and the reaction followed at 350 nm. The observed rates are plotted versus the final oxygen concentrations (0.28-0.5

mM). The observed rates are plotted versus the final oxygen concentrations (0.28-0.5). (A) fast phase; (B) slow phase, and (C) Co(II)N_4[11.3.1]$(N_3^-)_2$ (0.05 mM).

Potential antidote to azide toxicity in mice

We routinely employ the righting recovery behavior of mice to assess the ability of potential antidotes to ameliorate sublethal doses of toxicants (especially cyanide) [15, 176, 216]. In the present study, mice were injected (ip) with sodium azide ($t = 0$) and then, after "knockdown" (loss of consciousness), placed on their backs and the time until they "righted" themselves onto four feet were recorded. Mice given sodium azide exhibited a rather steep response curve (Figure 36): 25 mg/kg showed no effect, while 30 mg/kg was essential a lethal dose. This differs from the response observed with cyanide in that the molar LD_{50} dose for azide is ~4.5 times the molar cyanide LD_{50} dose. When given 26 mg/kg sodium azide, 12 week-old mice exhibited knockdowns at 7-8 min post injection, with the majority of mice surviving (88%) and exhibiting righting-recovery times of 40 (±8) min (Table 17).

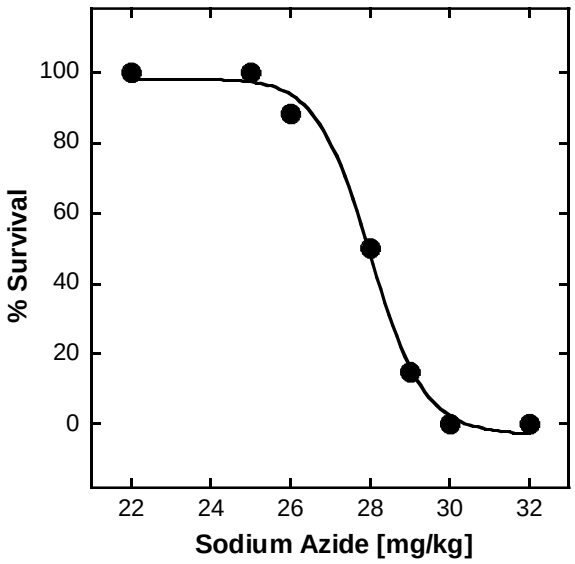

Figure 36. Survival curve of mice treated with sodium azide.

Swiss-Webster mice (12 weeks) were injected (ip) with sodium azide (22-32 mg/kg) and percent survival calculated. At least six mice were used per data point. The line represents a sigmoidal fit of the data.

Table 17. Antidotal activity of CoN_4[11.3.1] against azide toxicity in mice.

Experimental conditions	Number of knock-downs	Recovery Time (min)	% survivors
26 mg/kg NaN_3	8 of 8	40 (±8)	88
26 mg/kg NaN_3 + 24 mg/kg $NaNO_2$ (5 min later)	6 of 6	38 (±8)	83
26 mg/kg NaN_3 + 37 mg/kg CoN_4[11.3.1] (5 min later)	2 of 7	12 (±4)	100

The protective effect of CoN_4[11.3.1] against cyanide toxicity has previously been demonstrated in a mouse model [14, 15]. When CoN_4[11.3.1]Br_2 (37 mg/kg) was given at 5 min post sodium azide, all the mice recovered, the majority did not knockdown (71%) and those that did (29%) recovered by 12 min (Table 17). These results clearly demonstrate that CoN_4[11.3.1] is a potential antidote to azide toxicity, providing encouragement for the further development of scavenger-based therapeutics**.**

DISCUSSION

Principal toxicant species

It has been suggested that azide itself might not be responsible for the observed toxicity, with secondary metabolites, namely, cyanide [205] and nitric oxide [219], proposed as the principal species involved. We have previously shown [176, 216] that (i) administration of sodium nitrite to mice (at similar dose to that employed here) results in the appearance of >0.1 mM nitric oxide in the bloodstream, starting at less than 5 minutes and continuing up to about 20 minutes following the nitrite dose; and (ii) the administration of sodium nitrite/nitric oxide is markedly antidotal toward cyanide intoxication. Consequently, the available anecdotal evidence that sodium nitrite has no antidotal effect toward azide toxicity in human patients [209, 220] argues that neither nitric oxide nor cyanide can be key (secondary) toxicants in azide poisoning. If nitric oxide were involved, then sodium nitrite would be expected to exacerbate azide toxicity and, if cyanide were important, then sodium nitrite should ameliorate azide toxicity. Of course, we cannot categorically state that some other, presently unidentified, secondary metabolite of azide might not be involved, but this would only be speculation. At the present time, to the best of our knowledge, there are no other unambiguous data or rational and well-formulated hypotheses to suggest that the main toxicity of azide is due to anything except the N_3^- anion itself. Therefore, in the absence of any information to the contrary, it behooves us to continue working under the extremely reasonable assumption that N_3^- alone is responsible for the observed acute toxicity.

The observed duration of knockdown following the administration of toxicant were certainly longer for azide (40 and 8 min, respectively) compared to those previously found for cyanide (24 and 2 min, respectively). This slower onset and longer duration of knockdown in the case of azide can probably be explained by consideration of the two relevant acid dissociation

constants (K_as). The pK_a for hydrazoic acid is 4.7, indicating that at physiological pH, >98% of the azide will be present as the unprotonted anion (N_3^-). On the other hand, the pK_a for hydrocyanic acid is 9.2, indicating that at physiological pH >98% of the cyanide will be present as the molecular acid (HCN). HCN is free to diffuse across biological membranes and also quite soluble in aqueous media, while N_3^- must locate channels to efficiently cross membranes. It follows that diffusion of HCN to its mitochondrial site of inhibition from the bloodstream should be faster, resulting in quantitative transfer in less time than N_3^- is transported.

Antidotal activity

In our previous studies concerning the amelioration of cyanide toxicity by CoN_4[11.3.1] in mice, we found the complex to be an efficacious antidote when given either 5 min before or 2 min after an LD_{40} dose of cyanide (5 mg/kg NaCN) [14, 15]. The cobalt macrocycle was shown to bind two molecules of cyanide cooperatively [15], and extensive studies in mice showed it to be at least as good an antidote as cobinamide while measurably better than hydroxocobalamin [14]. Consequently, because azide is a slower acting toxicant, it is perhaps not surprising that preliminary experiments with CoN_4[11.3.1] in mice indicate that it will function as an azide antidote when given at least 5 min after the toxicant (Table 17). More remarkable is the apparent failure of established cyanide antidotes to display any ameliorative effect toward azide toxicity in human patients, particularly when they clearly protect mitochondrial function in an invertebrate model [131]. In fact, there is, seemingly, one case report in the literature suggesting that hydroxocobalamin might be of value as an azide antidote [221] and another to the contrary [222], but nothing of a less anecdotal nature. If we accept the consensual viewpoint that the target for both poisons is primarily cytochrome *c* oxidase, then it is reasonable to expect similarities in

behavior of azide and cyanide both in terms of their toxic mechanisms and responses to antidotes. That is, it might be possible to understand any quantitative difference in the manner in which these two toxicants behave based on knowledge of how each reacts with isolated cytochrome *c* oxidase. In oxygen turnover experiments, isolated cytochrome *c* oxidase has been reported to be inhibited by azide and cyanide with K_is of 22 μM and 0.2 μM, respectively [223]; indicating cyanide to be 150-fold more inhibitory than azide toward the enzyme. Intriguingly, the sodium azide dose used in the present study (400 μmol/kg) is only four-times the sodium cyanide dose (100 μmol/kg) used in our previous studies also monitoring knockdown and righting recovery.

The amount of CoN_4[11.3.1] employed to ameliorate azide toxicity was ~80 μmol/kg (37 mg/kg, Table 17) or approximately 20% of the azide dose (400 μmol/kg). Previously, to ameliorate cyanide toxicity, the most efficacious dose in mice was found to be approximately one-half the cyanide dose, consistent with CoN_4[11.3.1] binding two molecules of cyanide [14, 15]. The present dose of CoN_4[11.3.1] found to ameliorate azide toxicity would have maximally bound about 20% of the azide dose (based on 1:1 stoichiometry). This is low compared to the amount of antidote necessary to bind all the azide but would have the effect of lowering the residual (effective) azide dose from 26 mg/kg to ~21 mg/kg (assuming 20% bound) less than the 24 mg/kg at which we are able to observe minimal effects (Figure 36). Consequently, the findings appear reasonable, being in keeping with the steepness of the dose-response curve for azide toxicity in mice.

Mechanism of decorporation

The detoxification of cyanide by cobalt complexes has recently been suggested to consist of the toxicant binding to the reduced (substation labile) Co(II) forms, resulting in lowering of their oxidation potentials; this in turn facilitates oxidation to the (substitution inert) Co(III) cyanide

adducts that may then be excreted [15, 224-226]. That is, bound cyanide becomes trapped in kinetically stable forms from which it is slow to dissociate, preventing systemic redistribution of the toxicant and, thereby, nullifying its toxicity [14]. A somewhat similar mechanism of decorporation is plausibly operating in the case of the current preliminary experiments with azide intoxicated mice given Co(II)N_4[11.3.1] (Table 17) but differing in detail. Unlike the cyanide reaction, we observed no oxidation of Co(II) to Co(III) under anaerobic conditions following azide addition (Figure 28Figure 31). The oxidation of the azido-cobalt complex does occur however, but in the presence of oxygen and, although complicated (

Figure 35), it is faster than the oxidation of the cobalt complex itself (without azide). Given that inhibition of mitochondrial electron transfer *in vivo* must result in some increase in the prevailing oxygen level, any necessary requirement of available oxygen for conversion of the azide-bound complex to a kinetically stable Co(III) form does not seem to be a limiting issue. The affinity of the Co(II) form of the complex for azide appears to be suitably large enough for efficient decorporation purposes. From the EPR data (Figure 31), we estimate an association constant of ~10^4 for the binding of an azide anion. The kinetics of the reaction of Co(II)N_4[11.3.1] with azide is triphasic, with the first two reasonably facile phases seemingly representing independent azide binding processes (Figure 33

Figure 34). The second (intermediate rate) phase II, with an associated rate constant k_2 = 70 M^{-1} s^{-1} at 37 °C, is the majority process. While the rate constant for phase II is about an order of magnitude less than the analogous rate constant describing cyanide binding to Co(II)N_4[11.3.1] [98], the onset of symptoms in mice given azide intraperitoneally is about five-times slower than animals similarly administered cyanide (not shown). Thus, the rate of reaction appears to be at least adequate for a decorporation mechanism in which azide binds to Co(II)N_4[11.3.1].

The mechanism of decorporation of azide by CoN_4[11.3.1] differs in detail from that we have previously suggested for cyanide [98] and is more complicated. The major reaction pathway (represented by phase II in the kinetics) can most simply be considered a two-step process (e.g. Figure 37) but with the caveat that this does not take into account the possible involvement of protein-associated ligands *in vivo*. For the present purposes, the key finding is that while CoN_4[11.3.1] can clearly be antidotal toward sublethal azide intoxication (Table 17), the apparent binding of one azido ligand to the cobalt ion is likely to ultimatey prove an undesirable limitation. A better antidote might conceivably be some related macrocyclic structure of suitably low toxicity in which the central Co(II) ion is able to bind two azido ligands and then undergo oxidation to a substation inert Co(III) without any loss of bound azide.

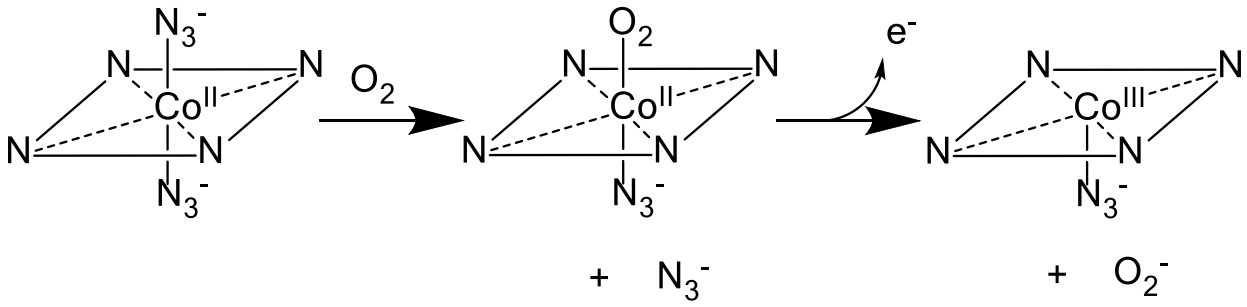

Figure 37. Minimal mechanism for reaction of excess sodium azide with Co(II)N_4[11.3.1] and subsequent oxidation by oxygen.

BIBLIOGRAPHY

1. Chugh, S., et al., *Toxicity of exposed aluminium phosphide.* The Journal of the Association of Physicians of India, 1993. **41**(9): p. 569-570.
2. ATSDR. *Phosphine*. 2014.
3. Dua, R. and K.D. Gill, *Effect of aluminium phosphide exposure on kinetic properties of cytochrome oxidase and mitochondrial energy metabolism in rat brain.* Biochimica et Biophysica Acta (BBA)-General Subjects, 2004. **1674**(1): p. 4-11.
4. Mehrpour, O., M. Jafarzadeh, and M. Abdollahi, *A systematic review of aluminium phosphide poisoning.* Arhiv za higijenu rada i toksikologiju, 2012. **63**(1): p. 61.
5. Soltaninejad, K., et al., *Unusual complication of aluminum phosphide poisoning: Development of hemolysis and methemoglobinemia and its successful treatment.* Indian journal of critical care medicine: peer-reviewed, official publication of Indian Society of Critical Care Medicine, 2011. **15**(2): p. 117.
6. Zamani, N., H. Hassanian-Moghaddam, and S. Ebrahimi, *Whole blood exchange transfusion as a promising treatment of aluminium phosphide poisoning.* Arhiv za higijenu rada i toksikologiju, 2018. **69**(3): p. 275-277.
7. Cha'on, U., et al., *Disruption of iron homeostasis increases phosphine toxicity in Caenorhabditis elegans.* Toxicological Sciences, 2007. **96**(1): p. 194-201.
8. Sinha, U., et al., *Histopathological changes in cases of aluminium phosphide poisoning.* Indian journal of pathology & microbiology, 2005. **48**(2): p. 177-180.
9. Okolie, N.P., J.U. Aligbe, and E.E. Osakue, *Phostoxin-induced biochemical and pathomorphological changes in rabbits.* 2004.
10. Domeneh, B.H., et al., *A review of aluminium phosphide poisoning and a flowchart to treat it.* 2016.
11. Shadnia, S., et al., *Successful treatment of acute aluminium phosphide poisoning: possible benefit of coconut oil.* Human & experimental toxicology, 2005. **24**(4): p. 215-218.
12. Brautbar, N. and J. Howard, *Phosphine toxicity: report of two cases and review of the literature.* Toxicology and industrial health, 2002. **18**(2): p. 71-75.
13. Chugh, S., et al., *A critical evaluation of anti-peroxidant effect of intravenous magnesium in acute aluminium phosphide poisoning.* Magnesium research, 1997. **10**(3): p. 225-230.
14. Cronican, A.A., et al., *A Comparison of the Cyanide-Scavenging Capabilities of Some Cobalt-Containing Complexes in Mice.* Chem Res Toxicol, 2018. **31**(4): p. 259-268.
15. Lopez-Manzano, E., et al., *Cyanide Scavenging by a Cobalt Schiff-Base Macrocycle: A Cost-Effective Alternative to Corrinoids.* Chemical research in toxicology, 2016. **29**(6): p. 1011-1019.
16. Praekunatham, H.G., K; Cronican, A; Frawley, K; Pearce, L; Peterson, J, *A Cobalt Schiff-base Complex as a Putative Therapeutic for Azide Poisoning.* Chemical Research in Toxicology, 2019.
17. Cotton, F.A. and G. Wilkinson, *Advanced Inorganic Chemistry*. Fifth ed. 1988: Wiley-Interscience.

18. Housecroft, C.E. and A.G. Sharpe, *Inorganic Chemistry*. 4th ed. 2012, Harlow U.K.: Pearson Education Ltd.
19. Sanaei-Zadeh, H., *Aluminum phosphide poisoning and development of hemolysis and methemoglobinemia.* Indian Journal of Critical Care Medicine, 2012. **16**(4): p. 248.
20. Mostafazadeh, B., et al., *Blood levels of methemoglobin in patients with aluminum phosphide poisoning and its correlation with patient's outcome.* Journal of Medical Toxicology, 2011. **7**(1): p. 40-43.
21. Aggarwal, P., et al., *Intravascular hemolysis in aluminium phosphide poisoning.* The American journal of emergency medicine, 1999. **17**(5): p. 488-489.
22. Wahdan, A. and E. Elmadah, *Methemoglobinemia and intravascular hemolysis; unusual presentations of metal phosphides poisoning.* Ain Shams Journal of Forensic Medicine and Clinical Toxicology, 2016. **26**(1): p. 129-139.
23. Lall, S., S. Peshin, and S. Mitra, *Methemoglobinemia in aluminium phosphide poisoning in rats.* 2000.
24. Shadnia, S., et al., *Methemoglobinemia in aluminum phosphide poisoning.* Human & experimental toxicology, 2011. **30**(3): p. 250-253.
25. Lakshmi, B., *Methemoglobinemia with aluminum phosphide poisoning.* The American journal of emergency medicine, 2002. **20**(2): p. 130-132.
26. Lam, W.W., R.F. Toia, and J.E. Casida, *Oxidatively initiated phosphorylation reactions of phosphine.* Journal of agricultural and food chemistry, 1991. **39**(12): p. 2274-2278.
27. Gurjar, M., et al., *Managing aluminum phosphide poisonings.* Journal of emergencies, trauma and shock, 2011. **4**(3): p. 378.
28. Mohney, G. *How water poured on rodenticide caused 4 deaths in a texas home*. 2017; Available from: https://abcnews.go.com/Health/water-poured-rodenticide-caused-deaths-texas-home/story?id=44526042.
29. Kumar, S.V., et al., *A study on poisoning cases in a tertiary care hospital.* Journal of natural science, biology, and medicine, 2010. **1**(1): p. 35.
30. CADPR, *Estimation of exposure to persons in california to phosphine due to use of aluminum phosphide, magnesium phosphide, and cylinderized phosphine gas*. 2014, Department of Pesticide Regulation.
31. Wilson, R., et al., *Acute phosphine poisoning aboard a grain freighter: epidemiologic, clinical, and pathological findings.* Jama, 1980. **244**(2): p. 148-150.
32. Van de Sijpe, P., et al., *Acute occupational phosphine intoxications in the maritime shipping sector: Belgian and French reported cases.* International Maritime Health, 2020. **71**(3): p. 151-159.
33. O'Malley, M., et al., *Inhalation of phosphine gas following a fire associated with fumigation of processed pistachio nuts.* Journal of agromedicine, 2013. **18**(2): p. 151-173.
34. Lineberry, T.W. and J.M. Bostwick. *Methamphetamine abuse: a perfect storm of complications*. in *Mayo Clinic Proceedings*. 2006. Elsevier.
35. Burgess, J.L., *Phosphine exposure from a methamphetamine laboratory investigation.* Journal of Toxicology: Clinical Toxicology, 2001. **39**(2): p. 165-168.
36. Willers-Russo, L.J., *Three fatalities involving phosphine gas, produced as a result of methamphetamine manufacturing.* Journal of Forensic Science, 1999. **44**(3): p. 647-652.
37. Lemoine, T.J., et al., *Unintentional fatal phosphine gas poisoning of a family.* Pediatric emergency care, 2011. **27**(9): p. 869-871.

38. Lauer, C. *Police investing accidental poisoning that killed 4 kids*. 2017 [cited 2021; Available from: https://apnews.com/article/6f09a65bbb5142cb8d2469f9c3cdd6aa.
39. *Phosphine pesticide used to kill bedbugs causes Fort McMurray baby's death*. 2015; Available from: https://www.cbc.ca/news/canada/edmonton/phosphine-pesticide-used-to-kill-bedbugs-causes-fort-mcmurray-baby-s-death-1.2969189.
40. Blum, D. *Dead tourists and a dangerous pesticide*. 2014; Available from: https://www.wired.com/2014/03/dead-tourists-and-a-dangerous-pesticide/.
41. Bumbrah, G.S., et al., *Phosphide poisoning: a review of literature.* Forensic science international, 2012. **214**(1-3): p. 1-6.
42. Anand, R., B. Binukumar, and K.D. Gill, *Aluminum phosphide poisoning: an unsolved riddle.* Journal of applied toxicology, 2011. **31**(6): p. 499-505.
43. Kordrostami, R., et al., *Forensic toxicology analysis of self-poisoning suicidal deaths in Tehran, Iran; trends between 2011-2015.* DARU Journal of Pharmaceutical Sciences, 2017. **25**(1): p. 1-10.
44. Thippaiah, S.M., M.S. Nanjappa, and S.B. Math, *Suicide in India: A preventable epidemic.* The Indian journal of medical research, 2019. **150**(4): p. 324.
45. Snowdon, J., *Indian suicide data: What do they mean?* The Indian journal of medical research, 2019. **150**(4): p. 315.
46. Etemadi-Aleagha, A., M. Akhgari, and F.S. Iravani, *Aluminum phosphide poisoning-related deaths in Tehran, Iran, 2006 to 2013.* Medicine, 2015. **94**(38).
47. Meena, M.C., S. Mittal, and Y. Rani, *Fatal aluminium phosphide poisoning.* Interdisciplinary toxicology, 2015. **8**(2): p. 65-67.
48. Yan, H., et al., *Phosphine analysis in postmortem specimens following inhalation of phosphine: fatal aluminum phosphide poisoning in children.* Journal of analytical toxicology, 2018. **42**(5): p. 330-336.
49. Farahani, M.V., D. Soroosh, and S.M. Marashi, *Thoughts on the current management of acute aluminum phosphide toxicity and proposals for therapy: An evidence-based review.* Indian journal of critical care medicine: peer-reviewed, official publication of Indian Society of Critical Care Medicine, 2016. **20**(12): p. 724.
50. Jaiswal, S., R. Verma, and N. Tewari, *Aluminum phosphide poisoning: Effect of correction of severe metabolic acidosis on patient outcome.* Indian journal of critical care medicine: peer-reviewed, official publication of Indian Society of Critical Care Medicine, 2009. **13**(1): p. 21.
51. *6 CFR Part 27 Appendix to Chemical Facility Anti-Terrorism Standards; Final Rule*, D.o.H. Security, Editor. 2007: Federal Register.
52. Fluck, E., *The chemistry of phosphine*, in *Inorganic Chemistry*. 1973, Springer. p. 1-64.
53. NIOSH. *Phosphine: Lung Damaging Agent*. Emergency Response Safety and Health Database 2011; Available from: https://www.cdc.gov/niosh/ershdb/emergencyresponsecard_29750035.html.
54. Bond, E. and T. Dumas, *Loss of warning odour from phosphine.* Journal of Stored Products Research, 1967. **3**(4): p. 389-392.
55. Musshoff, F., et al., *A gas chromatographic analysis of phosphine in biological material in a case of suicide.* Forensic science international, 2008. **177**(2-3): p. e35-e38.
56. Withnall, R. and L. Andrews, *FTIR spectra of the photolysis products of the phosphine-ozone complex in solid argon.* Journal of Physical Chemistry, 1987. **91**(4): p. 784-797.
57. Nath, N.S., et al., *Mechanisms of phosphine toxicity.* Journal of toxicology, 2011. **2011**.

58. Assem, L. and M. Takamiya. *Phosphine Toxicological overview*. 2007.
59. Sciuto, A.M., et al., *Phosphine toxicity: a story of disrupted mitochondrial metabolism.* Annals of the New York Academy of Sciences, 2016. **1374**(1): p. 41.
60. Anand, R., et al., *Effect of acute aluminum phosphide exposure on rats—A biochemical and histological correlation.* Toxicology letters, 2012. **215**(1): p. 62-69.
61. (IPCS), I.P.o.C.S., *Phosphine,* in *Poisons Information Monnograph*. 1997, WHO: Geneva.
62. Chaudry, M., *A review of the mechanisms involved in the action of phosphine as an insecticide and phosphine resistance in stored–product insect.* Pesticide Science, 1996. **49**: p. 213-228.
63. Price, N., *Some aspects of the inhibition of cytochrome c oxidase by phosphine in susceptible and resistant strains of Rhyzopertha dominicia.* Insect Biochemistry, 1980. **10**(2): p. 147-150.
64. Loddé, B., et al., *Acute phosphine poisoning on board a bulk carrier: analysis of factors leading to a fatal case.* Journal of occupational medicine and toxicology, 2015. **10**(1): p. 1-7.
65. Misra, U., et al., *Occupational phosphine exposure in Indian workers.* Toxicology letters, 1988. **42**(3): p. 257-263.
66. WARITZ, R.S. and R.M. BROWN, *Acute and subacute inhalation toxicities of phosphine, phenylphosphine and triphenylphosphine.* American Industrial Hygiene Association Journal, 1975. **36**(6): p. 452-458.
67. Wong, B., et al., *The physiology and toxicology of acute inhalation phosphine poisoning in conscious male rats.* Inhalation toxicology, 2017. **29**(11): p. 494-505.
68. Bond, E., J. Robinson, and C. Buckland, *The toxic action of phosphine absorption and symptoms of poisoning in insects.* Journal of stored products research, 1969. **5**(4): p. 289-298.
69. Chin, K., et al., *The interaction of phosphine with haemoglobin and erythrocytes.* Xenobiotica, 1992. **22**(5): p. 599-607.
70. Gautam, S., G. Opit, and E. Hosoda, *Phosphine resistance in adult and immature life stages of Tribolium castaneum (Coleoptera: Tenebrionidae) and Plodia interpunctella (Lepidoptera: Pyralidae) populations in California.* Journal of economic entomology, 2016: p. tow221.
71. Pimentel, M.A.G., et al., *Phosphine resistance, respiration rate and fitness consequences in stored-product insects.* Pest Management Science: formerly Pesticide Science, 2007. **63**(9): p. 876-881.
72. Ludwig, H., S. Cairelli, and J. Whalen, *Documentation for Immediately Dangerous to Life or Health Concentrations (IDLHs)*. 1994, US Department of Health and Human Services: Cincinnati, OH. p. 530.
73. Administration, N.O.a.A. *Acute Exposure Guideline Levels (AEGLs)*. 2021; Available from: https://response.restoration.noaa.gov/oil-and-chemical-spills/chemical-spills/resources/acute-exposure-guideline-levels-aegls.html.
74. Chefurka, W., K. Kashi, and E. Bond, *The effect of phosphine on electron transport in mitochondria.* Pesticide Biochemistry and Physiology, 1976. **6**(1): p. 65-84.
75. Nakakita, H., Y. KATSUMATA, and T. OZAWA, *The effect of phosphine on respiration of rat liver mitochondria.* The Journal of Biochemistry, 1971. **69**(3): p. 589-593.

76. Valmas, N., S. Zuryn, and P.R. Ebert, *Mitochondrial uncouplers act synergistically with the fumigant phosphine to disrupt mitochondrial membrane potential and cause cell death.* Toxicology, 2008. **252**(1-3): p. 33-39.
77. Zuryn, S., J. Kuang, and P. Ebert, *Mitochondrial modulation of phosphine toxicity and resistance in Caenorhabditis elegans.* Toxicological Sciences, 2008. **102**(1): p. 179-186.
78. Anand, R., et al., *Mitochondrial electron transport chain complexes, catalase and markers of oxidative stress in platelets of patients with severe aluminum phosphide poisoning.* Human & experimental toxicology, 2013. **32**(8): p. 807-816.
79. Nakakita, H., *Mitochondria of Maize Weevils, Sitophilus zeamais (M.): II. Components of Cytochromes and Effects of Phosphine on Adult Maize Weevil Mitochondria.* Applied entomology and zoology, 1976. **11**(4): p. 327-334.
80. Chugh, S., et al., *Plasma renin activity in shock due to aluminium phosphide poisoning.* The Journal of the Association of Physicians of India, 1990. **38**(6): p. 398-399.
81. Pimentel, M., et al., *Phosphine resistance in Brazilian populations of Sitophilus zeamais motschulsky (Coleoptera: Curculionidae).* Journal of Stored Products Research, 2009. **45**(1): p. 71-74.
82. Bolter, C.J. and W. Chefurka, *Extramitochondrial release of hydrogen peroxide from insect and mouse liver mitochondria using the respiratory inhibitors phosphine, myxothiazol, and antimycin and spectral analysis of inhibited cytochromes.* Archives of biochemistry and biophysics, 1990. **278**(1): p. 65-72.
83. Brandes, R.P., F. Rezende, and K. Schröder, *Redox regulation beyond ROS: why ROS should not be measured as often.* Circulation research, 2018. **123**(3): p. 326-328.
84. Liochev, S.I., *Reactive oxygen species and the free radical theory of aging.* Free Radical Biology and Medicine, 2013. **60**: p. 1-4.
85. Shields, H.J., A. Traa, and J.M. Van Raamsdonk, *Beneficial and Detrimental Effects of Reactive Oxygen Species on Lifespan: A Comprehensive Review of Comparative and Experimental Studies.* Frontiers in Cell and Developmental Biology, 2021. **9**: p. 181.
86. Memiş, D., et al., *Fatal aluminium phosphide poisoning.* European journal of anaesthesiology, 2007. **24**(3): p. 292-293.
87. Rahimi, N., et al., *Fresh red blood cells transfusion protects against aluminum phosphide-induced metabolic acidosis and mortality in rats.* PloS one, 2018. **13**(3): p. e0193991.
88. Wright, R.O., W.J. Lewander, and A.D. Woolf, *Methemoglobinemia: etiology, pharmacology, and clinical management.* Annals of emergency medicine, 1999. **34**(5): p. 646-656.
89. Curry, S. and A. Kang, *Hematologic syndromes: Hemolysis, methemoglobinemia, sulfhemoglobinemia.* Critical care toxicology, 2005: p. 339.
90. Belcher, J.D., et al., *Heme degradation and vascular injury.* Antioxidants & redox signaling, 2010. **12**(2): p. 233-248.
91. Benatti, U., et al., *A methemoglobin-dependent and plasma-stimulated experimental model of oxidative hemolysis.* Biochemical and biophysical research communications, 1982. **106**(4): p. 1183-1190.
92. Reeder, B.J., *The redox activity of hemoglobins: from physiologic functions to pathologic mechanisms.* Antioxidants & redox signaling, 2010. **13**(7): p. 1087-1123.
93. Eteiwi, S.M., et al., *Potassium permanganate poisoning: A nonfatal outcome.* Oman medical journal, 2015. **30**(4): p. 291.

94. Sudakin, D., *Occupational exposure to aluminium phosphide and phosphine gas? A suspected case report and review of the literature.* Human & experimental toxicology, 2005. **24**(1): p. 27-33.
95. Lauterbach, M., et al., *Epidemiology of hydrogen phosphide exposures in humans reported to the poison center in Mainz, Germany, 1983–2003.* Clinical toxicology, 2005. **43**(6): p. 575-581.
96. Singh, B. and B. Unnikrishnan, *A profile of acute poisoning at Mangalore (South India).* Journal of clinical forensic medicine, 2006. **13**(3): p. 112-116.
97. Wahab, A., et al., *Spontaneous self-ignition in a case of acute aluminium phosphide poisoning.* The American journal of emergency medicine, 2009. **27**(6): p. 752. e5-752. e6.
98. Praekunatham, H., L.L. Pearce, and J. Peterson, *Reaction Kinetics of Cyanide Binding to a Cobalt Schiff-Base Macrocycle Relevant to Its Mechanism of Antidotal Action.* Chemical research in toxicology, 2019. **32**(8): p. 1630-1637.
99. Pearson, R.G., *Hard and soft acids and bases, HSAB, part 1: Fundamental principles.* Journal of Chemical Education, 1968. **45**(9): p. 581.
100. Best, S.L. and P.J. Sadler, *Gold drugs: mechanism of action and toxicity.* Gold bulletin, 1996. **29**(3): p. 87-93.
101. Sadler, P.J. and R.E. Sue, *The chemistry of gold drugs.* Metal-Based Drugs, 1994. **1**(2-3): p. 107-144.
102. Nobili, S., et al., *Gold compounds as anticancer agents: chemistry, cellular pharmacology, and preclinical studies.* Medicinal research reviews, 2010. **30**(3): p. 550-580.
103. Ott, I., *On the medicinal chemistry of gold complexes as anticancer drugs.* Coordination Chemistry Reviews, 2009. **253**(11-12): p. 1670-1681.
104. *FDA Approved Drug Products*. 2006 [cited 2018 July 19]; Available from: https://www.accessdata.fda.gov/scripts/cder/daf/index.cfm?event=overview.process&ApplNo=084921.
105. Medici, S., et al., *Silver coordination compounds: A new horizon in medicine.* Coordination Chemistry Reviews, 2016. **327**: p. 349-359.
106. Barillo, D.J. and D.E. Marx, *Silver in medicine: A brief history BC 335 to present.* Burns, 2014. **40**: p. S3-S8.
107. Kalinowska-Lis, U., et al., *Synthesis, characterization and antimicrobial activity of water-soluble silver (I) complexes of metronidazole drug and selected counter-ions.* Dalton Transactions, 2015. **44**(17): p. 8178-8189.
108. Kean, W., C. Lock, and H. Howard-Lock, *Gold complex research in medical science. Difficulties with experimental design.* Inflammopharmacology, 1991. **1**(2): p. 103-114.
109. Narayanaswamy, R., et al., *Synthesis, structure, and electronic spectroscopy of neutral, dinuclear gold (I) complexes. Gold (I)-gold (I) interactions in solution and in the solid state.* Inorganic Chemistry, 1993. **32**(11): p. 2506-2517.
110. Ciompi, M., et al., *Sodium-gold thyosolphatum therapy: an open, viewed, multicenter trial in rheumatoid arthritis patients followed for two years.* Reumatismo, 2002. **54**(3): p. 251-256.
111. Van Roon, E.N., et al., *Parenteral gold preparations. Efficacy and safety of therapy after switching from aurothioglucose to aurothiomalate.* The Journal of rheumatology, 2005. **32**(6): p. 1026-1030.

112. Ferraccioli, G., et al., *Long-term outcome with gold thiosulphate and tiopronin in 200 rheumatoid patients.* Clinical and experimental rheumatology, 1989. **7**(6): p. 577-581.
113. Darabi, F., et al., *Reactions of model proteins with aurothiomalate, a clinically established gold (I) drug: the comparison with auranofin.* Journal of inorganic biochemistry, 2015. **149**: p. 102-107.
114. Amberson Jr, J.B., B. McMahon, and M. Pinner, *A clinical trial of sanocrysin in pulmonary tuberculosis.* American Review of Tuberculosis, 1931. **24**(4): p. 401-435.
115. Brown, H., *Sodium aurothiosulfate. A simple method for its preparation.* Journal of the American Chemical Society, 1927. **49**(4): p. 958-959.
116. Kean, W. and I. Kean, *Clinical pharmacology of gold.* Inflammopharmacology, 2008. **16**(3): p. 112-125.
117. *Aurothioglucose*. 2021; Available from: https://www.sigmaaldrich.com/US/en/product/usp/1045508?context=product.
118. *Sodium Aurothiomalate Hydrate*. 2021; Available from: https://www.sigmaaldrich.com/US/en/product/aldrich/157201?context=product.
119. *Gold(I) sodium thiosulfate hydrate*. 2021; Available from: https://www.fishersci.com/shop/products/gold-i-sodium-thiosulfate-hydrate-99-9-metals-basis-alfa-aesar-3/AA3974103.
120. Starek, M., et al., *Stability of Metronidazole and Its Complexes with Silver (I) Salts under Various Stress Conditions.* Molecules, 2021. **26**(12): p. 3582.
121. WHO, *The impact of pesticides on health: Preventing intentional and unintentional deaths from pesticide poisoning*. 2006.
122. *Preparation of silver thiosulfate (STS) solution*. 2003; Product information sheet]. Available from: www.phytotechlab.com.
123. Ratte, H.T., *Bioaccumulation and toxicity of silver compounds: a review.* Environmental Toxicology and Chemistry: An International Journal, 1999. **18**(1): p. 89-108.
124. Leblanc, G.A., et al., *The influence of speciation on the toxicity of silver to fathead minnow (Pimephales promelas).* Environmental Toxicology and Chemistry: An International Journal, 1984. **3**(1): p. 37-46.
125. Lansdown, A.B., *Silver in health care: antimicrobial effects and safety in use.* Biofunctional textiles and the skin, 2006. **33**: p. 17-34.
126. Drake, P.L. and K.J. Hazelwood, *Exposure-related health effects of silver and silver compounds: a review.* The Annals of occupational hygiene, 2005. **49**(7): p. 575-585.
127. Fung, M.C. and D.L. Bowen, *Silver products for medical indications: risk-benefit assessment.* Journal of toxicology: Clinical toxicology, 1996. **34**(1): p. 119-126.
128. Rungby, J. and G. Danscher, *Hypoactivity in silver exposed mice.* Acta pharmacologica et toxicologica, 1984. **55**(5): p. 398-401.
129. Atkins, P.W. and L.L. Jones, *Chemical Principles The Quest for Insight*. 5 ed. 2010, New York, NY: W. H. Freeman and Company.
130. Frawley, K.L., et al., *A Comparison of Potential Azide Antidotes in a Mouse Model.* Chemical Research in Toxicology, 2020. **33**(2): p. 594-603.
131. Frawley, K.L., et al., *Assessing modulators of cytochrome c oxidase activity in Galleria mellonella larvae.* Comparative Biochemistry and Physiology Part C: Toxicology & Pharmacology, 2019. **219**: p. 77-86.
132. Lionakis, M.S., *Drosophila and Galleria insect model hosts: new tools for the study of fungal virulence, pharmacology and immunology.* Virulence, 2011. **2**(6): p. 521-7.

133. Champion, O.L., S. Wagley, and R.W. Titball, *Galleria mellonella as a model host for microbiological and toxin research.* Virulence, 2016. **7**(7): p. 840-5.
134. Tsai, C.J., J.M. Loh, and T. Proft, *Galleria mellonella infection models for the study of bacterial diseases and for antimicrobial drug testing.* Virulence, 2016. **7**(3): p. 214-29.
135. Nathan, S., *New to Galleria mellonella: Modeling an ExPEC Infection.* Virulence, 2014 April 1. **5**(3): p. 371-374.
136. Desbois, A.P. and P.J. Coote, *Utility of Greater Wax Moth Larva (Galleria mellonella) for Evaluating the Toxicity and Efficacy of New Antimicrobial Agents.* Adv Appl Microbiol, 2012. **78**: p. 25-53.
137. Hsu, C.-H., et al., *Phosphine-induced oxidative damage in rats: attenuation by melatonin.* Free radical biology and medicine, 2000. **28**(4): p. 636-642.
138. Hay, R.W., G.A. Lawrance, and N.F. Curtis, *A convenient synthesis of the tetra-aza-macrocyclic ligands trans-[14]-diene, tet a, and tet b.* Journal of the Chemical Society, Perkin Transactions 1, 1975(6): p. 591-593.
139. Curtis, N., *855. Transition-metal complexes with aliphatic Schiff bases. Part I. Nickel (II) complexes with N-isopropylidene-ethylenediamine schiff bases.* Journal of the Chemical Society (Resumed), 1960: p. 4409-4413.
140. Long, K.M. and D.H. Busch, *Cobalt (II) complexes of the quadridentate macrocycle 2, 12-dimethyl-3, 7, 11, 17-tetraazabicyclo [11.3. 1] heptadeca-1 (17), 2, 11, 13, 15-pentaene.* Inorganic Chemistry, 1970. **9**(3): p. 505-512.
141. Lacy, D.C., C.C. McCrory, and J.C. Peters, *Studies of cobalt-mediated electrocatalytic CO2 reduction using a redox-active ligand.* Inorganic chemistry, 2014. **53**(10): p. 4980-4988.
142. Gnaiger, E., *The oxygraph for high resolution respirometry.* 2011, Oroboros Instruments Corp.: Innsbruck, Austria.
143. Aw, W.C., et al., *Assessing bioenergetic functions from isolated mitochondria in Drosophila melanogaster.* Journal of Biological Methods; Vol 3, No 2 (2016), 2016.
144. EPA, *Physicochemical Properties for TRI Chemicals and Chemical Categories*. 2002.
145. Crawley, J.N., *What's wrong with my mouse?: behavioral phenotyping of transgenic and knockout mice*. 2007: John Wiley & Sons.
146. Spector, A., *Oxidative stress-induced cataract: mechanism of action.* The FASEB Journal, 1995. **9**(12): p. 1173-1182.
147. Frawley, K.L., et al., *Sulfide Toxicity and Its Modulation by Nitric Oxide in Bovine Pulmonary Artery Endothelial Cells.* Chem Res Toxicol, 2017. **30**(12): p. 2100-2109.
148. Pearce, L.L., et al., *Reversal of cyanide inhibition of cytochrome c oxidase by the auxiliary substrate nitric oxide: an endogenous antidote to cyanide poisoning?* J Biol Chem, 2003. **278**(52): p. 52139-45.
149. Gibson, Q.H., G. Palmer, and D.C. Wharton, *The binding of carbon monoxide by cytochrome c oxidase and the ratio of the cytochromes a and A3.* Journal of Biological Chemistry, 1965. **240**(2): p. 915-920.
150. Van Gelder, B., *On cytochrome c oxidase I. The extinction coefficients of cytochrome a and cytochrome a3.* Biochimica et Biophysica Acta (BBA)-Enzymology and Biological Oxidation, 1966. **118**(1): p. 36-46.
151. Nicholls, P., et al., *Sulfide inhibition of and metabolism by cytochrome c oxidase.* Biochem Soc Trans, 2013. **41**(5): p. 1312-6.

152. Hargrove, A.E., et al., *Algorithms for the determination of binding constants and enantiomeric excess in complex host: guest equilibria using optical measurements.* New Journal of Chemistry, 2010. **34**(2): p. 348-354.
153. Meng, F. and A.I. Alayash, *Determination of extinction coefficients of human hemoglobin in various redox states.* Analytical biochemistry, 2017. **521**: p. 11-19.
154. Mishara, B.L., *Prevention of deaths from intentional pesticide poisoning.* Crisis, 2007. **28**(S1): p. 10-20.
155. Hosseinian, A., et al., *Aluminum phosphide poisoning known as rice tablet: A common toxicity in North Iran.* Indian journal of medical sciences, 2011. **65**(4): p. 143.
156. Navabi, S.M., et al., *Mortality from aluminum phosphide poisoning in Kermanshah Province, Iran: characteristics and predictive factors.* Epidemiology and health, 2018. **40**.
157. Singh, Y., et al., *Acute aluminium phosphide poisoning, what is new?* The Egyptian journal of internal medicine, 2014. **26**(3): p. 99-103.
158. Soltaninejad, K., et al., *Fatal aluminum phosphide poisoning in Tehran-Iran from 2007 to 2010.* Indian J Med Sci, 2012. **66**(3-4): p. 66-70.
159. Flesch, J.P., J.C. Ganser, and G. Kullman, *Preventing phosphine poisoning and explosions during fumigation.*
160. NIPC. *Inhalation Risks from Phosphide Fumigants*. 2017; Available from: http://npic.orst.edu/mcapro/phosphine.html.
161. NCCEH, *Phosphine poisoning as an unintended consequence of bed bug treatment*. 2015.
162. Yan, H., S. Nottingham, and A. Stapleton. *Texas pesticide deaths: Chemical may have sickened, but cleanup was fatal*. 2017; Available from: https://www.cnn.com/2017/01/03/health/texas-pesticide-deaths/index.html.
163. Earnshaw, A. and N.N. Greenwood, *Chemistry of the Elements*. Vol. 60. 1997: Butterworth-Heinemann Oxford.
164. Burkett, B.N., *Respiration of Galleria mellonella in relation to temperature and oxygen.* Entomologia Experimentalis et Applicata, 1962. **5**(4): p. 305-312.
165. Popovic, D.M., et al., *Similarity of cytochrome c oxidases in different organisms.* Proteins, 2010. **78**(12): p. 2691-8.
166. Darley-Usmar, V.M., D. Rickwood, and M.T. Wilson, *Mitochondria, a practical approach*. 1987: IRL press.
167. Kanai, A.J., et al., *Identification of a neuronal nitric oxide synthase in isolated cardiac mitochondria using electrochemical detection.* Proceedings of the National Academy of Sciences, 2001. **98**(24): p. 14126-14131.
168. Yonetani, T. and G.S. Ray, *Studies on cytochrome oxidase VI. Kinetics of the aerobic oxidation of ferrocytochrome c by cytochrome oxidase.* Journal of Biological Chemistry, 1965. **240**(8): p. 3392-3398.
169. Sinjorgo, K.M., et al., *Bovine cytochrome c oxidases, purified from heart, skeletal muscle, liver and kidney, differ in the small subunits but show the same reaction kinetics with cytochrome c.* Biochimica et Biophysica Acta (BBA)-Bioenergetics, 1987. **893**(2): p. 251-258.
170. Fairchild, G.A., *Measurement of respiratory volume for virus retention studies in mice.* Applied microbiology, 1972. **24**(5): p. 812-818.

171. Reinicke, H. and K. Wunderlich, *Untersuchungen über die Resorption intramuskulärer Gold-und Wismut-Depots beim Kaninchen in ihrer Abhängigkeit von der Dosis.* Archiv für klinische und experimentelle Dermatologie, 1957. **204**(2): p. 103-115.
172. Mascarenhas, B.R., J.L. Granda, and R.H. Freyberg, *Gold metabolism in patients with rheumatoid arthritis treated with gold compounds—reinvestigated.* Arthritis & Rheumatism: Official Journal of the American College of Rheumatology, 1972. **15**(4): p. 391-402.
173. Balfourier, A., et al., *Gold-based therapy: from past to present.* Proceedings of the National Academy of Sciences, 2020. **117**(37): p. 22639-22648.
174. Alzahrani, S.M. and P.R. Ebert, *Stress pre-conditioning with temperature, UV and gamma radiation induces tolerance against phosphine toxicity.* PloS one, 2018. **13**(4): p. e0195349.
175. Proudfoot, A.T., *Aluminium and zinc phosphide poisoning.* Clinical toxicology, 2009. **47**(2): p. 89-100.
176. Cambal, L.K., et al., *Acute, sublethal cyanide poisoning in mice is ameliorated by nitrite alone: complications arising from concomitant administration of nitrite and thiosulfate as an antidotal combination.* Chem Res Toxicol, 2011. **24**(7): p. 1104-12.
177. Cronican, A.A., et al., *Antagonism of Acute Sulfide Poisoning in Mice by Nitrite Anion without Methemoglobinemia.* Chemical Research in Toxicology, 2015. **28**(7): p. 1398-1408.
178. Registry, A.f.T.S.a.D., *Toxic Substances Portal-Hydrogen Sufide.* April 8, 2019.
179. Taylor, J., et al., *Toxicological Profile for Cyanide*. 2006, Agency for Toxic Substances and Disease Registry, U.S. Department of Health and Human Services: Atlanta, GA.
180. Jones, M., et al., *A re-examination of the reactions of cyanide with cytochrome c oxidase.* Biochemical Journal, 1984. **220**(1): p. 57-66.
181. Issa, S.Y., et al., *Fatal suicidal ingestion of aluminum phosphide in an adult Syrian female-A clinical case study.* Journal of Pharmacology & Clinical Toxicology, 2015. **3**: p. 1061-1064.
182. Akhtar, S., et al., *Accidental phosphine gas poisoning with fatal myocardial dysfunction in two families.* 2015.
183. Bogle, R., et al., *Aluminium phosphide poisoning.* Emergency Medicine Journal, 2006. **23**(1): p. e03-e03.
184. Potter, W.T., et al., *Phosphine-mediated Heinz body formation and hemoglobin oxidation in human erythrocytes.* Toxicology letters, 1991. **57**(1): p. 37-45.
185. Misra, U., et al., *Acute phosphine poisoning following ingestion of aluminium phosphide.* Human toxicology, 1988. **7**(4): p. 343-345.
186. Garrett, K.K., et al., *Antidotal Action of Some Gold (I) Complexes toward Phosphine Toxicity.* Chemical research in toxicology, 2019. **32**(6): p. 1310-1316.
187. Gutsche, C.D., *Calixarenes.* Accounts of Chemical Research, 1983. **16**(5): p. 161-170.
188. Ikeda, A. and S. Shinkai, *Novel cavity design using calix [n] arene skeletons: toward molecular recognition and metal binding.* Chemical reviews, 1997. **97**(5): p. 1713-1734.
189. Sawyer, D.T., *Redox Thermodynamics for Oxygen Species*, in *Oxygen Chemistry*. 1991, Oxford University Press, Inc.: New York. p. 21.
190. *Silver Lactate 96% ACROS Organics*. 2021, Fisher Scientific.
191. Nesbitt Jr, R. and B. Sandmann, *Solubility studies of silver sulfadiazine.* Journal of pharmaceutical sciences, 1977. **66**(4): p. 519-522.

192. Information, N.C.f.B. *PubChem Compound Summary for CID 24470, silver nitrate.* 2021 [cited 2021 August 17]; Available from: https://pubchem.ncbi.nlm.nih.gov/compound/Silver-nitrate.
193. Babizhayev, M.A., *Generation of reactive oxygen species in the anterior eye segment. Synergistic codrugs of N-acetylcarnosine lubricant eye drops and mitochondria-targeted antioxidant act as a powerful therapeutic platform for the treatment of cataracts and primary open-angle glaucoma.* BBA clinical, 2016. **6**: p. 49-68.
194. Vinson, J.A., *Oxidative stress in cataracts.* Pathophysiology, 2006. **13**(3): p. 151-162.
195. Siegfried, C.J., et al., *Oxygen distribution in the human eye: relevance to the etiology of open-angle glaucoma after vitrectomy.* Investigative ophthalmology & visual science, 2010. **51**(11): p. 5731-5738.
196. Arrese, E.L. and J.L. Soulages, *Insect fat body: energy, metabolism, and regulation.* Annual review of entomology, 2010. **55**: p. 207-225.
197. Thompson, J., P. Casey, and J. Vale, *Deaths from pesticide poisoning in England and Wales 1990-1991.* Human & experimental toxicology, 1995. **14**(5): p. 437-445.
198. Wort, S.J. and T.W. Evans, *The role of the endothelium in modulating vascular control in sepsis and related conditions.* British medical bulletin, 1999. **55**(1): p. 30-48.
199. *Exposure Factors Handbook 2011 Edition (Final Report)*, U.S.E.P. Agency, Editor. 2011: Washington, DC.
200. *Poisonings uncover lax sodium azide controls*, in *The Japan Times*. 1998, The Japan Times.
201. *Sodium azide poisoning at a restaurant - Dallas County, Texas, 2010.* MMWR Morb Mortal Wkly Rep, 2012. **61**(25): p. 457-60.
202. Schwarz, E.S., et al., *Multiple Poisonings with Sodium Azide at a Local Restaurant.* The Journal of Emergency Medicine, 2014. **46**(4): p. 491-494.
203. Stewart, D., *Sodium azide found in coffee pot from Yale School of Medicine hazmat incident*, in *Fox 61*. 2017, Fox 61.
204. Chang, S. and S.H. Lamm, *Human health effects of sodium azide exposure: a literature review and analysis.* Int J Toxicol, 2003. **22**(3): p. 175-86.
205. Welling, P.G., *Differences between pharmacokinetics and toxicokinetics.* Toxicol Pathol, 1995. **23**(2): p. 143-7.
206. Berndt, J.D., N.L. Callaway, and F. Gonzalez-Lima, *Effects of chronic sodium azide on brain and muscle cytochrome oxidase activity: a potential model to investigate environmental contributions to neurodegenerative diseases.* J Toxicol Environ Health A, 2001. **63**(1): p. 67-77.
207. Ishikawa, T., B.L. Zhu, and H. Maeda, *Effect of sodium azide on the metabolic activity of cultured fetal cells.* Toxicol Ind Health, 2006. **22**(8): p. 337-41.
208. Smith, L., H. Kruszyna, and R.P. Smith, *The effect of methemoglobin on the inhibition of cytochrome c oxidase by cyanide, sulfide or azide.* Biochem Pharmacol, 1977. **26**(23): p. 2247-50.
209. Kurt, T.L. and W. Klein-Schwartz, *Azide poisonings*, in *Toxicology of Cyanids and Cyanogens: Experimental, Applied and Clinical Aspects*, A.H. Hall, G.E. Isom, and G.A. Rockwood, Editors. 2015, John Wiley & Sons, Ltd. p. 330-336.
210. Borron, S.W. and F.J. Baud, *Antidotes for acute cyanide poisoning.* Curr Pharm Biotechnol, 2012. **13**(10): p. 1940-8.

211. Long, K.M. and D.H. Busch, *Cobalt(II) complexes of the quadridentate macrocycle 2,12-dimethyl-3,7,11,17-tetraazabicyclo[11.3.1]heptadeca-1(17),2,11,13,15-pentaene.* Inorganic Chemistry, 1970. **9**(3): p. 505-512.
212. Lacy, D.C., C.C.L. McCrory, and J.C. Peters, *Studies of Cobalt-Mediated Electrocatalytic CO2 Reduction Using a Redox-Active Ligand.* Inorganic Chemistry, 2014. **53**(10): p. 4980-4988.
213. Hill, Z.D. and P. MacCarthy, *Novel approach to Job's method: An undergraduate experiment.* Journal of Chemical Education, 1986. **63**(2): p. 162.
214. Vosburgh, W.C. and G.R. Cooper, *Complex Ions. I. The Identification of Complex Ions in Solution by Spectrophotometric Measurements.* Journal of the American Chemical Society, 1941. **63**(2): p. 437-442.
215. Skoog, D.A., D.M. West, and F.J. Holler, *Molecular Absorption Spectroscopy*, in *Fundamentals of Analytical Chemistry*, D.A. Skoog, D.M. West, and F.J. Holler, Editors. 1992, Saunders College Publishing: the United States of America. p. 583-584.
216. Cambal, L.K., et al., *Comparison of the relative propensities of isoamyl nitrite and sodium nitrite to ameliorate acute cyanide poisoning in mice and a novel antidotal effect arising from anesthetics.* Chem Res Toxicol, 2013. **26**(5): p. 828-36.
217. Crankshaw, D.L., et al., *A Novel Paradigm for Assessing Efficacies of Potential Antidotes against Neurotoxins in Mice.* Toxicology letters, 2007. **175**(1-3): p. 111-117.
218. Nakamoto, K., *Infrared and Raman spectra of inorganic and coordination compounds, part B: applications in coordination, organometallic, and bioinorganic chemistry*. 2009: John Wiley & Sons.
219. Smith, R.P., et al., *Acute neurotoxicity of sodium azide and nitric oxide.* Fundam Appl Toxicol, 1991. **17**(1): p. 120-7.
220. Klein-Schwartz, W., et al., *Three fatal sodium azide poisonings.* Med Toxicol Adverse Drug Exp, 1989. **4**(3): p. 219-27.
221. Barteka-Mino, K., et al., *Hydroxocobalamin: An antidote for sodium azide poisoning?* Clinical toxicology, 2014. **52**: p. 314.
222. Lim, K., et al. *Hemodialysis failure secondary to hydroxocobalamin exposure*. in *Baylor University Medical Center Proceedings*. 2017. Taylor & Francis.
223. Petersen, L.C., *The effect of inhibitors on the oxygen kinetics of cytochrome c oxidase.* Biochim Biophys Acta, 1977. **460**(2): p. 299-307.
224. Benz, O.S., et al., *The Metalloporphyrin Co(III)TMPyP Ameliorates Acute, Sub-lethal Cyanide Toxicity in Mice.* Chemical research in toxicology, 2012. **25**(12): p. 2678-2686.
225. Yuan, Q., L.L. Pearce, and J. Peterson, *Relative Propensities of Cytochrome c Oxidase and Cobalt Corrins for Reaction with Cyanide and Oxygen: Implications for Amelioration of Cyanide Toxicity.* Chemical Research in Toxicology, 2017. **30**(12): p. 2197-2208.
226. Benz, O.S., et al., *Effect of Ascorbate on the Cyanide-Scavenging Capability of Cobalt(III) meso-Tetra(4-N-methylpyridyl)porphine Pentaiodide: Deactivation by Reduction?* Chem Res Toxicol, 2016. **29**: p. 270-278.